Order Number 9224833

# Mathematical/kinetic models for low density lipoprotein pathway in non-hepatic human cells (using historic experimental data on human fibroblasts)

Lim, Kwang-Hee

The City University of New York, 1992



U·M·I
300 N. Zeeb Rd.
Ann Arbor, MI 48106

# Mathematical/Kinetic Models for Low Density Lipoprotein Pathway in Non-Hepatic Human Cells

(Using Historic Experimental Data on Human Fibroblasts)

by

**Kwang-Hee Lim**

A dissertation submitted to the Graduate Faculty
in Engineering in partial fulfillment
for the degree of Doctor Philosophy,
The City University of New York

1992

This manuscript has been read and accepted for the Graduate Faculty in Engineering in satisfaction of the dissertation requirement for the degree of Doctor of Philosophy.

23 March 1992
Date

David S. Rumschitzki
Professor David S. Rumschitzki
Chair of Examining Committee

April 6, 1992
Date

Gerald G. Lowen
Professor Gerald G. Lowen
Executive Officer

Prof. David S. Rumschitzki

Prof. Reuel Shinnar

Prof. Sheldon Weinbaum

Prof. Herbert Weinstein

Dr. R. Ramakrishnan
Supervisory Committee

The City University of New York

## Abstract

**Mathematical/Kinetic Models for Low Density Lipoprotein Pathway in Non-Hepatic Human Cells**

**by**

**Kwang-Hee Lim**

Adviser: **Professor David S. Rumschitzki**

This goal of this thesis is to kinetically model the so-called cellular LDL pathway using historical data, mainly taken for human fibroblasts by the Brown and Goldstein group. Such quantitative kinetic modeling can point to inconsistencies in qualitative models and suggest more appropriate modifications whose predictions agree with the data. They also have the potential to play a role in the development of an overall transport and reaction theory of lipoprotein cholesterol in and through the artery wall which may help pinpointing the earliest events in lesion formation and their causal interrelation. The thesis is divided into two parts, the first entitled, "Uptake," and the second, "Regulation."

Part One focuses exclusively on the uptake and degradation of low density lipoproteins (LDL) using, as noted, the historical human fibroblast-derived data of Brown and Goldstein and of other groups. For these data, unlike for data taken on (bovine) smooth muscle cells, it appears necessary to explicitly account for the transfer of cell surface-mobile LDL receptors to receptors bound

to coated pits. In addition, kinetic analysis suggests that receptors that have bound LDL molecules before attaching to coated pits have a significantly reduced rate of subsequently becoming attached to coated pits. This agrees qualitatively with one of two alternative explanations of the experimental results of Barak and Webb[1,2] (*JCB*, 90, 595 (1981) & 95, 846) and Tank *et al.*[3] (*JCB*, 101, 148 (1985)), showing even a quantitatively similar disparity in the surface diffusion coefficients of ligand-free and LDL-bound receptors. A closer analysis, both in terms of an order of magnitude calculation and of two detailed models that do not *a priori* assume diffusion control, reveals, however, that diffusion seems to be too fast to account for the kinetically-determined parameters. One possible explanation, which the models herein support, is that this process is primarily binding, rather than diffusion controlled.

As is well known, many types of human non-hepatic cells prefer to satisfy their need for cholesterol by importing exogenous lipoprotein cholesterol via the path described in Part One. Part Two moves on to examine the regulation processes that such cells use to avoid a shortage or an over-accumulation of cholesterol. Brown and Goldstein have shown that these include cellular *de novo* synthesis of cholesterol when the exogenous supply is too low and cholesterol esterification to store excess free cholesterol when the cell has too much of it. In addition, in response to extended periods of high exogenous LDL supply, the cells sharply down-regulate the number of surface LDL receptors that they express and thereby their rate of LDL uptake.

We propose kinetic models to account for each of the regulatory processes and use available data to test these models

and to determine their parameters. The models for the control of cellular *de novo* cholesterol synthesis and for the total receptor tally are gene-level-based, as opposed to that for cholesterol esterification. Its model has the novel feature that LDL-derived cholesterol that has recently enterred via the receptor pathway is postulated to be able to expanding the size of the esterifiable cholesterol pool and thereby controlling the rate of esterification. This model turns out to be capable of explaining a number of experimental observations. Finally, the combined model seems to be quite capable of predicting experimental results even when all of the regulatory processes are at play.

## Acknowledgments

I would like to express my sincere gratitude to my advisor, Professor David S. Rumschitzki for his great guidance throughout this research. In particular, his continuous encouragement has given me the strength to overcome the hardships we often encounter in dealing with tough problems.

I also wish to thank Professor Weinbaum for motivating with his superb understanding of biomechanical phenomena in this research.

I would also like to thank Professor Roberto Mauri and Professor Charles Maldarelli for their kind suggestion whenever I discussed scientific or other matters with them, and the NIH and the NSF for the partial support under grants E49657-4653 and CTS 8658147 (both to Professor David Rumschitzki), respectively.

Most of all I want thank to my wife, Anna, for her constant support encouragement and love.

## Table of Contents

## List of Tables

# List of Figures

Descriptions of experimental procedures are taken essentially verbatim from the original papers of M.S. Brown and J.L. Goldstein.

**Part one: Uptake** page

**Part two: Regulation**

# Part One: Uptake

# I. Introduction

High serum concentrations of low density lipoprotein cholesterol (LDL) correlate strongly with the development of atherosclerosis. In fact, LDL is the major lipoprotein in plasma and the bulk of the plasma cholesteryl ester that is a source of lesion cholesterol. The precise mechanistic link between these events, and the manner in which cofactors such as smoking contribute, is and has been a major active area of research. It does, however, seem likely that high plasma cholesterol levels would tend to raise the local cholesterol concentration in the artery wall (and, in particular, in the intima where lesions begin) where it may cause mischief. An important factor in determining this local concentration is the rate at which arterial endothelial cells take up this LDL cholesterol and keep it from accumulating. In addition, the amount of cellular uptake on the whole body level, affects the LDL concentration, of the circulating plasma. The source of this cholesterol is dietary. Dietary fat is processed in the intestines and eventually makes its way to the liver (Fig. $1^{110}$). The liver cells package the cholesterol, cholesteryl ester and other minor components together with a protein into the LDL "molecule." LDL is soluble to a much higher degree in plasma than is free cholesterol and the protein component of the LDL allows recognition and binding to many types of body cells. Most cell need cholesterol as the major component of their membranes. A group of fascinating and important steps in the overall cholesterol pathway comprises the cellular pathway (Fig. $2^{110}$) by which non-hepatic cells and, in particular, arterial endothelial and smooth muscle cells take up

LDL from blood, digest it and use it to produce new membrane. In times of famine, these cells can produce their own supplies of cholesterol and, in times of feast, they have mechanisms to protect themselves from drowning in cholesterol. For their vast pioneering work on deciphering this cellular pathway, M. S. Brown and J. L. Goldstein were awarded the Nobel Prize in Biology or Medicine in 1985.

At the early stage of arterial lesion formation, plasma LDL infiltrates across endothelial cell monolayer and accumulates in the intima of artery wall. Monocytes, white blood cells, then attach to and penetrates the arterial endothelial cell monolayer and enter the intima. The monocytes turn into macrophages and scavenge the accumulated LDL at the intimal region and usually return to the lumen. However, when intimal LDL concentrations are very high, some macrophages lodge there and turn into foam cells that contain high level of lipid. This seems to be the beginning of a legion, which grows to include both monocyte-derived and smooth muscle cell-derived foam cells. The key questions seem to be what controls the local cholesterol concentration in the artery wall, what triggers monocyte entry and when are macrophages unable to clear the intima? Thus, in order to eventually gain an understanding of the overall origins of coronary artery disease, it seems that one will need models that take into account the cholesterol transport through the artery wall (e.g., *Yuan et al*[111]) and the subsequent responses of the endothelial and smooth muscle cells as well as the myriad lymphocytes (e.g., monocytes) to the resulting elevated subendothelial LDL concentration. It seems, therefore, reasonable to suspect that any such theory will require a good

model for quantitative or semi-quantitative as well as qualitative prediction of the local LDL concentration in the intima and the arterial wall; clearly then, a kinetic understanding of the steps of the cellular pathway, which is a major "sink" term (in fact, between one half[4] and two thirds[5] of the total body LDL degradation occurs by this pathway) in the overall dynamic of the local cholesterol concentration, is vital. This is the motivation for the present and a subsequent article aimed at constructing just such a model, verifying it and determining its parameters by comparison with the ample experimental data available in the literature.

Brown and Goldstein conducted their experiments, by and large, on human fibroblasts, as a model for the behaviour of human arterial endothelial cells. As is by now quite well known, they found that the surfaces of normal human endothelial, fibroblast and many other cells possess a type of high affinity LDL receptor which specifically binds the apoprotein B component of the LDL packet (it can also bind the apoproteins B and E containing $\beta$VLDL molecule and the apoprotein E containing $HDL_c$ molecule) and ferries the bound LDLs into the cell. These receptors, mobile on the membrane surface, can stick to the clathrin-lined areas (called coated pits) that make up 1%-2% of the cell membrane; the coated pits periodically (with a half-life of about 3-5 minutes[6]) invaginate, undergo endocytosis and deliver their contents to the endosomes[7]. After the receptor separates in order to recycle to the surface, the lysosome degrades the LDL protein component and hydrolyzes its cholesteryl esters; the hydrolysis product contributes to the cell's cholesterol pool. Should famine deplete this pool, the cell activates the enzyme

HMG CoA Reductase to catalyze the rate limiting step in a cellular *de novo* cholesterol synthesis. Feast, on the other hand, stimulates the cell to activate the enzyme or enzymes Acyl-CoA: Cholesterol Acyl Transferase (ACAT) which act to prevent a cholesterol oversupply by esterifying excess cholesterol. Finally, prolonged feast induces the cell to inhibit the production of new receptors, thereby allowing the cell to reduce the total receptor tally by up to 90% by attrition[8,9].

Whereas receptor binding can take place over a time scale of hours, surface receptor motion towards coated pits, their invagination and the subsequent recycling of receptors and coated pit clathrin take place over time scales of minutes. *De novo* synthesis and esterification turn on and off over a period of hours and receptor numbers change significantly over tens of hours or days (the half-life of an LDL receptor is about 25 hrs.[8]). Our strategy in modeling this complex web of interrelated processes is that of the kineticist: We begin modeling the fastest processes under the assumption that the slower variables do not change on the fast time scale. With models in hand for the fast processes that are consistent with observation, we proceed to the processes that are on the next fastest time scale; the working assumption on this scale is that the fast processes are quasi-steady at values consistent with the instantaneous values of the variables associated with the slower processes currently being modeled. At the end of this modeling process, we combine all of the models. We endeavor, whenever possible, to invoke "well mixed" models that do not require the introduction of quantities whose values depend on local position within or on

the cells. When alternate models become necessary, we take care to distinguish between such models and the well mixed type.

In part I of this thesis, we focus exclusively on the steps or "reactions" up to and including the lysosomal actions which, other than binding, are fast enough so that one may take the regulatory processes to be stationary. The complementary models of the regulatory processes, their justifications and combination into an overall model will be the subject of part II.

In addition to the receptor-mediated processes just described, free cholesterol can exchange between LDL packets and the plasma membrane.[10] There also exists a non-specific bulk-phase pinocytotic pathway of transporting lipoprotein cholesterol into the cells, but this route does not affect the cholesterol regulatory processes discussed above.[11] In this work, we focus exclusively on the high affinity receptor pathway.

The paper's outline is as follows. Section II briefly reviews the previous modeling efforts of receptor-mediated pathways in general and of the LDL receptor pathway in particular. It also discusses more detailed models of cell surface motions of receptors and puts the current work in the context of these other efforts. Section III presents a hierarchy of models and argues in favour of one of these. We then analyze the chosen model and estimate the associated rate constants in a few intuitive ways from the available literature data. The results then suggest two physical interpretations. Finally, we bring numerical and statistical methods to bear on the available data to find the best fits for the model's rate parameters.

Section IV examines the question of which physical interpretation given in section IV is more likely. It approaches this

question by constructing two new models or variants of models for the receptor surface diffusion and binding to coated pits. These models' results tie in directly to the kinetic models of the last section. Finally, section V summarizes, draws some conclusions, examines some fine points and presents the outlook for future work.

## II. Modeling of Receptor Dynamics

Cells make use of a variety of surface-mobile specific receptor mechanisms as means for introducing a number of different molecules (including LDL, epidermal growth factor (EGF), transferrin, insulin, etc.) present in the surrounding medium into the cell's interior. Some of these mechanisms have already lent themselves to modeling. For example, the receptor mechanism for EGF is the subject of a number of studies (e.g., [12] [13] [14] [15]). Other studies (e.g., [16]), while ostensibly constructing a general model for receptor-mediated endocytotic processes, defer to particulars of the EGF system. The LDL system is also the focus of modeling efforts (e.g., [17] [18] [19] [20]) aimed at understanding binding, receptor-mediated endocytosis and degradation for experiments done on bovine smooth muscle cells as well as others (e.g., [21]) that attempt to describe the regulation of receptor number in response to changes in serum cholesterol levels. Finally, another group of theoretical works (e.g., [22-27]) focuses on the details of the processes by which the

receptors diffuse and bind[28] to the coated pits. A short discussion will put the present work in the context of these prior investigations.

Whereas most of the receptor-mediated endocytotic mechanisms discovered thus far have very similar general outlines, they frequently differ in various crucial particulars; it is these particulars which can radically alter the properties that the system's model must possess and thereby strongly affect the model's applicability. Attempting to include too many alternative features in a given model so that it can potentially encompass explanations for many receptor mechanisms can complicate the model to a point that interferes with its utility and can introduce large numbers of adjustable or partially adjustable parameters which make results hard to interpret.

As an example of how individual receptor mechanisms may vary, consider the EGF system. A number of authors listed above have presented detailed models for this system and one might hope or speculate that these models might carry over to the LDL system. However, unlike the EGF system where receptors do not cluster in coated pits until after they have bound a ligand,[13 29] LDL receptors cluster in coated pits with or without LDL in the medium.[6] Unlike the EGF system where the lysosome degrades a substantial fraction of the receptors that are internalized,[30] the LDL receptor appears to separate from its ligand in the endosome and to quickly recycle to the cell surface.[31 32] Unlike the EGF system where receptors have a half life of about three hours,[33] LDL receptors have a half life of 20-25 hours.[31] As a result, the time needed to replace an internalized surface LDL receptor may be as short as a matter of seconds[34] and there is no

appreciable inventory of LDL receptors internal to the cell[32] as opposed to the EGF system which, since it lysosomally degrades its internalized receptors, has a replacement time of many minutes to an hour and maintains a large internal stock of receptors.[14] As a result, important issues of EGF-receptor trafficking[14] and sorting efficiency,[12] apparently central to EGF-receptor models, are not pertinent in the LDL case.

Most of the modeling work on the LDL receptor system derives from experiments of the Boston (Harvard Medical School, MIT and Tufts) group[17-20] on Bovine smooth muscle cells. As we shall see by examining some of Brown and Goldstein's data for human fibroblasts, the Boston model, although quite good for the smooth muscle case, is not capable of even qualitatively explaining some important features of the fibroblast system. Rather, we use the Boston model, which neglects the need for receptors to find coated pits in order to internalize their ligands, as the first in a hierarchy of models, each of which includes more detail than its predecessor. After analysis and selection of one of these models, we cite other experimental work which tends to substantiate our changes to the Boston model.

Yuan, Weinbaum, Pfeffer and Chien's (1991)[21] work on the LDL metabolism problem is similar in spirit to ours in that it attempts to advance an overall model for the entire cellular pathway for the dynamics on a time scale of days; yet it differs immensely in its treatment of the biological data and its approach to modeling. Their approach is, for each process (i.e., binding and internalization, *de novo* synthesis, esterification, cholesterol efflux), to curve-fit a set of experimental data to a convenient (often non-kinetic) algebraic form and to combine the

results into a cholesterol balance. These algebraic forms sometimes tacitly assume relationships not in agreement with other available data. They then fit an algebraic form to relate the receptor synthesis rate to the cholesterol level suggested by this balance; this results in a prediction for the dynamics of the overall receptor tally. Our work attempts to *kinetically* model the processes involved and, in doing so, to remain faithful to as much of the broad range of experimental observations for each of the individual processes as possible.

In the context of our modeling below, we will determine rate constants for the processes that take free receptors and receptors laden with LDL to coated pits. We will then attempt to compare these numbers to the experimental diffusion coefficients for free and LDL-bound receptors along the cell membranes of fibroblast cells. This will lead us to a discussion of whether and to what extent these processes are limited by receptor diffusion or by the rate of receptor binding to coated pits. The work of the last group of authors mentioned in the opening paragraph of this section concerns this question and so we defer our review of their work until then (section IV).

## III. Hierarchy of Models

### III.1 Motivation and Models:

As noted in the introduction, this paper concerns itself exclusively with the modeling of the binding, uptake, internalization and degradation processes of LDL by cultured human

fibroblasts, based predominantly on the experimental results of Brown, Goldstein and coworkers. In presenting models below we shall adhere strictly to the convention of mass action kinetics, whereby the rate of a reaction *as written* is proportional to the product of the concentrations of the reactant species for the said reaction, each raised to the power given by the stoichiometric coefficient (possibly zero) of that species on the reactant (tail) side of the reaction arrow. Thus, translation from mechanism to kinetic differential equations is a totally unambiguous, prescribed procedure; in fact, we will usually omit this explicit translation.

One motivation for our hierarchy of models derives from the experiment described in Figure 3.[11,6] It begins with fibroblasts whose receptors have already bound $^{125}$I-LDL at 4°C (where internalization essentially does not occur) suddenly being warmed to 37°C in the presence of unlabeled LDL. The figure follows the time course of the concentrations of: (i) the labeled LDL which dissociates from the cells upon administration of heparin to the culture medium. This value is believed to represent the labeled LDL that is still on the cell's surface, whether or not it is in coated pits; (ii) the trichloroacetic acid soluble material, representing the degraded protein component of the degraded labeled LDL; and (iii) the radioactive material that remains associated with the cell after the previous two assays, which represents the labeled LDL taken to be the internalized fraction. At first glance, the figure's curves qualitatively show the classic forms for the series reactions that take reactant (surface bound LDL) to product (degraded LDL) via an intermediate (internalized LDL).

Such an interpretation leads to the model that we have called the Boston model which explains other types of experiments on bovine smooth muscle cells quite well. In that model, an LDL molecule (L) binds to a receptor ($R^P$) that is either prepositioned in a coated pit or can subsequently find it in a time short relative to the time scales of the other processes under consideration. The resulting complex ($L^P$) internalizes with its coated pit, quickly separates its internalized LDL molecule ($L^i$) and returns its receptor to the surface ($R^P$). The cell then degrades $L^i$ into the degradation product $L^d$. One can summarize the Boston model in mechanistic shorthand by:

$$L + R^P \rightarrow L^P \rightarrow L^i + R^P$$
$$L^i \rightarrow L^d \qquad (1)$$

(The Boston group originally included a step for LDL dissociation from its receptor, but found its rate constant to be negligible.[20 9]) Note that this mechanism conserves the total number of receptors given by $R^P+L^P$ and requires them to essentially always be on the cell's surface, i.e, that the time that receptors spend inside the cell is short compared with all other processes of interest and no appreciable inventory of receptors exists within the cell.

There are, however, a few noteworthy features in figure 3. First, a conservation of LDL molecules would require the sum of data points from the three curves at any given time to remain time-invariant. The experimental procedure has clearly led to

some violation of this principle, with the measurement taken at approximately three minutes being the only one that is beyond a reasonable fluctuation (~18% from the mean). This is probably due to the variation of total reactivity amongst parallel dishes, and one can probably infer that the internalization value at three minutes is a bit high. We shall return to this point later when discussing the extraction of rate constants for models that implicitly assume mass conservation from data that, as just mentioned, slightly violate this requirement.

Another important feature is that rather than displaying an exponential decay characterized by a single decay constant as required by model (1), the "surface bound" curve seems to clearly exhibit (at least) *two* time scales of decay[1], in figure 3, 6a and 6b: A fast decay having a characteristic time of about five minutes which depletes 60% to 80% of the surface-bound labelled LDL molecules precedes a slow decay that is not yet complete after two hours[2]. This may be a sign that the processes involved are more complicated than a simple series of two first order reactions with linear kinetics. It is also noteworthy that

1. Actually, the curve may seem to suggest *three* time scales, but there is too little data to substantiate such a claim.
2. These numbers do not change appreciably when one corrects for the non-specific binding of LDL to the plasma membrane by comparing with data[35] (in most cases in this paper, from parallel incubations) on homozygote familial hypercholesteremic (FH) cells, as Brown and Goldstein themselves do[36]; having, by hypothesis, no receptors, FH cells' total binding is non-specific. Whereas there is some question in using data from one study to quantitatively correct another, particularly when certain quantities, e.g., receptor number[38], might vary even with identical preparation, the non-specific bindings from a number of studies under conditions almost identical to the relevant ones (Fig. 5f[37] (4°C and 37°C) and Fig. 3a[35] (37°C)) are, in particular at the value of L~10$\mu$g/ml, consistently similar in size and a factor of about four lower than figure 3's tail. Thus non-specific binding cannot account for this tail.

under similar experimental conditions the half-life of coated pits on the fibroblast cell surface (as well as the half-life prior to internalization of the receptors bound to them) is about three to five minutes[6] and the fraction of receptors located in coated pits is between 50% and 80% of the total.[6] This suggests one possible explanation for the presence of two time scales: that LDL-bound receptors $L^p$ located in coated pits at the beginning of the experiment internalize quickly and *LDL-bound receptors $L^a$ initially located outside of coated pits have difficulty (i.e., the process is slow) becoming LDL receptors $L^p$ bound to coated pits*. Naturally one will need other evidence to corroborate this suggestion. (In section V we consider and argue against another possibility that the process taking non-coated pit-bound receptors to coated-pit-bound receptors is reversible.)

Distinguishing between $L^a$ and $L^p$ requires the model to also distinguish between unliganded receptors ($R^p$) bound to coated pits and those (R) that are not. Analogous to $L^a \rightarrow L^p$, R can bind to a coated pit to give $R^p$. Internalization of a coated pit containing $R^p$ returns a free receptor R to the surface. The mechanistic shorthand for this model is:

$$\begin{array}{l} L + R^p \rightarrow L^p \rightarrow L^i + R \\ \qquad\quad\ \uparrow \\ L + R \ \rightarrow L^a \\ L^i \rightarrow L^d \\ R \rightleftarrows R^p \end{array} \qquad (2)$$

This model (and model (3) below) assume that the concentration of coated pits on the cell's surface remains time-invariant and thereby lumps its constant value into the rate constants for $L^a \rightarrow L^p$ and $R \rightarrow R^p$. Like mechanism (1), mechanism (2) also conserves the total number of receptors, given here by $L^a+L^p+R+R^p$, and again requires all receptors to essentially always remain on the cell's surface.

In contrast to the ligand-bound receptors, the transformation of a non-LDL-bound receptor R to one bound to a coated pit $R^p$ cannot be slow since the steady distribution of LDL receptors in the absence of LDL shows 50% to 80% receptors bound to coated pits.[6] Therefore, one may guess that the "reaction" (in the sense of it being a modeled kinetic process) $L^a \rightarrow L^p$ is much slower than $R \rightarrow R^p$. This does not seem to contradict the observation of Goldstein *et al.*[34] that receptor clustering in coated pits occurs in the presence or the absence of LDL in the medium. Rather, $L^a \rightarrow L^p$ can occur, just at a slower rate than $R \rightarrow R^p$. Moreover, since the processes of LDL binding to a ligand-free receptor and receptor search for coated pits both compete for non-LDL-bound receptors not yet located in coated pits, it is conceivable that many receptors might bind to coated pits before binding ligand, *even in the presence of LDL-containing medium.* Other corroborative evidence follows later in section III.2.

A third, more detailed, possible model accounts for the possibility that while being short, the time spent by receptors inside the cell is not entirely negligible. The modeling of this feature, together with those of model (2), requires the tracking

of an additional dependent variable, the internal receptor inventory $R^i$, which results in model (3):

$$
\begin{array}{l}
L + R^P \rightarrow L^P \rightarrow L^i + R^i \\
\qquad\quad\ \uparrow \\
L + R \ \rightarrow L^a \\
\\
L^i \rightarrow L^d \\
R \rightarrow R^P \\
\uparrow \ \downarrow \\
\ R^i
\end{array}
\qquad (3)
$$

Like its predecessors, this model conserves the total number of receptors, given here by $R+R^P+R^i+L^a+L^P$. In contrast to models (1) and (2), model (3) allows for some of the receptors ($R^i$) to reside inside to reactor.

As a result of the discussion of figure 3 and some notes at the beginning of section V, we shall concentrate less on model (1) than on (2) and (3). By virtue of the experimental evidence suggesting small internalized receptor inventories and fast recycling, we shall focus primarily on model (2) and refer to model (3) only later on. Before entering into a detailed discussion aimed at checking the fidelity of this model to a variety of experimental data and at determining the appropriate rate constants via non-linear and statistical parameter fitting techniques, we present a couple of back-of-the-envelope calculations to check

this model's reasonableness and to estimate the orders of magnitude of the rate constants.

### III.2 Estimation of Rate Constants for Model (2):

The differential equations for model (2), using the same symbol for a species and its concentration, are:

$$\frac{dR}{dt} = -k_0'R + k_2R^p - k_1LR + k_2L^p$$

$$\frac{dR^p}{dt} = k_0'R - k_2R^p - k_1LR^p$$

$$\frac{dL^a}{dt} = k_1LR - k_0L^a$$

$$\frac{dL^p}{dt} = k_1LR^p + k_0L^a - k_2L^p$$

$$\frac{dL^i}{dt} = k_2L^p - k_3L^i \qquad (4)$$

For the experiment in figure 3, the concentration of labeled L is zero for $t \geq 0$ and so there is no new binding of labeled LDL to unliganded receptors once the experiment begins. Thus the equations for $L^a$, $L^p$ and $L^i$ decouple from those for R and $R^p$ and comparison with figure 3 ($(L^a+L^p)(t)$, $L^i(t)$, $L^d(t)$) require only solution of the former. These reduce to:

$$\frac{dL^a}{dt} = -k_0L^a$$

$$\frac{dL^p}{dt} = k_0L^a - k_2L^p$$

$$\frac{dL^i}{dt} = k_2 L^p - k_3 L^i \qquad (5)$$

with solutions

$$L^a(t) + L^p(t) = \frac{k_2 L^a(0)}{k_2 - k_0} \left(e^{-k_0 t} - e^{-k_2 t}\right) + \left(L^a(0) + L^p(0)\right) e^{-k_2 t}$$

$$L^i(t) = \frac{k_2 L^p(0)}{k_3 - k_2} \left(e^{-k_2 t} - e^{-k_3 t}\right) + L^i(0) e^{-k_3 t} + \frac{k_2 k_0 L^a(0)}{k_2 - k_0} \left( \frac{e^{-k_0 t} - e^{-k_3 t}}{k_3 - k_0} - \frac{e^{-k_2 t} - e^{-k_3 t}}{k_3 - k_2} \right). \qquad (6)$$

The rationale for model (2) was the separation of time scales evident in the binding curve of figure 3; one can express this scale separation as $k_2 \gg k_0$. As such, one should be able to obtain estimates of the rate constants for the internalization ($k_2$) and for $L^a \rightarrow L^p$ ($k_0$) by comparing the limit for $k_2 \gg k_0$ of (5) in the appropriate time regimes with the corresponding data points from figure 3. Thus, for short ($t \ll 1/k_0$) and for intermediate ($1/k_0 \approx t \gg 1/k_2$) times, one finds, respectively, a pure exponential decay of the receptors prepositioned in coated pits and a pure exponential decay of the non-prepositioned receptors:

$$L^a(t)+L^p(t) \approx L^a(0) + L^p(0) e^{-k_2 t} \qquad (t \ll 1/k_0);$$

$$L^a(t)+L^p(t) \approx L^a(0) e^{-k_0 t} \qquad (1/k_0 \approx t \gg 1/k_2). \qquad (7)$$

The resulting estimates for the rate constants are $k_0 \approx 10^{-2}$-$10^{-3}$/min. and $k_2 \approx .2$/min., the latter of which corresponds quite well with the number calculated (~.23/min.) from Brown and Goldstein's estimate[6] of the half-life (~3 min.) of a coated pit.

As a check on $k_0$, one can easily calculate a lower bound for this quantity. (Goldstein *et al.*[39] arrive at essentially this same estimate as a limit of a more complex model.) The model assumes that $L^a \rightarrow L^p$ is slow. The most extreme case, yielding a lower bound on $k_0$, would have the LDL-bound receptors outside of coated pits either immobile or totally unable to bind to coated pits. Nevertheless, eventually such receptors would become internalized due to the continual internalization and random formation of new coated pits, sooner or later directly below the stranded $L^a$, i.e., as "the mountain coming to Mohammed." A calculation of $k_0$ solely due to surface renewal is analogous to a half-life calculation, where one notes that coated pits occupy 1%-2% of the cell surface and have a half-life of about 3 minutes[6]. The cell surface thus has a 1/200-1/100th life of 3 minutes, which gives a value $k_0 \approx 10^{-3}$/min. at the lower limit of the estimate of the last paragraph, as expected.

It also behooves us to estimate the rate constant $k_0'$ for $R \rightarrow R^p$. Brown and Goldstein[6] report that in the absence of LDL, 50%-80% of the receptors reside in coated pits. In the absence of LDL, our model reduces to $R \underset{\leftarrow}{\overset{\rightarrow}{}} R^p$, with the rate constant for

the reverse process being that for internalization, $k_2$. At steady state, one has $k_0' = k_2 R^p/R$. Thus $k_0' \approx .2\text{-}.8$/min.

As a result, one can see that the experimental data, when interpreted in the context of our model, suggest that the ratio $k_0'/k_0 \approx 10^{-2}$. It is very interesting to note that Webb and coworkers[1 2 3] have measured the two-dimensional surface diffusion coefficients of LDL-bound and free receptors (by two different methods) on the surface of human fibroblasts and have found, in fact, that the ratio of the measured diffusivities is $(2.7\text{x}10^{-9}\ \text{cm}^2/\text{min.})/(1.2\text{x}10^{-7}\ \text{cm}^2/\text{min.}) \approx 10^{-2}$, also a difference of two orders of magnitude. There is some dispute as to whether the faster value corresponds simply to a faster diffusion of R or to a temporary electric field-induced disruption of R's cytoskeletal interaction.[3] Indeed if the processes $R \rightarrow R^p$ and $L^a \rightarrow L^p$ are diffusion controlled, that is, if their rates depend solely on the arrival of a receptor at the site of a coated pit, whereupon binding to the coated pit is very fast, then what we have is a kinetic confirmation of the simple interpretation of Webb *et al.*'s[2 3] experimental findings. On the other hand, if

3. Tank *et al.*[3] argue, "the LDL particle may...interact with immobilized components [e.g., fibronectin] of the extracellular matrix or lamina and hence show reduced mobility." The alternative is that electric field exposure causes the system to resemble fast diffusion of $L^a$ on cytoskeleton-detached blebs. However[3], the blebs may be artifactitious: "the exoskeleton may be depleted from cell surface blebs, explaining the observed rapid lateral diffusion of the $L^a$ in that system." Moreover, the alternate must explain the fact that postfield labeling "inhibits relaxation,"[3] i.e., restores slow diffusion and "postfield immobilization by ligand binding has also been observed for lecithin."

the binding rate of the receptor to the coated pit is significantly slow, then the situation becomes more involved. We defer further discussion of this point until (section IV) after we have estimated the binding constant (below) and discussed the "best" fitting of all of the rate constant to the experimental data (in sub-section III.3).

To get an estimate for the order of magnitude of the binding constant, one can proceed in at least two ways. The first centers on data taken with normal cells. Since the inventory of receptors not on the cell surface is small, one can estimate a lower bound on the total number of receptors (at a value - in the units of Brown and Goldstein's figure[11] - of ~200 ng/$\mu$g) from an experiment (figure 4a[11]) which measures the heparin-releasable labelled LDL from cells that are initially LDL-starved for 48 hours and then incubated for five hours with a very high concentration of labelled LDL. One can then turn to an experiment where one subjects identically prepared cells to a step change in LDL concentration (from 0 to, say, 10 $\mu$g/(ml protein)). Since at the start of the experiment $L^a$=$L^p$=0 and L remains time-independent throughout, the initial rate of increase of $L^a$+$L^p$ is due purely to binding. Thus, the initial rate $[d(L^a+L^p)/dt](t=0) \approx k_1 L\ (R+R^p)$. We (under)estimate the initial derivative from figure 4b[11] as the ratio of the first data point (at 37° C) and the time (30 min.) at which it was taken. The result of this calculation is $k_1 \approx .001$ ml/($\mu$g-min.).

One can obtain a second estimate of the binding rate constant from the internalization-deficient cells from the patient J.D. J.D.'s cells' receptors are unable to bind to coated pits[11]

[41] [6] and therefore are unable to internalize significant amounts of LDL, although they seem to bind LDL at rate close to normal.[11] Also, LDL-receptor dissociation seems to be much more significant than in normal cells[4]. Thus, for J.D. cells, the $k_0 - k_0' \approx 0$. Ignoring the slow internalization due to coated pit recycling and including a step for LDL-receptor dissociation, the model for J.D.'s cells becomes:

$$R + L \underset{\leftarrow}{\overset{\rightarrow}{}} L^a. \qquad (8)$$

The dissociation rate constant derives from figure 5a[11] as ~.008/min. and the binding constant from figure 5b[11] as ~.001 ml/($\mu$g-min), in agreement with the previous estimate. One can probably take J.D.'s binding rate again as a lower bound on the binding rate for normal cells.

The take-home lesson of these estimates is that simple calculations utilizing data from a variety of different experiments and different types of experiments yield consistent estimates. This suggests that the model advanced may, in fact, be a good representation of the true processes. In order to investigate this further we proceed to carry out a more proper parameter estimation scheme, compare the forms of the resulting model-generated curves with the data used to generate the parameters,

4. The rate of spontaneous dissociation from normal cells is "very slow."[9] If it were as high for normal cells at 37°C then it would result in a mass balance deficit in fig. 3 that would be larger than the observed trendless mass balance fluctuations. In fact, inclusion of dissociation in a best fit parameter scheme for normal cell data yields a negligible rate constant.

and then compare model predictions with experimental data not used in the parameter estimation process.

### III.3 "Best" Fit Parameters for Model (2)

Given the estimates obtained in the last section as a guideline for approximate parameter size, we now present "best" fit parameter schemes. Parameters thus obtained allow one to compare data from various sources and, in particular, to see if the model taken with parameters obtained from one set of experiments has predictive value for a qualitatively different set of experiments.

In essence, Brown, Goldstein and coworkers carried out three qualitatively different types of experiments on the LDL binding, uptake and degradation system which interest us. In order to allow comparison of the data from these various types of experiments, though, they employed a uniform, standard cell preparation scheme.[38] The first type of experiment, as exemplified in figure 3, begins with the receptors loaded with the entire charge of labelled LDL at the beginning of the experiment and watches the unsteady progress of the labelled components through the system. We call this a *pulse* experiment. As is well known, an experiment containing the equivalent information is the so-called *step* experiment in which cells initially starved of LDL (here for 48 hours) prior to the start of the experiment, are exposed to an assumed time-invariant concentration of labelled LDL for the duration of the experiment. Again, one records the time-progress of the labelled material through the system. Finally, the third type of experiment is a set of (presumed almost) steady

state[5] values of the labelled quantities as a function of the presumed-time-independent concentration of labelled LDL in the medium.

The gist of a best fit parameter estimation scheme is to find a set of parameters which minimizes the norm (e.g., least square) of the error between the data and the prediction of the model taken at those parameters. This invites a short discussions of the data, the model prediction and of the minimization scheme. Whereas the set of curves for binding, internalization and degradation for any given experiment are not independent measurements, one must incorporate (or weight) them in an appropriate (Bayesian[20 42]) manner in formulating the least squares error function. Another point for which the Bayesian procedure accounts is that one is extracting rate constants from data that, at least in the pulse experiment, do not conserve mass exactly, for a model that implicitly does. Rather than arbitrarily "correcting" the data to conserve mass, the statistical procedure just minimizes the error, which takes into account that within the data itself.

To complete the error function one must compute the model prediction for a given set of parameters by (usually numerically) solving the coupled, typically non-linear set of ordinary differential equations corresponding to the experiment at hand. Finally, one must choose a non-linear minimization scheme suited for efficiently minimizing with respect to many parameters whose values are not discrete, an object function that may have many

5. The measurements were taken either 5 or 6 hours after introducing LDL into the medium, while the unsteady step experiments suggest that steady behaviour obtains after ~2 hrs.

local minima. For parameter estimation based on steady state data where the solution of the steady equations is cheap and for estimation based on pulse data where one has an analytic solution for the model's predictions, we employed Kirkpatrick's simulated annealing,[43] adapted to continuous parameter system[6], with a temperature scheduling consisting of reducing the temperature by a fixed percentage (say, 20%) after a number of steps equal to 15-20 (and sometimes significantly more) times[44] the number of parameters at a given temperature. Since calculation of the model's predictions for unsteady step data is considerably more computationally expensive, we chose Bremermann's optimization scheme,[45 46] involving far fewer object function evaluations, based on the way in which chemotactic bacteria home in on their chemoattractants. The main feature of this algorithm is that it can see over nearby hills and valleys and avoid getting stuck in relatively poor local minima.

Figures 6 $a^6$ ( $b^6$), $c^{11}$, $d^{11}$ are prototypical experimental results (corrected, as described earlier, for non-specific binding by subtracting the amount of non-specific binding in FH cells from the same experiment) for the three types of experiments discussed above and table 1 gives the parameter values determined independently from each of these curves (in columns 1, 2, 3,

6. Our experience led us to chose an updating scheme different from that suggested by Vanderbilt and Louie (1984).[44] We chose the update (on each parameter) from a random number generator governed by a Gaussian distribution of mean zero and standard deviation one sixth of the difference between the given upper and lower bounds for that parameter. In order to assure that we did not bias the annealing scheme to search almost exclusively within the order of magnitude of the given upper bounds for the parameters, we ran all annealing schemes twice, once for the parameters themselves and once for their logarithms.

respectively) as determined by the methods outlined above. The figures also contain, for comparison, the model-generated curves based on the parameters in table 1. It is worth noting that although the types of experiments were quite different from one another, possibly resulting in slightly different actions of the regulatory processes ignored in the current treatment, the values determined for each of the parameters are generally in good agreement with one another and with the estimates of the last section, with the largest variation in the rate constant $k_0'$ for the migration of free receptors. Moreover, we have compared the model prediction (actually, postdiction, after S. Lifson) with an array of historic data taken under various conditions (figures 7[6 37 47 48 53]). Considering the variety of sources of the data, the agreement is quite good. In these plots, the only parameter that was adjusted was the total number of receptors, a quantity (which can vary - see footnote 2) not given explicitly in the experiments reported. It is worth mentioning that the model underpredicts the steady degradation curve in figure 6d for low LDL concentrations, which may point to a flaw in the assumption of a steady rate of degradation for the said experiment.

Table 2 is an error analysis along the lines of Waters *et al.*[15] for the parameters in table 1. Due to the large number of graphs this would entail considering the number of parameters and experiments, we have presented the results in the form of ten times the fractional change in the (Bayesian) error function F minimized that accompanies a ten percent shift in the said parameter, i.e., $(\delta F/F)/(\delta k/k)$; $\delta k/k=.1$. Only the magnitudes and not the precise values are significant (the larger, the more significant) as fig. 8 exhibits by giving actual Waters *et al.*[15]

plots for $k_0$ and the three experiments in table 1. Since the experimental papers do not include error bars, table 2 only reflects the error introduced by the fitting procedure. Clearly different experiments are more significant for different rate constants.

## IV. Receptor Motion towards and Binding to Coated Pits

Of note in the results of the last section is that the rate constant determined for $L^a \rightarrow L^p$ is about an order of magnitude larger than the lower bound estimated for the extreme case of $L^a$ being totally immobile or totally unable to bind to coated pits[7]. Thus the $L^a$ do have significant mobility/binding ability. Nevertheless, in keeping with the diffusion coefficient measurements of Webb and coworkers discussed in section III.2, it is still one to two orders of magnitude slower than the best fit values for $k_0'$ the rate constant for $R \rightarrow R^p$. Given numerical values for these effective kinetic rate constants and for the experimental diffusivities (according to the simple explanation of Tank *et al.*'s experiments), one should now be able to assess whether

7. Although the fit of "bound" data in figure 6a and 6b, might suggest that the determined value for the constant is somewhat high, use of the lower value significantly depresses the fit of the degradation curve in the same figure (In fact, no values will accommodate both the binding and the degradation data because, as noted earlier, these data violate mass conservation). It would also lead to a spurious, large accumulation of $L^a$ and to $L^I$ going through a maximum at moderate L in the fit to the step data from figure 6c.

either diffusion of receptors or their binding to coated pits is the controlling (i.e., significantly slower) process in $k_0$ and $k_0'$.

Ours is certainly not the first attempt to investigate this question. B. Goldstein and coworkers have examined the recycling of both coated pits[25] and of LDL receptors.[24 26 39] Our concern is only with the latter of these since we assume that the coated pit recycling is not dependent on the receptor recycling and provides a steady, time-independent surface coated pit concentration.

The Goldstein group begins by assuming that there is no need to distinguish between ligand-free receptors (R or $R^p$) and LDL-bound receptors ($L^a$ or $L^p$). Using data from the ligand-free system they fit the parameters for the models (in our notation) $R + [P] \underset{\leftarrow}{\overset{\rightarrow}{}} R^p \rightarrow 0$ or $R + [P] \underset{\leftarrow}{\overset{\rightarrow}{}} R^p \rightarrow R^i \rightarrow R$. In these models, "0" represents "outside of the system" and [P] represents the time-invariant surface-concentration of coated pits, a quantity that one can simply lump into the forward rate constant. Finally, assuming that the process $R \rightarrow R^p$ is diffusion controlled, i.e., that binding to coated pits is instantaneous upon arrival of a receptor at a coated pit, they construct and solve various diffusion models to relate the diffusivity to the rate parameter determined from the kinetic model. If the literature value of the diffusivity and the one calculated from this kinetic model are similar in magnitude, they conclude that diffusion control is not inconsistent with observation.

Unfortunately, even though they obtain their rate constant from an equilibrium measurement of $R^P/(R+R^P)$ on the ligand-free system, they use a literature value for the diffusivity for LDL-bound receptors[1,2] which assumes that $k_0=k_0'$ and is thus only consistent with the interpretation that Tank *et al.*'s (1985)[3] later results are electric-field induced artifacts. According to its simple interpretation, the diffusivity of ligand-free receptors ($D=1.2\times10^{-7}$ cm.$^2$/min.) is two orders of magnitude larger, and thus gives a value for the rate constant for $R\rightarrow R^P$ (under the assumption of instantaneous binding to coated pits) that is much larger than the kinetically determined value. A simple, back-of-the-envelope estimation can also show this: If the rate constant $k_0'$ is solely due to diffusion, then $k_0'\sim (1/\tau) \sim D/(\ell^2) = 1.2\times10^{-7}/(10^{-4})^2 \sim 12.05$/min. $>>$ .5, the kinetic value, where we take the characteristic length $\ell$ to be half the mean distance between coated pits. According to this interpretation, the simplest conclusion that one can draw is that binding to coated pits is not instantaneous relative to diffusion. A similar conclusion follows for $L^a$ independently of the interpretation of Tank *et al.*[3] if one accepts that $k_0<<k_0'$, as established in section III. Thus, even though the initial goal in reference[1] was only to show that diffusion limitation is not the cause of J.D.'s receptors' defect, one can also infer from their data that, possibly or likely, neither does diffusion limit free receptors becoming receptors in coated pits in normal cells.

Keizer, Ramirez and Peacock-Lopez (1985)[28] arrive at a similar conclusion, although they still do not distinguish between ligand-free and LDL-bound receptors. Rather, they use a non-equilibrium thermodynamic method to conclude that the system can be no more than "84% diffusion controlled." Unfortunately, aside from neglecting the distinction between ligand-free and LDL-bound receptors, Keizer *et al.*[28] begin their analysis with an equation (their equation (9)) that simultaneously contains a term modelling the *local* diffusion of receptors along the surface to a *particular coated pit* and another term where the surface is considered "well mixed" and represented by a *uniform* pit concentration $\rho_p$ (their notation). Unless the receptor concentration is almost uniform, i.e., unless the system is presumed *a priori* to be "reaction controlled," it is hard to understand this type of equation.

Below, we investigate the possibility that coated pit binding is not diffusion controlled. We present two types of models to relate the kinetically measured rate constants to the measured diffusivities and the not-measured rate constants for coated pit binding. The first type of model is for systems whose characteristic times (~1/k) are shorter than the mean lifetime of coated pits (~3-5 min.) such as the ligand-free receptor case ($1/k_0'$~1 min.). The second model, on the contrary, allows for systems with much longer characteristic times, such as the LDL-bound receptor system ($1/k_0$~50-100 min.). As such, unlike previous models, ours distinguish between LDL-bound and ligand-free receptors.

The first model attempts to account for the local diffusion of receptors in an annular-shaped region extending from the radius of a coated pit (s~.1 $\mu$M) to half the average distance between coated pits (b~1 $\mu$M), their binding to coated pits, their internalization and their recycling. Since the diffusion takes place over much longer length scales (~1 $\mu$M) than the characteristic coated pit size, we choose to treat the region exterior to the coated pits with partial differential equations, while treating the small pits themselves as "well mixed" regions, i.e., with ordinary differential equations.

The first model does, though, deliberately confuse certain local (in the sense of describing the processes surrounding a single coated pit) concepts with global (in the sense of an average over all coated pits on the entire membrane at any given time) concepts. In particular, even though it considers diffusion to a single coated pit and the internalization of receptors only after they have bound to the coated pit, the model itself does not allow the pit itself to disappear. The feeling is that if, as suggested by the above interpretation of the R data, diffusion turns out to be fast relative to binding to coated pits and relative to the lifetimes of coated pits, then there will be established a steady, almost uniform receptor concentration (and a steady diffusive flux of receptors to coated pits) that will not be appreciably affected by the internalization or formation of a *particular* coated pit. Thus one will effectively have a steady, almost homogeneous type model. The mixing of local and global concepts here is somewhat similar to the situation we critiqued earlier from Keizer *et al.*'s,[28] except that here the machinery needed to analyze the model is much simpler; the

present model also yields a self-consistent result that diffusion is by far the faster process.

Model I contains balances for receptors R not in coated pits, those ($R^W$) located in but not bound to coated pits and those ($R^P$) bound to coated pits, all in the same units of number/area, but where one defines R only on the annular region between r=s and r=b, and $R^W$ and $R^P$ only on the (homogeneous) region r<s. These balances contain rate parameters and geometric factors that account for random insertion of recycled receptors and for appropriate units corrections, as follows:

$$\frac{\partial R}{\partial t} = D\,\nabla^2 R + \left\{\frac{s^2}{(b^2-s^2)}\,\frac{(b^2-s^2)}{b^2}\right\} k_2 R^P$$

$$\frac{dR^W}{dt} = -\frac{2}{s}\,(-D\,\nabla R)\Big|_{r=s} - k' R^W + \left\{\frac{s^2}{b^2}\right\} k_2 R^P$$

$$\frac{dR^P}{dt} = k' R^W - k_2 R^P. \qquad (9)$$

Note that the binding constant k' is explicit in this formulation. The boundary and initial conditions, assuming circular symmetry, are continuity of R at the coated pit radius r=s ($R(r=s,t)=R^W(t)$), no flux at the outer radius r=b ($\frac{\partial R}{\partial r}(r=b,t)=0$) and an initially uniform receptor concentration ($R(r,t=0)$).

As noted above, one need now consider only the steady version of these equations (i.e., all time derivatives set to zero). One easily solves for R to within a constant $\eta$ (proportional to the total number of receptors) as

$$R(r) = \eta \left[ \frac{D\, b^2}{k' s^2} + \frac{b^2}{2} \ln (r/s) - \frac{1}{4} (r^2 - s^2) \right]. \qquad (10)$$

In order to relate the result of this model to the rate constant determined in section III, we compare this model to the lumped overall kinetic model (here we denote variables in the lumped model with a subscript $\ell$) $R_\ell \underset{\leftarrow}{\rightarrow} R_\ell^p$ in the absence of LDL. Recall that this model has forward rate constant $k_0'$ and reverse rate constant $k_2$, both determined in section III. To facilitate the comparison, we equate $R_\ell^p = (s^2/b^2)R^p$ and $\frac{dR_\ell^p}{dt} = (s^2/b^2)\frac{dR^p}{dt}$, which give, $k_0' R_\ell = (s^2/b^2)k' R^w$, where we set $R_\ell = \left\{ \int_s^b 2\pi r\, R(r)\, dr + \pi s^2 R^w \right\} / (\pi b^2)$. For $k_0' = 0.8$/min., numerical calculation gives a binding constant (including the supposed-time-invariant value of the coated pit binding site concentration) of $k' = 84$/min.

With values for $k'$ and for $D$ in hand, we would now like to determine, in some standard way, the per cent diffusion and per cent "reaction" (i.e., binding) control in $k_0'$. One such method is to consider the steady overall rate $k_0' R_\ell \pi b^2$ per coated pit of $R_\ell \rightarrow R_\ell^p$ as the steady rate of two first order processes in series, a diffusion $k_m (R_\ell - R^w) 2\pi s$ in terms of a mass transfer coefficient $k_m = D/\Lambda$ ($\Lambda$ ($s \leq \Lambda \leq b$), the only unknown, is an effective or average diffusion length which needs to be determined), followed by binding $k' R^w \pi s^2$. (Note that the relatively large value of $k'$

determined above is now multiplied by the small quantity $\pi s^2$.) It is well known that in such cases the rate constants act like capacitances in series, and add as follows:

$$(k_0')^{-1} = \left(\frac{2s}{b^2} k_m\right)^{-1} + \left(\frac{s^2}{b^2} k'\right)^{-1}. \qquad (11)$$

Solving (11) gives, $\Lambda = \frac{2s}{b^2} D\left(\frac{1}{k_0'} - \frac{b^2}{s^2 k'}\right) = 1.6s$ for $b = 10s = 1\mu$, and $k_m = .0077$ cm./min.; thus $k_0'$ is 95% and 5% reaction $\left(\frac{k_m}{(s/2)k' + k_m}\right)$ and diffusion $\left(\frac{(s/2)k'}{(s/2)k' + k_m}\right)$ controlled, respectively.

This brings us to the second model which, as noted earlier, is non-steady and of particular relevance when the processes of interest are not faster than the mean lifetime of the coated pits, e.g., the LDL-bound receptors. The model considers the unsteady diffusion through the annular region between r=s and r=b to a coated pit beginning at the time of the coated pit's emergence, together with the time-dependent binding of the (LDL-bound) receptors $L^a$ to the coated pits. Again, we take the pit itself to be homogeneous, the binding to coated pits not to be limited by the number of available pit binding sites and the receptor concentration to be continuous at r=s. In addition, in anticipation again of an either diffusion- or binding-limited situation, we assume that the receptor concentration $L^a(r=s)$ at,

but not yet bound to the coated pit very quickly reaches a quasi-steady value which only changes on the controlling time scale. Thus, the equations describing this model are:

$$\frac{\partial L^a}{\partial t} = D \nabla^2 L^a \qquad (12)$$

with boundary and initial conditions:

$$L^a(r, t=0) = L^a(0)$$

$$\frac{\partial L^a}{\partial r}(r=b,\ t) = 0$$

$$2\pi s\ D\ \nabla L^a(r=s, t>0) - \pi s^2\ k'' L^a(r=s, t>0) = 0. \qquad (13)$$

Using the orthogonality following from of the boundary/initial conditions, one can solve for $L^a(r,t)$ as

$$L^a(r,t) = \sum_{n=1}^{\infty} A_n\ U_0(\lambda_n r)\ e^{-\lambda_n^2 Dt}, \text{ where} \qquad (14)$$

$$A_n = \{L^a(0)(sh/(\lambda_n^2)U_0(\lambda_n s)\} \ /\ \{(s^2/2)[\frac{(4b^2/(s^2\pi^2)}{\lambda_n^2 b^2 Y_1^2(\lambda_n b)} -$$

$$(1+(h/\lambda_n)^2)U_0^2(\lambda_n s)]\}, \qquad (15)$$

$$h = sk''/(2D). \qquad (16)$$

The eigenvalues $\lambda_n$ and the functions $U_0$ and $U_1$ satisfy

$$U_1(\lambda_n s) = -\frac{h}{\lambda_n} U_0(\lambda_n s) \tag{17}$$

$$U_j(\lambda_n r) = J_j(\lambda_n r) - \frac{J_1(\lambda_n b)}{Y_1(\lambda_n b)} Y_j(\lambda_n r), \tag{18}$$

$J_j$ and $Y_j$ being the usual Bessel and Neumann functions of order j.

In order to compare this detailed model with the lumped kinetic model, we compare with the solution $L_\ell^a(\tau=0)e^{-k_0\tau}$ of the simple model equation $L_\ell^a \rightarrow L_\ell^p$ with rate constant $k_0$ for an imaginary pulse experiment beginning with a pulse of pure $L_\ell^a$. The comparison proceeds by presuming, as do Goldstein *et al.*,[24] that the overall membrane surface, whose LDL-bound receptor concentration $L_\ell^a$ describes, is comprised of a large number of coated pits, whose ages are exponentially distributed. In chemical engineering parlance, as far as coated pits are concerned, the surface is considered to be a steady state, continuous flow stirred tank reactor which has an exponential internal age distribution. The model above gives the state of a single coated pit system of age t whose uniform initial condition was $L^a(0)$. Thus, $L_\ell^a(\tau)$ at a lumped-model time $\tau$, an average of the local variable $L^a$ over the entire cell surface A at $\tau$, is equivalent to an average over the pit age distribution i(t) of the average of $L^a$ over the pit system of age t, i.e.,

$$L_\ell^a(\tau) = (A)^{-1}\int_A L^a(\underline{x};\tau;L_\ell^a(0))dA = \frac{1}{\pi b^2}\left\{ \int_0^\tau dt\ i(t) \left\{2\pi\int_s^b dr\ r\right.\right.$$

$$\left. L^a(r,t;L^a(0)-L_\ell^a(\tau-t)) + \pi s^2 L^a(s,t;L^a(0)-L_\ell^a(\tau-t))\right\} + \int_\tau^\infty dt\ i(t)$$

$$\left.\left\{2\pi\int_s^b dr\ r\ L^a(r,\tau;L^a(0)-L_\ell^a(0)) + \pi s^2 L^a(s,\tau;L^a(0)-L_\ell^a(0))\right\}\right\}. \quad (19)$$

One calculates the $L_\ell^a(\tau)$ curve in this way (using, say, the first 100 terms of $L^a$) and compares it with the simple solution of the lumped model to see, first, if the form of the lumped model is satisfactory and, second, to determine a value for k". It is a noteworthy advantage that this model compares an entire curve to determine the parameter of interest, rather than just a single value as in our previous model or other models where one compares based on a single number such as the mean capture time.

The result of this calculation is that k"~1.03/min. The procedure for dividing the rate constant into percentage diffusion and percentage binding control gives $k_r$=5.1x10$^{-6}$ cm./min. and $k_d$=1.8x10$^{-4}$ cm./min., or 97% binding controlled. It is worth noting that application of this dynamic model to the previous case of ligand-free receptors yields a result (95% binding control) almost indistinguishable from that of model (9).

## V. Discussion and Conclusions

Based on the fact the the surface-bound curve in figure 3 was not a simple exponential decay, coupled to the fact that its intermediate time value (~30-60 min.) coincided closely with the estimated value of the initial concentration of LDL-bound receptors not located in coated pits, we suggested that receptors not yet in coated pits that have already bound an LDL molecule have trouble becoming coated pit-bound. Actually, what we postulated, based on this and other data, was a major distinction between ligand-free receptors and those that have already bound LDL, the latter being (one to two orders of magnitude) slower in becoming coated pit-bound. At that point we could have asked whether experiments other than figure 3 (which model (1) fails to explain unless one postulates a non-specific binding four times that previously observed) also suggested that model (1) required such drastic modification. In fact, fitting schemes show that model (1), even with dissociation, can account for neither the steady step nor the unsteady step data (Figs. 6c and d) when required at the same time to give an internalization rate constant that is close to the well established (from studies of coated pit recycling) value of .25±.05/min.[6 24] (A fit to these data would require an internalization value more than a factor of three lower.) Even augmenting model (1) with dissociation and an exocytosis reaction ($k_{-2}$) does not account for the unsteady step data when required to give a reasonable value for the internalization constant. On the other hand, we could have suggested another possible modification to explain figure 3 that did include migration/binding to coated pits: That there was no difference in coated pit binding between LDL-bound and ligand-free receptors (i.e., $k_0$=$k_0'$), but that receptors already bound to

coated pits might also unbind. That is, the reactions $R \rightarrow R^p$ and $L^a \rightarrow L^p$ might be reversible. Let us call the reverse rate constant $k_{-0}$ and consider this possibility. The argument below is similar to one in [24].

From the steady state fraction of receptors located in coated pits in the absence of ligand, one obtains the steady state relation $(k_2+k_{-0})/k_0 = R/R^p \sim 1-.3$. Since $k_2 \sim .3/\text{min.}$, it follows that $k_0 \geq k_2 \sim .3/\text{min}$. Thus, in order for $L^a$ to remain appreciable beyond a couple of $(1/k_2)$ time units, as is the case in figure 3, $k_{-0}$ must also be of the same order of magnitude. Since $k_2$ will very quickly deplete $L^p$ and the interplay of large $k_0$ and $k_{-0}$ will quickly redistribute the $L^a$ between coated-pit bound and non-coated-pit-bound, the surface bound LDL will be forced to decay on $(1/k_2)$ time scales, thereby contradicting observation. Thus, this model cannot, in fact, explain figure 3. One can also see this mathematically, by simply solving the (in this case, linear) differential equations for this model applied to figure 3's experiment, but we omit the details here.

One might then suggest that one include the above-mentioned reverse reaction *in addition to* allowing for a distinction between the LDL-bound and ligand-free receptors. Since we are generally interested in a "minimal" description of the system, that is, one with a minimum number of reactions and, therefore, a minimum number of parameters to be harvested from the data, and since model II of the text seems to be quite accurate in describing an array of even qualitatively different experiments, we have

opted to only include the latter effect. Moreover, we are not aware of any independent experimental evidence to support the proposition that the unbinding is appreciable in receptor-normal individuals. Finally, unbinding does not seem to happen in bovine smooth muscle cells,[20] as we shall note below.

Another point of interest is the distinction between the experiments done on bovine smooth muscle cells and those done on human fibroblasts. First, the binding constants from these experiments seem to differ by a factor of 2-5, apparently a model-independent result.[8] Also as noted in the text, model I describes the former well, yet cannot describe figure 3. In fact, analysis of the bovine data using model II instead of model I gives similar values for many of the parameters determined in the human fibroblast case, *except for* $k_0$ *and* $k_0'$ *which turn out to be significantly larger than all other bovine rate constants* and much larger than the corresponding constants for human fibroblasts. That is, model II reduces to model I for these data, a satisfying result. (Similarly, preliminary calculations suggest that model III reduces to model II based on the human fibroblast data, which is consistent with the observation of a negligible inventory of receptors within the cell.) The question remains, however, why is there such a difference between these two cell types? Pure speculation based on results suggesting[50] that the maximum number of LDL receptors that bovine smooth

8. At steady state, the rates of binding and degradation are equal. Comparison of $k_1$ for the two cell types obtained from actual binding and degradation rates at, say, LDL=50μg/ml, and from the maximal binding as LDL gets large (corresponding to the total number of receptors) yields this factor (cf., [11] [17]).

muscle cells express is far fewer (in LPDS: sparse - 55; confluent - 43.2 ng LDL/mg cell protein; the # cells/mg cell protein for SMCs ($1.5x10^5$)[17] and for fibroblasts ($1.9x10^5$)[61] are comparable) than one routinely finds in fibroblasts (~200).[6 9 49] Thus, their receptor recycling may be more efficient: If surface diffusion is really slow then smooth muscle cells might recycle receptors preferentially close to coated pits rather than randomly; if diffusion is fast, then they might recycle them directly bound to coated pits.

While on the subject of random or non-random insertion[52] of recycled receptors, we mention an interesting result. Throughout this paper we have made the random insertion hypothesis. Based on this we initially calculated the rate constants from data from the three canonical types of experiments and listed them in table 1. We found it remarkable that although the experiments were quite different from one another, the rate constants turned out to be very similar. Yet, there was some variation. If, instead, one introduces a new parameter $\alpha$ to account for possible non-random insertion ($\alpha$ = fraction of receptors that recycle to non-coated pit regions) in the lumped model II and includes it in the list of parameters to be fit by the regression on, say, the steady state data, then the resulting parameters ($k_1$~.0056, $k_2$~.32, $k_3$~.01, $k_0$~.03, $k_0'$~.3, $R^p(0)/R(0)$~ 160/40, $\alpha$=.41), all with the same units as in table 1) yield a prediction for the unsteady step and pulse experiments that is *as good as the best fit values for those experiments*! Predictions for the experimental data in figures 7 is similarly excellent. Even though this new

procedure introduces a new parameter into the calculation, its ability to unify the data is striking.

Finally, it is worth commenting on the magnitudes of a characteristic time determined in our analysis. First, the characteristic times from $k_0$ and $k_0'$ are order 50 minutes and order 1 minute, respectively. One might ask, if the half-life of a coated pit is only 3-5 minutes, then how do ligand-bound receptors ever get internalized? The scenario that suggests itself is based on the fact that LDL-binding is also relatively slow at moderate LDL concentrations. Thus, most receptors bind to coated pits before they bind their LDL; they then bind LDL during the time remaining before coated pit invagination. The few receptors that bind ligand before attaching to coated pits then provide a more slowly-depleted reserve of LDL on the cell's surface, possibly to continue providing exogenous LDL during brief periods when the lumen LDL concentration drops. Lest one, however, doubt the significance of migration, varying $k_0$ with all other rate constants fixed drastically varies the ratio of bound to (the sum of) internalized and degraded LDL.

Table 1: Summary of Best-Fit Parameter Values by Least Squares

| Process | Rate Constant | Pulse-Unsteady | Step-Unsteady | Step-Steady |
|---|---|---|---|---|
| Migration of $L^a$ | $k_0$ | 0.01/min | 0.029/min | 0.03/min |
| Migration of R | $k_0'$ | 0.34-1.36/min | .49/min | 2.1/min |
| Binding of $L+R^{(p)}$ | $k_1$ | n/a | $.004\frac{(ml/\mu g)}{min}$ | $0.002\frac{(ml/\mu g)}{min}$ |
| Internalization | $k_2$ | 0.33/min | 0.33/min | 1.0/min |
| Degradation | $k_3$ | 0.018/min | 0.0095/min | 0.011/min |

Table 2: Error Analysis of Rate Constants from Table 1

Sensitivity of Error Function F to 10% Shift in Rate Constant ($\frac{\delta F/F}{\delta k/k}$; $\delta k/k = .1$)

| Fitted Quantity | Step-Unsteady | Step-Steady | Pulse-Unsteady |
|---|---|---|---|
| $k_0$ | 5.7 | 5.3 | 0.10 |
| $k_0'$ | 3.2 | 2.3 | n/a |
| $k_1$ | 8.1 | 1.4 | n/a |
| $k_2$ | 0.66 | 3.4 | 1.3 |
| $k_3$ | 6.6 | 7.8 | 1.5 |
| $R^t$ (total)* | 9.1 ($239\frac{\mu g}{mg}$) | 4.5 ($219\frac{\mu g}{mg}$) | n/a |
| $R^p(t=0)$* | max ($.7R^t$) | 0.21 (110) | n/a |
| $L^i(t=0)$* | n/a | n/a | max (10ng/mg) |
| $L^a(t=0)$* | n/a | n/a | 0.54 (10.9ng/mg) |
| $L^p(t=0)$* | n/a | n/a | 1.5 (33.3ng/mg) |

*: Fitted value in parentheses; "max" denotes maximum of input search range.

## Figures

Descriptions of experimental procedures are taken essentially verbatim from the original papers of M.S. Brown and J.L. Goldstein.

**Fig. 1**[110]: Overall pathway of exogenous and endogenous fat-transport

**Fig. 2**[110]: Cellular LDL-uptake pathway

**Fig. 3**[6 11]: Internalization and degradation at 37° C of $^{125}$I-LDL previously bound to the LDL receptor at 4°C in normal human fibroblasts: Cells were incubated in growth medium containing 10% lipoprotein-deficient serum for 48 hr prior to the experiment. On day 7 of cell growth, each dish received 2 ml of ice-cold medium containing 10 μg of protein per ml of $^{125}$I-LDL (169 cpm/ng). The $^{125}$I-LDL was allowed to bind to the cells at 4°C for 2 hr, after which each monolayer was washed extensively. Each dish then received 2 ml of warm medium containing 10 mg of protein per ml of unlabeled LDL, and all the dishes were incubated at 37°C. After the indicated time at 37°C, groups of dishes were rapidly chilled to 4°C, the medium was removed, and its content of $^{125}$I-labeled trichloroacetic acid-soluble material [degraded] was measured. The amounts of surface-bound (heparin-releasable) $^{125}$I-LDL (bound) and internalized (heparin-resistant) $^{125}$I-LDL that remained associated with the cells were also determined. Each value represents the average of duplicate incubations.

**Fig. 4a**[11]: Cell surface binding (shown), internalization, degradation of $^{125}$I-LDL at 37°C as a function of $^{125}$I-LDL concentration in normal fibroblasts: On day 7 of cell growth, each monolayer received 2 ml of medium containing the indicated concentration of $^{125}$I-LDL (37 cpm/ng). After incubation for 5 hrs at 37°C, the medium was removed and its content of $^{125}$I labeled trichloroacetic acid soluble material [degraded] was measured. The cell monolayers were then washed by the standard procedure and the amounts of heparin-releasable [bound] and heparin-resistant [internalized] $^{125}$I-LDL were determined. Each value represents the average of duplicate incubations.

Figure represents the bound LDL at steady state incorporating best fit values for the rate constants, used in model (2). The curve's asymptote represents the total number of receptors.

**Fig. 4b**[11]: Unsteady kinetics of $^{125}$I-LDL in normal human fibroblast: On day 7 of cell growth, monolayers of cells were placed for 30 mins in incubators (without $CO_2$) adjusted to 37°C.

The growth medium was then removed and replaced with 2 ml of medium containing 10 mg protein per ml of $^{125}$I-LDL (124 cpm/ng) that had been adjusted to the appropriate temperature. After the indicated interval, the medium was removed and replaced with ice-cold wash buffer and the cell monolayers were placed on an ice-cold surface. The medium was saved for measurement of its content of $^{125}$I-labeled trichloroacetic acid soluble material (degraded-not shown). The chilled cell monolayers were washed in

a 4°C room by the standard procedure and the amounts of heparin-releasable (bound) and heparin-resistant (internalized-not shown) $^{125}$I-LDL were determined. Each value represents the average of duplicate incubations.

Figure includes curve incorporating best fit values used in model (2).

**Figs. 5a & 5b**[11]: a. Unsteady binding kinetics for J.D. cells: On day 7 of cell growth, each dish received 2 ml of ice-cold medium containing 10 mg protein per ml of $^{125}$I-LDL (169 cpm/ng). The $^{125}$I-LDL was allowed to bind to the cells at 4°C for 2 hr. Remainder of procedure was same as in Fig. 3. Figure includes curve for the model $L^a \rightarrow L + R$ , together with the best fit value (0.008/min) for its rate constant.

b. Steady binding kinetics for J.D. cells: Experimental procedure was the same as in Fig. 4a. Figure includes curve for model $L+R \underset{\leftarrow}{\overset{\rightarrow}{}} L^a$ with reverse rate constant from Fig. 5a and best fit forward rate constant (0.001/(min($\mu$g/ml))). Best fit receptor total was 160 ng/mg protein.

**Fig. 6**: a.[6] Experiment same as Fig. 3. Data adjusted for non-specific binding as described in text. Figure includes curves generated from model (2) with best fit parameters (table 1, column 1 and table 2, column 3). Best fit value of $L^P/(L^a+L^P)(t=0)$ was .74.

b.[6] The plots in log scale of Fig. 6a.

c.[11] Experimental procedure same as Fig. 4b. Figure includes curves generated from model (2) with best fit parameters (table 1, column 2). Data were adjusted for non-specific internalization and degradation by subtraction of values for JD from same experiment. Best fit receptor total and $R^P/(R+R^P)(t=0)$ were 239 ng/mg and 0.7. Inset: Binding curve on an expanded scale.

d.[11] Experimental procedure same as Fig. 4a. Figure includes curves generated from model (2) with best fit parameters (table 1, column 3). Data adjusted for non-specific internalization and degradation as in 6c. Best fit receptor total and $R^P/(R+R^P)(t=0)$ (needed for calculation of degradation) were 219 ng/mg and 0.5.

**Fig. 7a**[47]: Prediction: Nonconfluent normal monolayers were prepared and incubated for 48 hrs in medium containing lipoprotein-deficient serum (LPDS). On day 7, the medium in each dish was replaced with 2 ml of medium that contained 5% lipoprotein deficient serum & 10 mg protein /ml of $^{125}$I-LDL (124 cpm/ng). Figure includes curves predicted from model (2) together with parameters from table 1, column 2. Data not adjusted for non-specific processes. Receptor total (to scale curve) and $R^P/(R+R^P)(t=0)$ used were 264 ng/mg and 0.7.

**Fig. 7b**[4]: Prediction: The normal cells were grown under standard conditions except that the growth medium was switched to 5% human LPDS on Day 5. After 48 hrs in LPDS (Day 7), cell monolayers received 2 ml growth medium containing 5% human LPDS and 10 mg of protein/ml of $^{125}$I-LDL (116 cpm/ng of protein). After incubation at 37°C for the indicated time, the amounts of cellular

binding and proteolytic degradation of the $^{125}$I-LDL were determined under typical experimental procedure. Figure includes curves predicted from model (2) together with parameters from table 1, column 2. Data not adjusted for non-specific processes. Receptor total (to scale curves) and $R^P/(R+R^P)(t=0)$ used were 432 ng/mg and 0.7.

**Fig. 7c**[6]: Prediction: Experimental procedure was similar to Fig. 6d. Figure includes curves predicted from model (2) together with parameters from table 1, column 3. Data were adjusted for nonspecific processes by deducting the values shown by F.H. homozygote cells in same experiment. Receptor total (to scale curves) and $R^P/(R+R^P)(t=0)$ (needed for calculation of degradation) used were 280 ng/mg and 0.5. Inset shows binding curve on an expanded scale.

**Fig. 7d**[37]: Prediction: On day 7, each dish received 2 ml of medium containing 10 mg of $^{125}$I-LDL (441 cpm/ng). After incubation for the indicated time, each monolayer was washed by the standard technique, after which 2 ml of medium containing 10 mg/ml of heparin were added to each dish. The dishes were then incubated at 4°C for 60 min, after which the heparin-containing medium was removed and an aliquot was counted to determine the amount of heparin-releasable $^{125}$I radioactivity. The cells were dissolved in NAOH, and an aliquot was counted to determine the amount of $^{125}$I-LDL remaining bound to the cells after heparin treatment. The total cellular binding of $^{125}$I-LDL represents the sum of the heparin releasable radioactivity and the radioactivity remaining in the dish. Figure includes curves predicted from model (2) together with parameters from table 1, column 2. Data were adjusted for nonspecific processes by deducting the values shown by F.H. homozygote cells in same experiment. Receptor total (to scale curves) and $R^P/(R+R^P)(t=0)$ used were 240 ng/mg and 0.7.

**Figs. 7e & f**[53]: Prediction: Cells from one normal subject were plated (day 0) into 94 petri dishes (60 mm) at the concentration of 1x10 cells/dish in 3 ml of growth medium containing 10% fetal calf serum. On day 7, monolayer was washed with 3 ml of PBS, after which 2 ml of fresh growth medium containing 5% LPDS (2.5 mg protein/ml) was added. After 24 hrs (day 8), the medium was replaced with 2 ml fresh medium containing 5% LPDS and $^{125}$I-LDL (120 cpm/ng protein) at a concentration of either 5 mg protein/ml (Fig. 7f) or 25 mg protein/ml (Fig. 7e). [To correct for nonspecific processes,] high affinity $^{125}$I-LDL binding [plus internalization] and degradation were calculated by subtracting the amount of radioactivity bound or degraded in the presence of 395 μg protein/ml of unlabeled LDL from that bound or degraded in its absence. Figure includes curves predicted from model (2) together with parameters from table 1, column 2. Receptor total (to scale curves) and $R^P/(R+R^P)(t=0)$ used were 256 ng/mg and 0.7.

**Fig. 7g**[11]: Prediction: Experimental procedure was the same as in Fig. 4b. Figure includes the curve for model $L+R \rightleftarrows L^a$ with rate constants taken from Fig. 5. Receptor total (to scale curves) used were 160.

**Fig. 8a,b,c:** Sensitivity of model-generated curves (fig. 6) to a 10% increase in the best fit values of $k_0$ from table 1 for pulse unsteady (a) and (b), step unsteady (c) and step steady (d) experiments. The plots for bound ($L^b-L^a+L^p$), internalized ($L^i$) and degraded ($L^d$) LDL show, e.g., $(\delta L^b/L^b)/(\delta k_0/k_0)$, with $\delta k_0/k_0=.1$, after[15], as explained in the text.

# Fig. 1

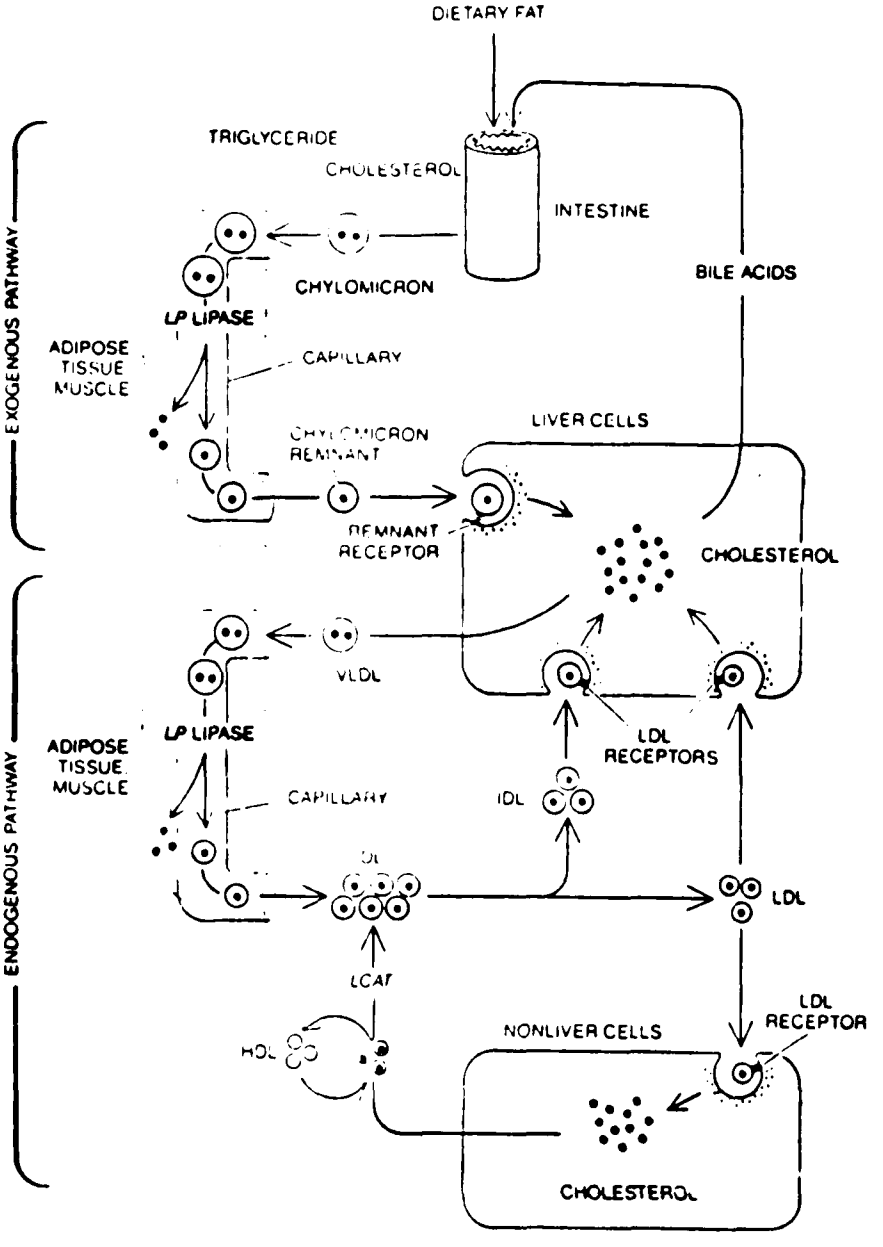
DIETARY FAT
TRIGLYCERIDE
CHOLESTEROL
INTESTINE
BILE ACIDS
CHYLOMICRON
LP LIPASE
ADIPOSE TISSUE MUSCLE
CAPILLARY
LIVER CELLS
CHYLOMICRON REMNANT
REMNANT RECEPTOR
CHOLESTEROL
EXOGENOUS PATHWAY
VLDL
LP LIPASE
ADIPOSE TISSUE MUSCLE
LDL RECEPTORS
CAPILLARY
IDL
LDL
LCAT
HDL
NONLIVER CELLS
LDL RECEPTOR
CHOLESTEROL
ENDOGENOUS PATHWAY

# Fig. 2

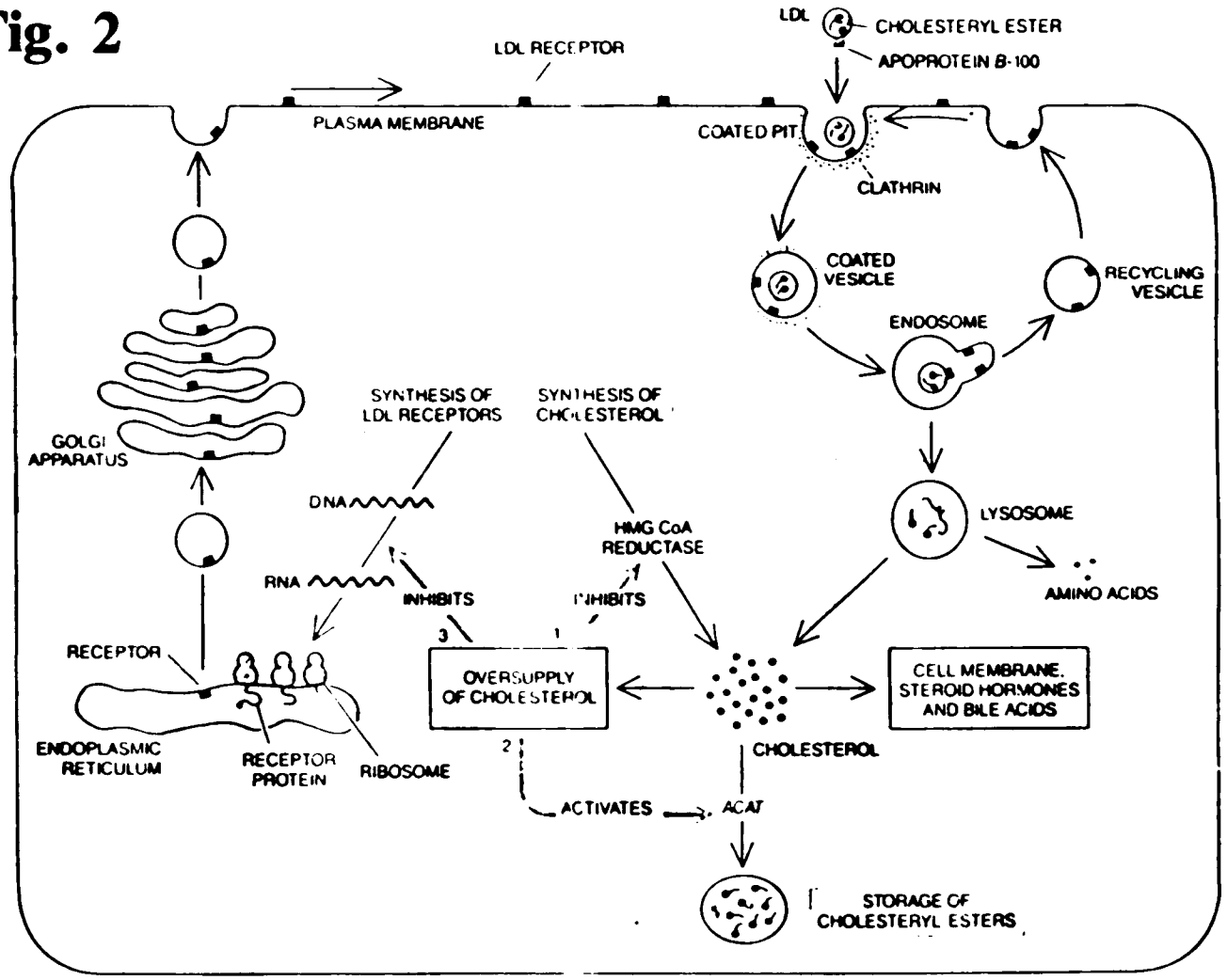
LDL
CHOLESTERYL ESTER
APOPROTEIN B-100
LDL RECEPTOR
PLASMA MEMBRANE
COATED PIT
CLATHRIN
COATED VESICLE
RECYCLING VESICLE
ENDOSOME
LYSOSOME
AMINO ACIDS
GOLGI APPARATUS
SYNTHESIS OF LDL RECEPTORS
SYNTHESIS OF CHOLESTEROL
DNA
RNA
INHIBITS
HMG CoA REDUCTASE
INHIBITS
RECEPTOR
ENDOPLASMIC RETICULUM
RECEPTOR PROTEIN
RIBOSOME
OVERSUPPLY OF CHOLESTEROL
CELL MEMBRANE, STEROID HORMONES AND BILE ACIDS
CHOLESTEROL
ACTIVATES
ACAT
STORAGE OF CHOLESTERYL ESTERS

# Fig. 3

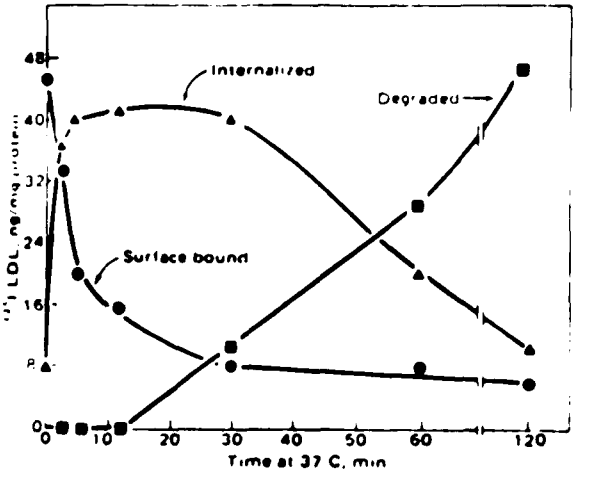
Internalized
Degraded
Surface bound
48
40
32
24
16
8
0
0
10
20
30
40
50
60
120
Time at 37 C, min

**Fig. 4a**

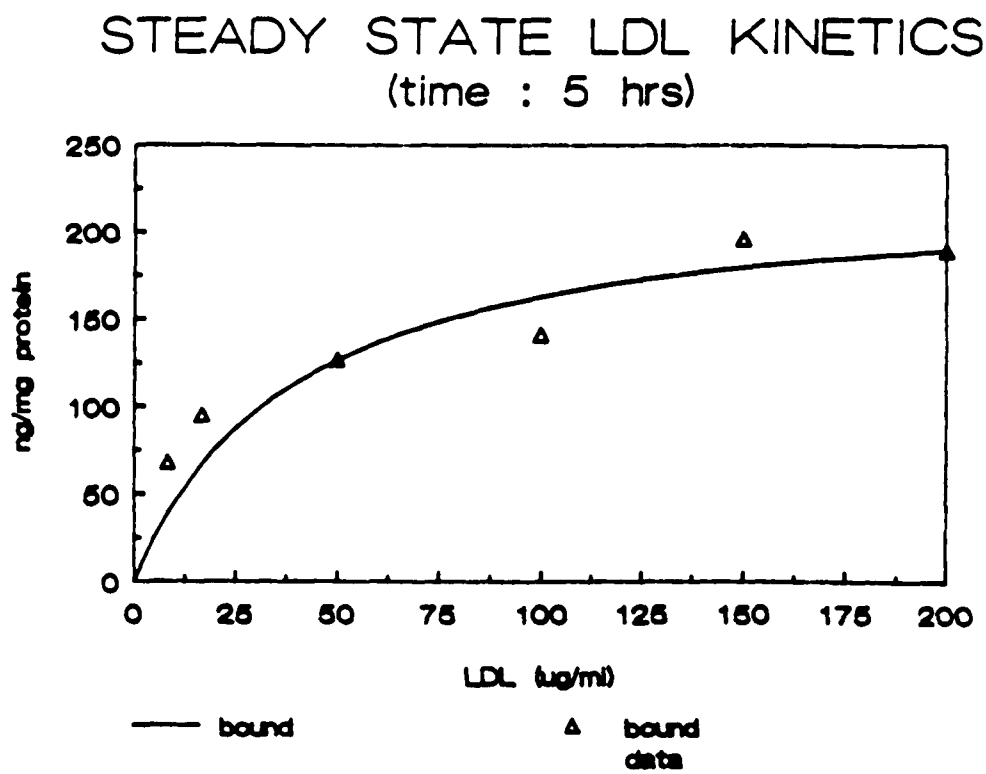
STEADY STATE LDL KINETICS
(time : 5 hrs)
250
200
150
100
50
0
ng/mg protein
0
25
50
75
100
125
150
175
200
LDL (ug/ml)
bound
bound data

**Fig. 4b**

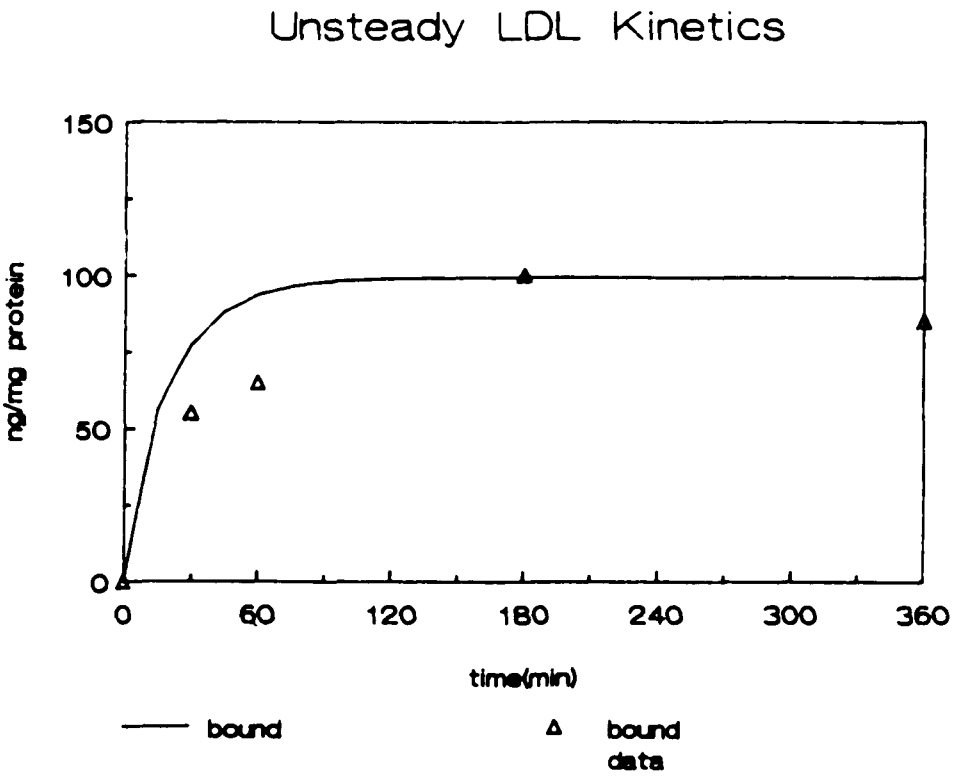
Unsteady LDL Kinetics
150
100
50
0
ng/mg protein
0
60
120
180
240
300
360
time(min)
bound
bound data

**Fig. 5a**

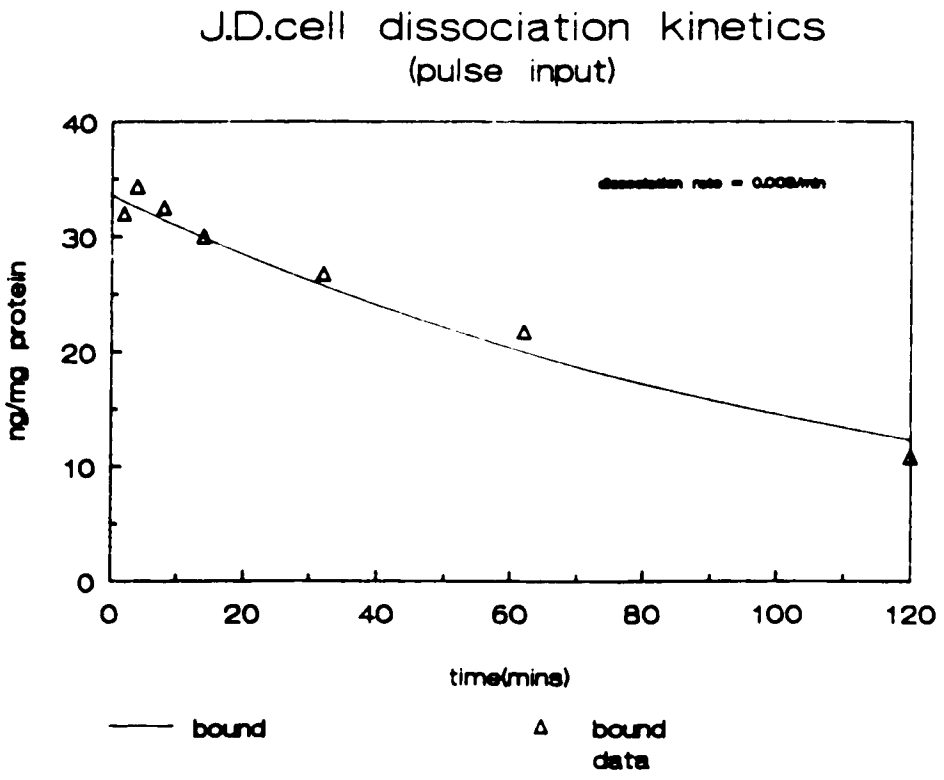
J.D.cell dissociation kinetics
(pulse input)
dissociation rate = 0.008/min
ng/mg protein
40
30
20
10
0
0
20
40
60
80
100
120
time(mins)
bound
bound data

**Fig. 5b**

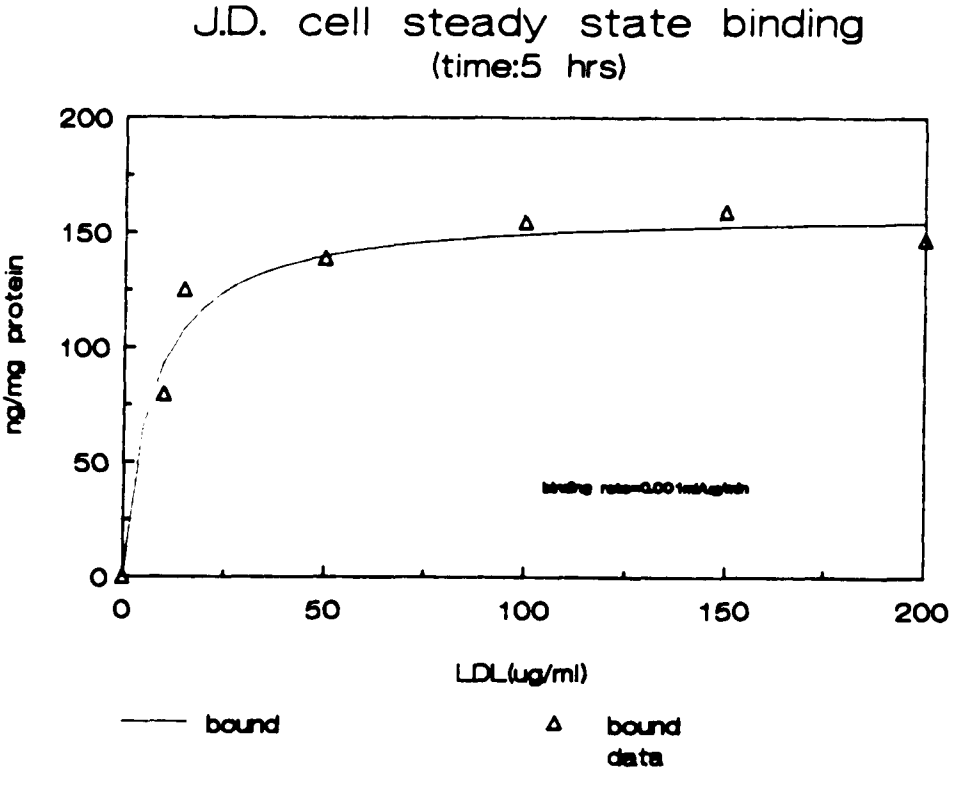
J.D. cell steady state binding
(time:5 hrs)
200
150
100
50
0
ng/mg protein
0
50
100
150
200
LDL(ug/ml)
bound
bound data

**Fig. 6a**

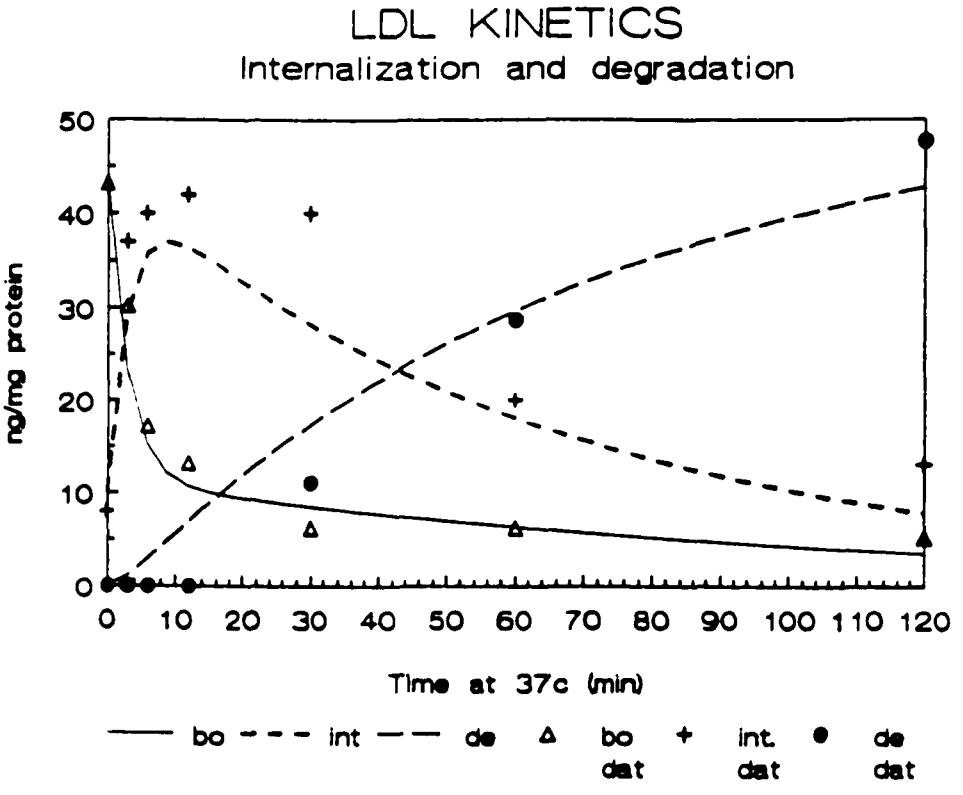
LDL KINETICS
Internalization and degradation
ng/mg protein
50
40
30
20
10
0
0 10 20 30 40 50 60 70 80 90 100 110 120
Time at 37c (min)
bo
int
de
bo dat
int. dat
de dat

# Fig. 6b

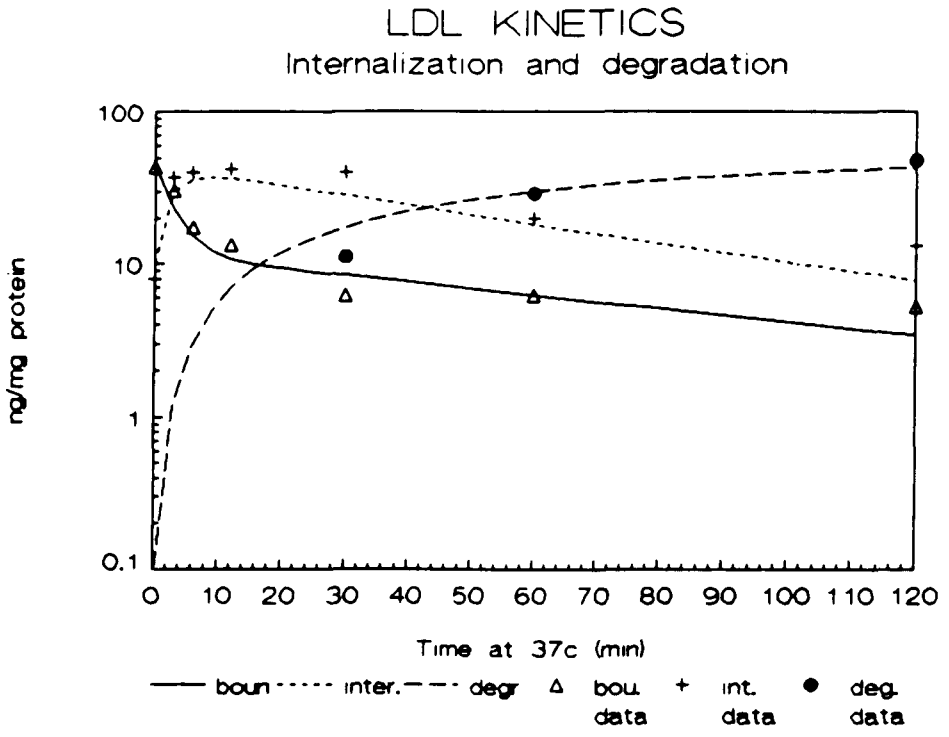
LDL KINETICS
Internalization and degradation
100
10
1
0.1
ng/mg protein
0 10 20 30 40 50 60 70 80 90 100 110 120
Time at 37c (min)
boun
inter.
degr
bou. data
int. data
deg. data

**Fig. 6c**

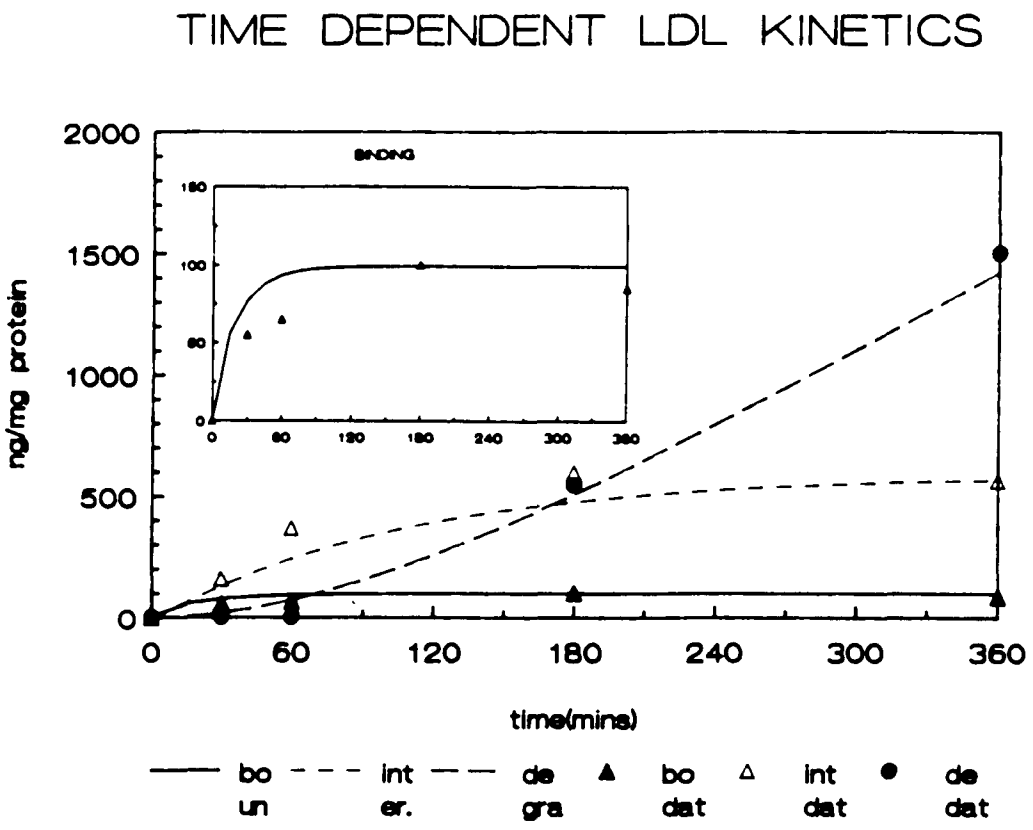
TIME DEPENDENT LDL KINETICS
2000
1500
1000
500
0
ng/mg protein
0
60
120
180
240
300
360
time(mins)
BINDING
bo un
int er.
de gra
bo dat
int dat
de dat

**Fig. 6d**

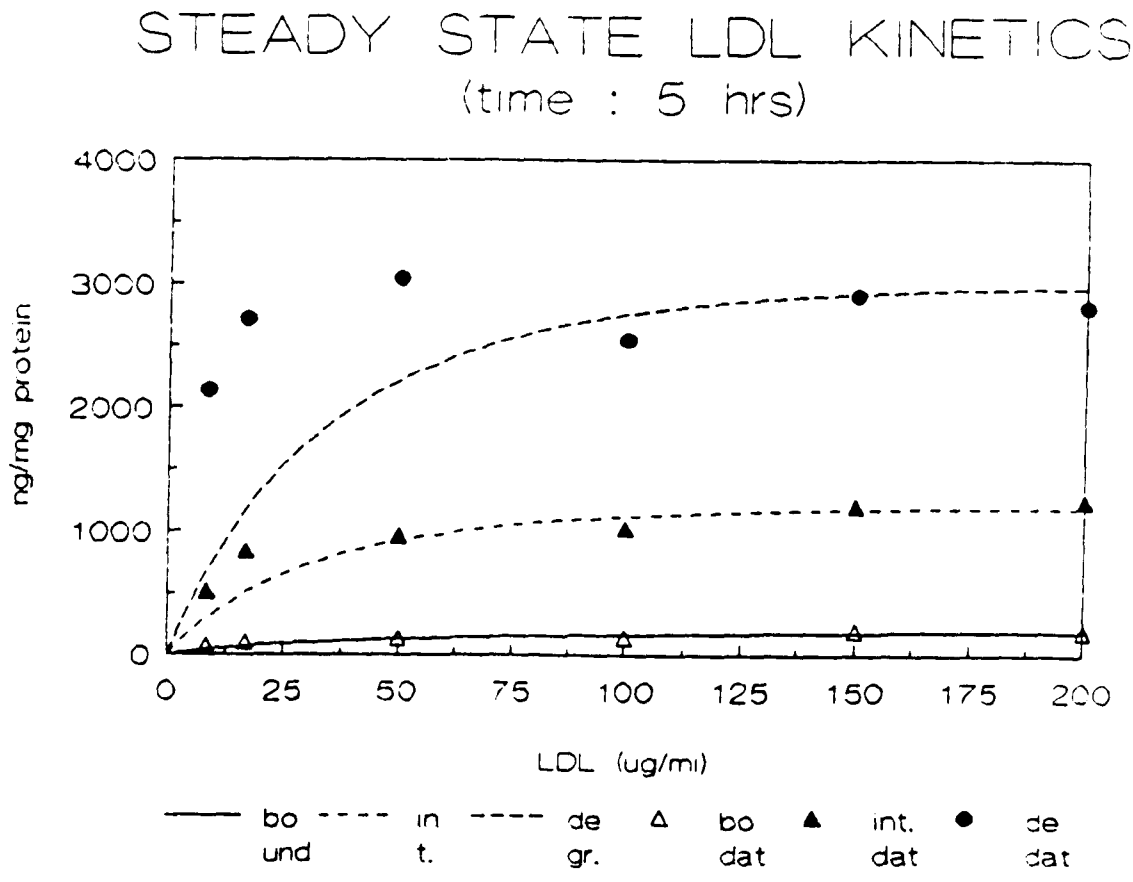
STEADY STATE LDL KINETICS
(time : 5 hrs)
4000
3000
2000
1000
0
ng/mg protein
0
25
50
75
100
125
150
175
200
LDL (ug/ml)
bo und
in t.
de gr.
bo dat
int. dat
de dat

**Fig. 7a**

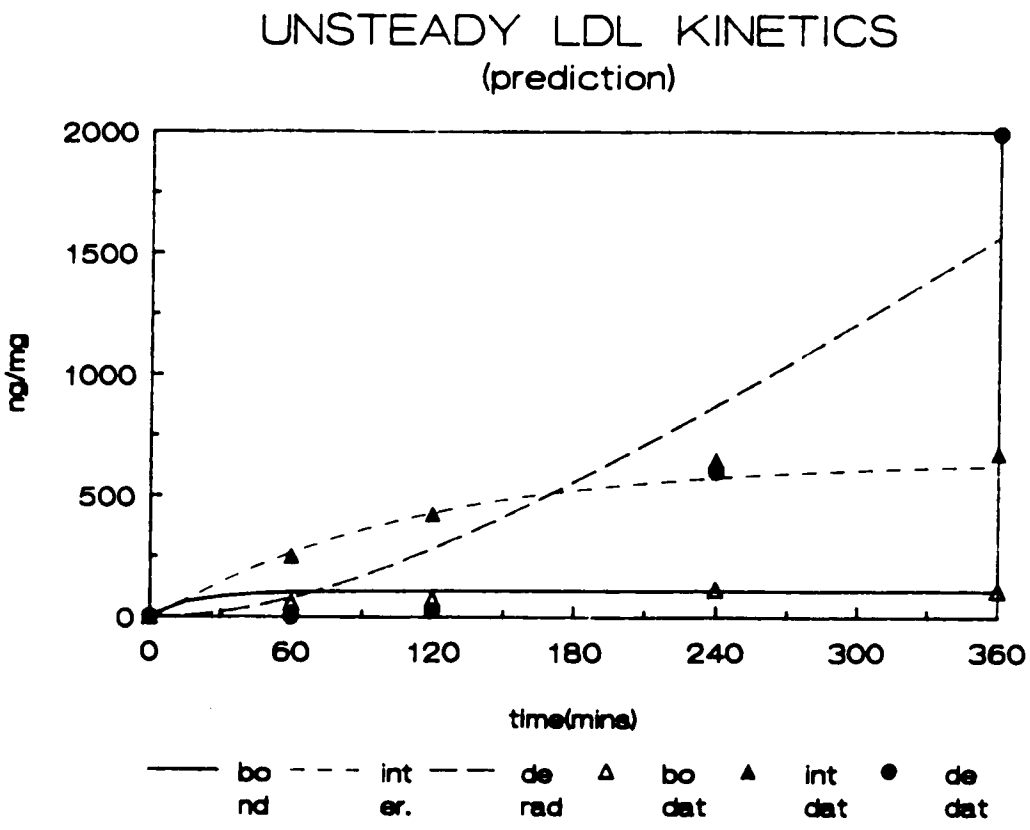
UNSTEADY LDL KINETICS
(prediction)
2000
1500
1000
500
0
ng/mg
0
60
120
180
240
300
360
time(mins)
bo nd
int er.
de rad
bo dat
int dat
de dat

**Fig. 7b**

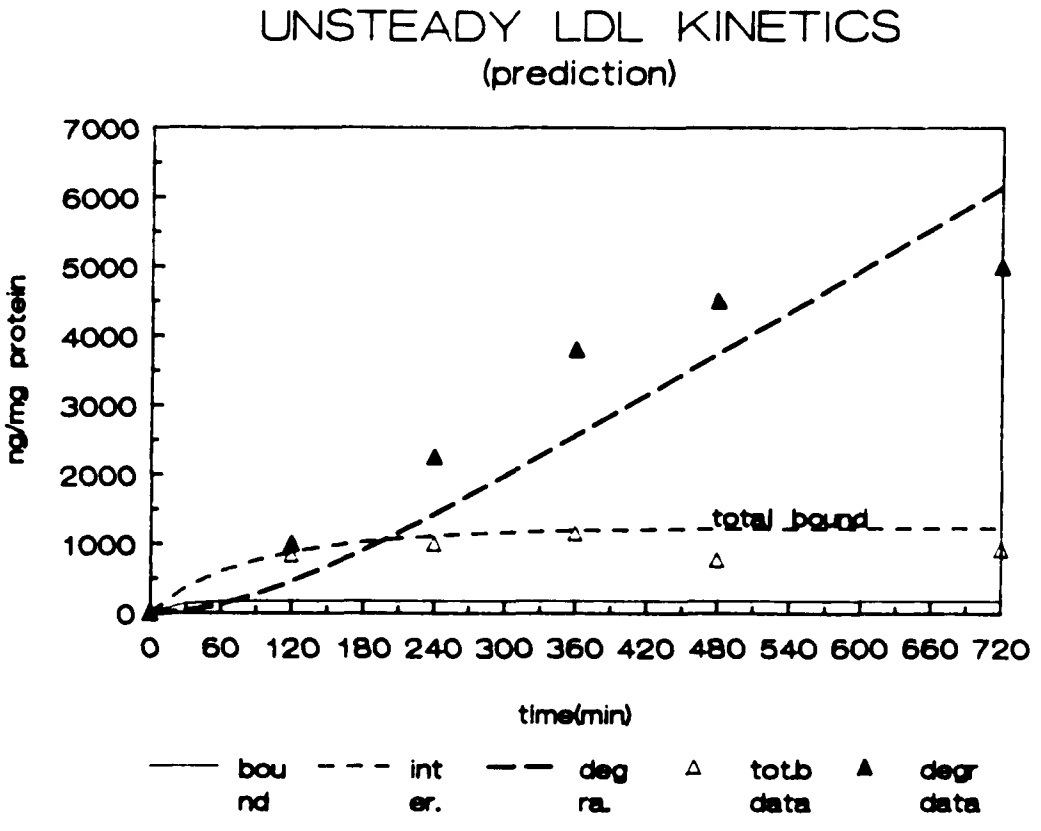
UNSTEADY LDL KINETICS
(prediction)
ng/mg protein
7000
6000
5000
4000
3000
2000
1000
0
0 60 120 180 240 300 360 420 480 540 600 660 720
time(min)
total bound
bound
interer.
degra.
totb data
degr data

**Fig. 7c**

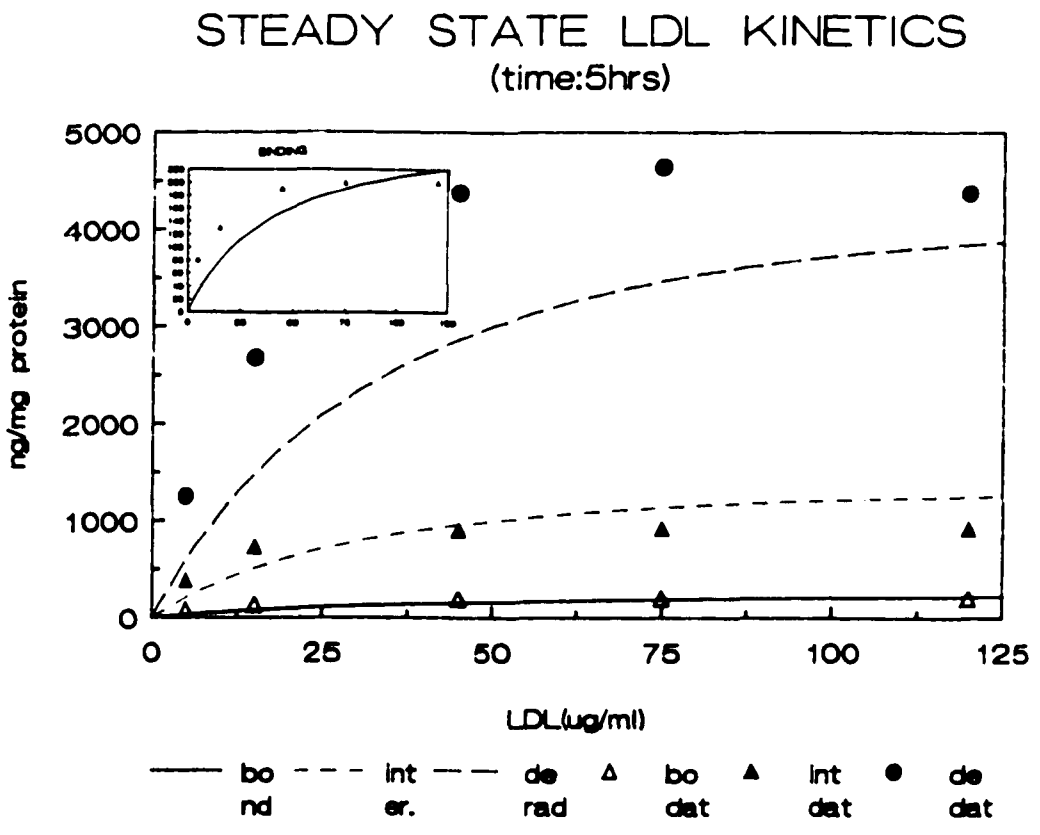
STEADY STATE LDL KINETICS
(time:5hrs)
ng/mg protein
5000
4000
3000
2000
1000
0
0
25
50
75
100
125
LDL(ug/ml)
bo nd
int er.
de rad
bo dat
int dat
de dat

# Fig. 7d

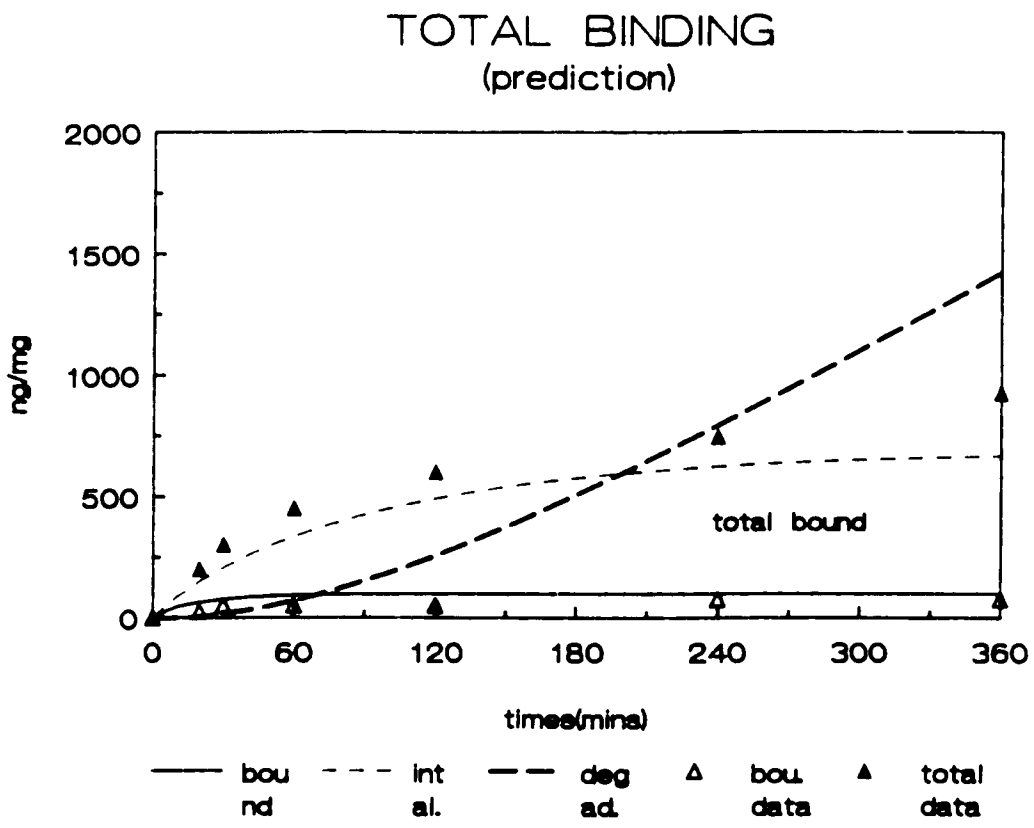
TOTAL BINDING
(prediction)
2000
1500
1000
500
0
ng/mg
total bound
0
60
120
180
240
300
360
times(mins)
bou nd
int al.
deg ad.
bou data
total data

# Fig. 7e

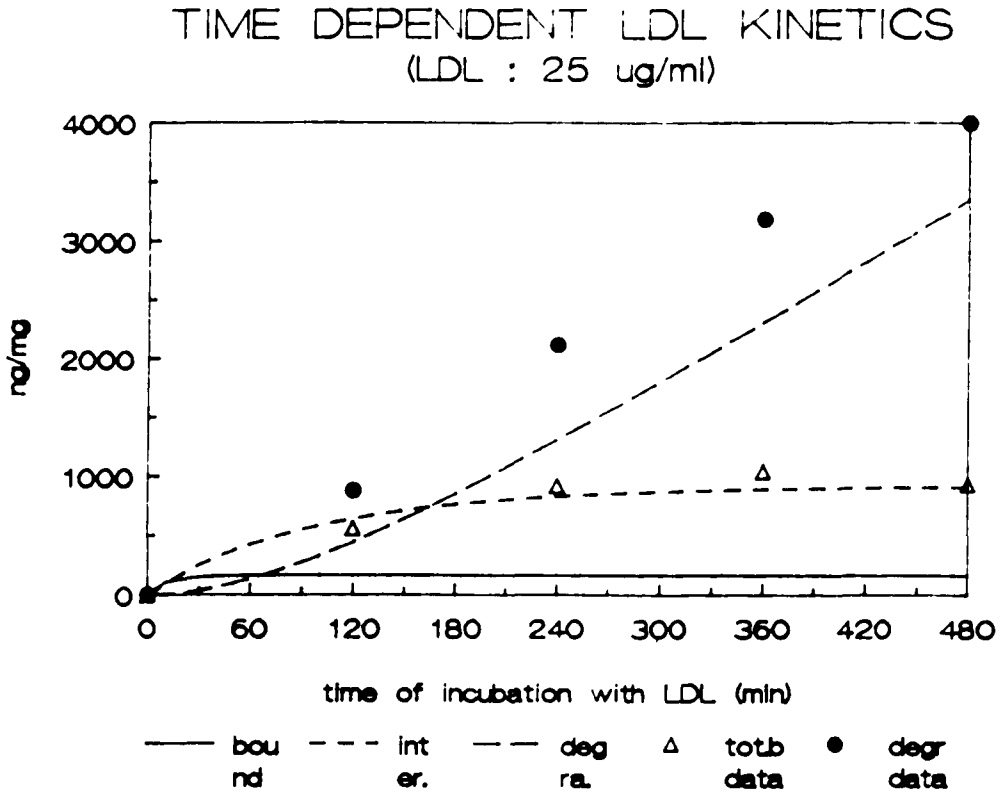
TIME DEPENDENT LDL KINETICS
(LDL : 25 ug/ml)
4000
3000
2000
1000
0
ng/mg
0
60
120
180
240
300
360
420
480
time of incubation with LDL (min)
bou nd
int er.
deg ra.
totb data
degr data

**Fig. 7f**

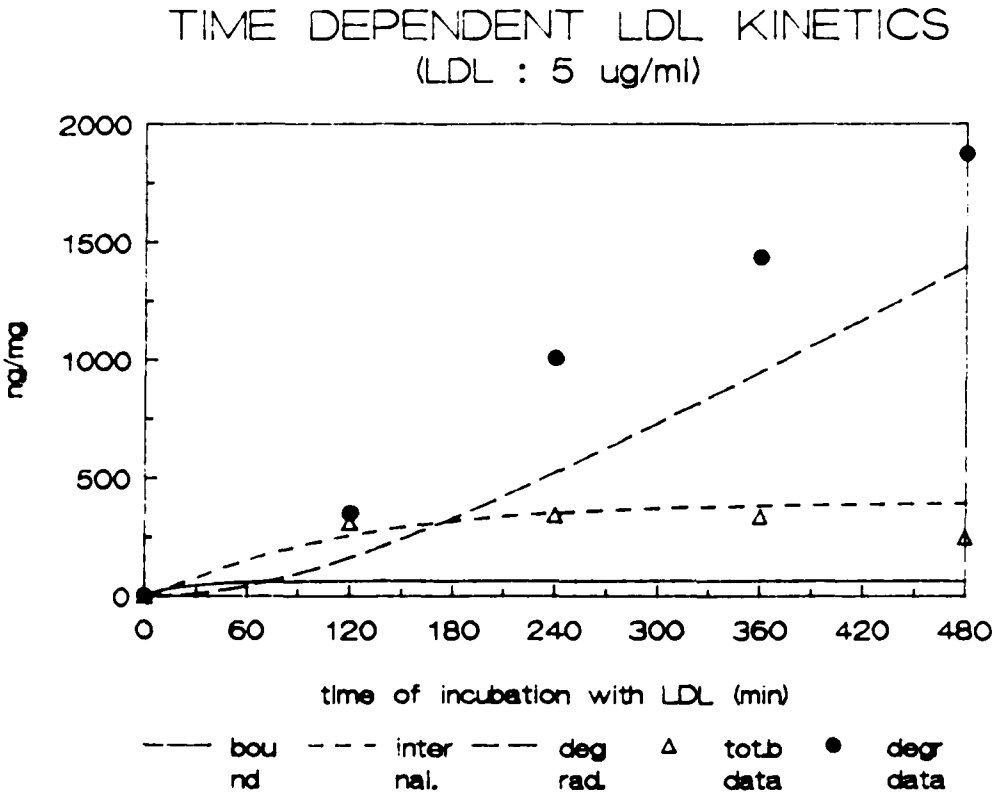
TIME DEPENDENT LDL KINETICS
(LDL : 5 ug/ml)
2000
1500
1000
500
0
ng/mg
0
60
120
180
240
300
360
420
480
time of incubation with LDL (min)
bound
internal.
degrad.
totb data
degr data

# Fig. 7g

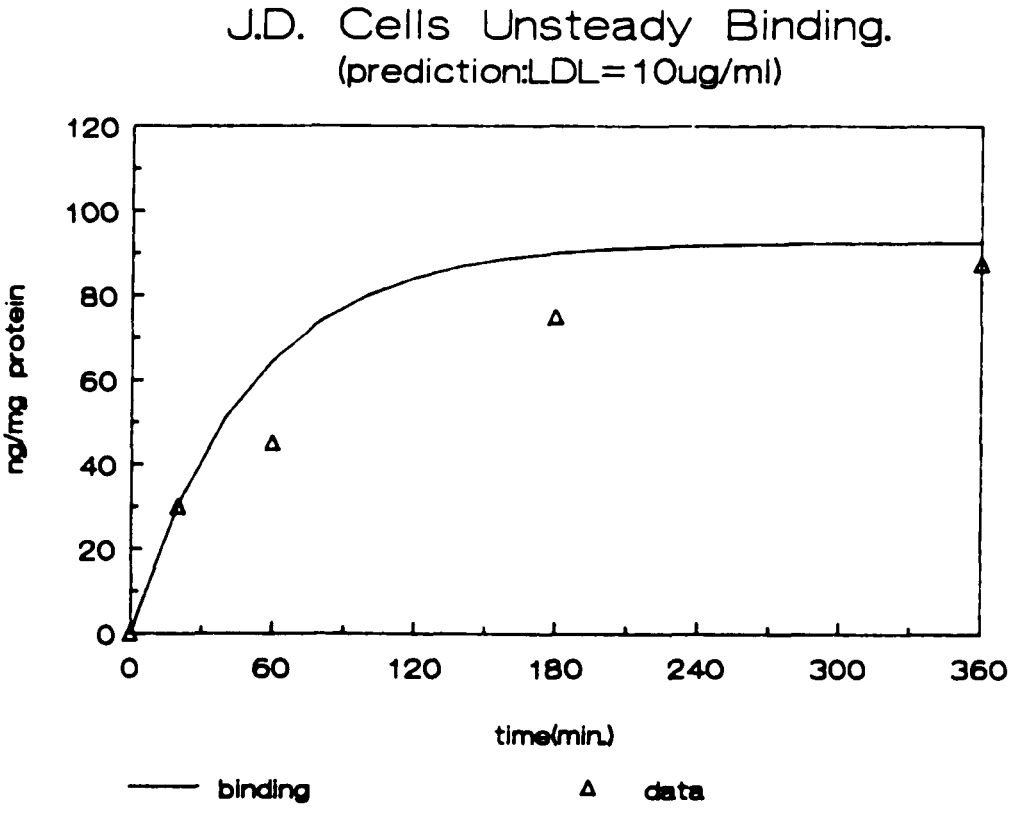
J.D. Cells Unsteady Binding.
(prediction:LDL=10ug/ml)
ng/mg protein
120
100
80
60
40
20
0
0
60
120
180
240
300
360
time(min.)
binding
data

**Fig. 8a**

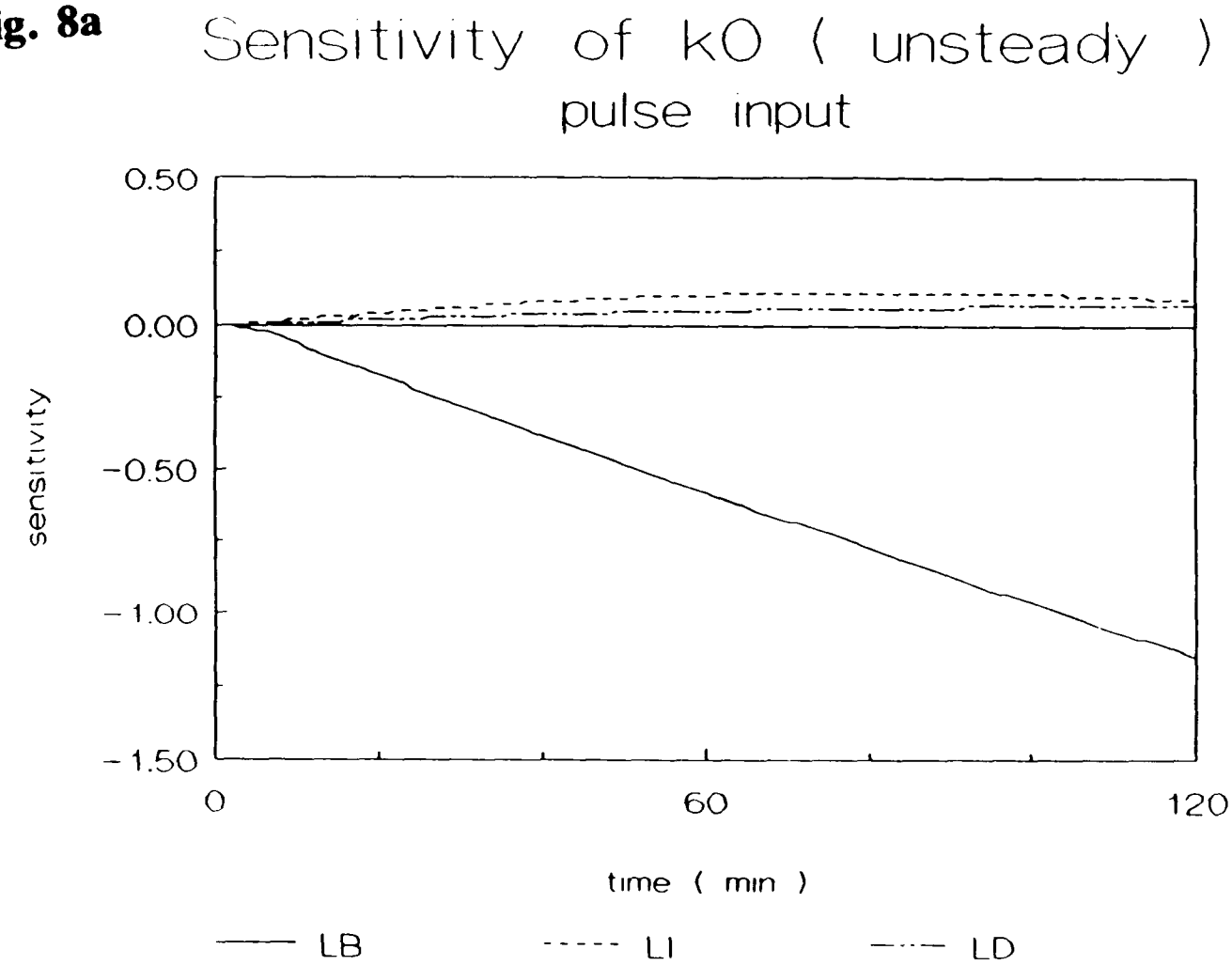
Sensitivity of kO ( unsteady )
pulse input
0.50
0.00
-0.50
-1.00
-1.50
sensitivity
0
60
120
time ( min )
LB
LI
LD

**Fig. 8b**

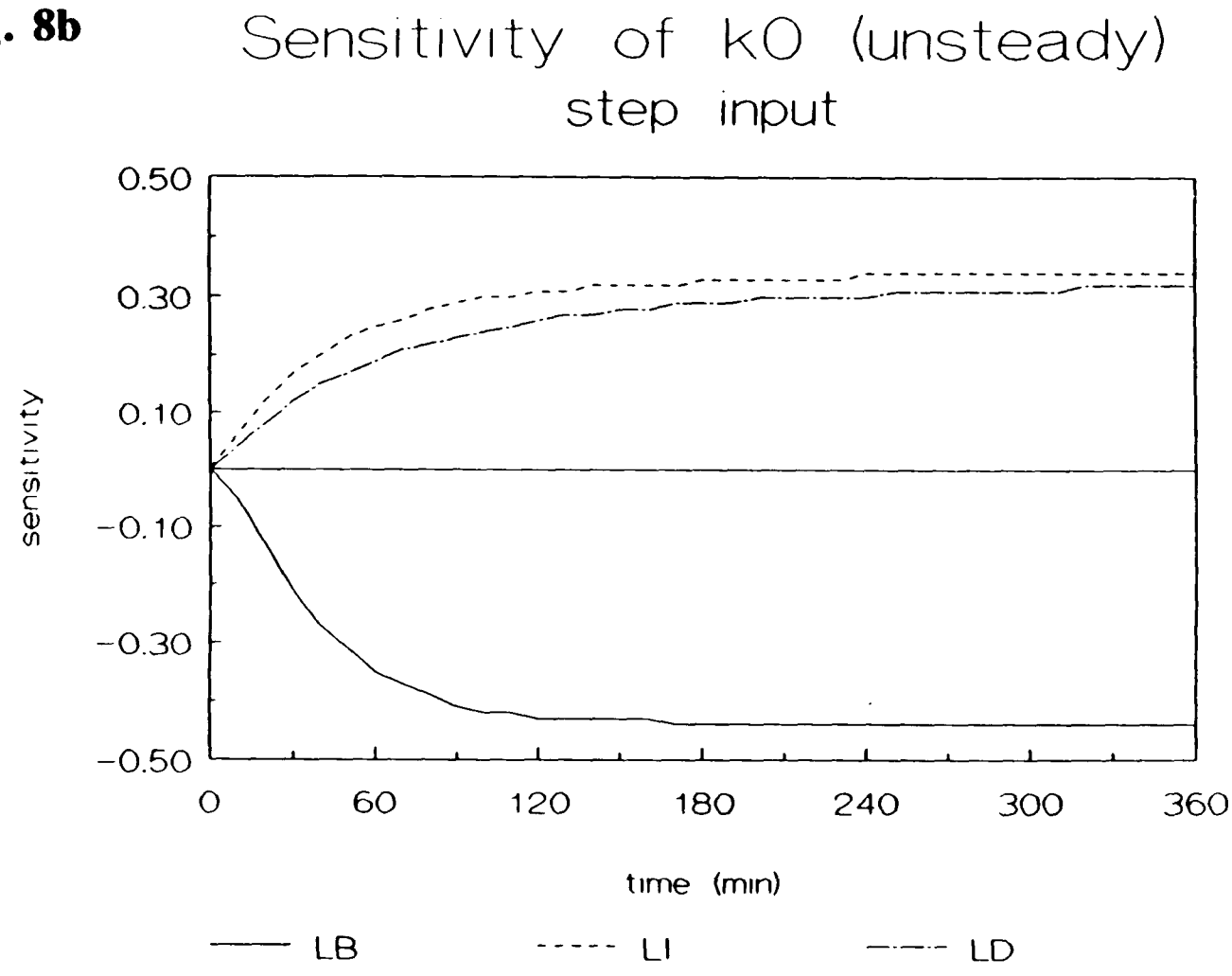
Sensitivity of kO (unsteady)
step input
0.50
0.30
0.10
-0.10
-0.30
-0.50
sensitivity
0
60
120
180
240
300
360
time (min)
LB
LI
LD

**Fig. 8c**

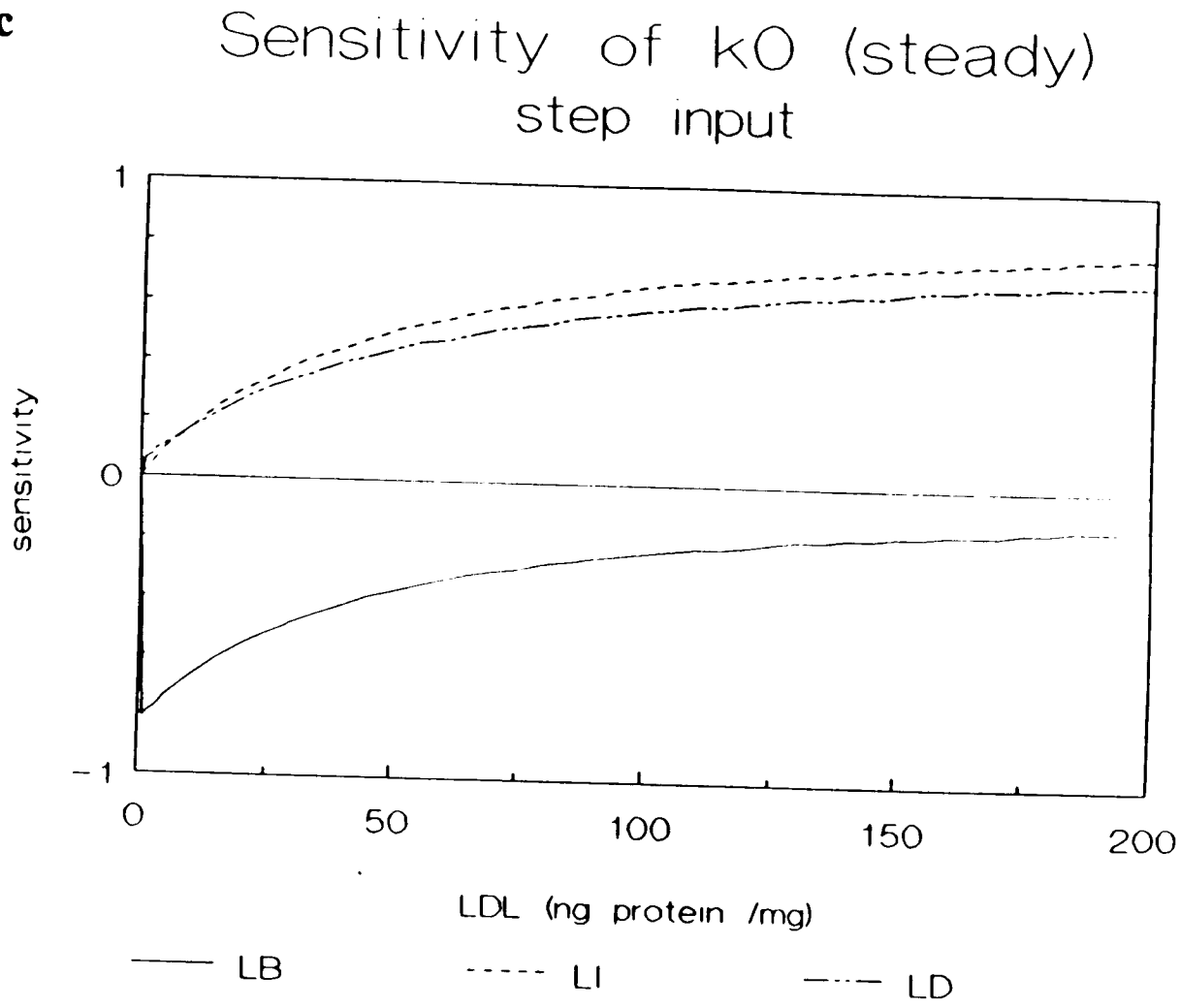
Sensitivity of kO (steady)
step input
1
0
-1
sensitivity
0
50
100
150
200
LDL (ng protein /mg)
LB
LI
LD

# Part Two: Regulation

# VI. Introduction

As noted in the general introduction, our overall goal for this thesis is to come up with a kinetic model to describe the major steps in the Brown and Goldstein cellular cholesterol pathway. In the work described thusfar, we have shown that a quantitative, kinetic approach can, in addition to its long-term usefulness as part of an overall transport model for cholesterol within the artery wall, suggest some insights into some of the details of the individual processes themselves.

Recall that the pathway by which many non-hepatic cells such as fibroblasts and arterial endothelial cells maintain cholesterol homeostasis is by taking up LDL cholesterol packets circulating in the blood via a specific receptor process. In extreme circumstances of either very low or very high plasma LDL concentrations, these cells have the facility to nevertheless keep their cholesterol levels fairly steady. At this point, having what we feel is a good model for binding, uptake and degradation of LDL by human fibroblasts, we would like to proceed towards the development of models for these various regulatory processes that are at play in human fibroblast and, by assumption, in human endothelial cells. (It is probably worth remarking that most experiments are probably performed on fibroblasts rather than on endothelial or smooth muscle cells because of the relatively plentiful supply of normal fibroblast cells (from circumcision) and because fibroblasts, like endothelial cells but unlike smooth muscle cells, form confluent monolayers.)

Before continuing, a word about our modeling philosophy is in order: Even though the actual processes being modeled may be quite complex, involving many intricate and important steps, the modeler is limited in the detail of description to which the model can aspire by the availability of experimental data that is specific enough to be useful for kinetic analysis. In particular, experiments where too many quantities vary may very well lead to significant qualitative insights yet at the same time be completely inappropriate for kinetic study. Furthermore, even if there is a lot of available data, it is usually the case even for complex processes, that a very small subset of the "reaction steps" accounts for the major trends observed in experiments and in normal function; it is first and foremost these that the modeler attempts to model. In view of these perspectives, the detail that we will attempt to incorporate into the models briefly described below will be the minimum necessary to account for the observations and hopefully be no worse than proportional to the amount of (kinetically useful) data available for the process in question.

The major regulatory processes that are the subjects of the ensuing chapters are the manufacture of cholesterol *de novo* in low LDL environments the activation of enzymes that store cholesterol by esterifying it and the down-regulation of LDL receptor number in high LDL environments.

Such an investigation begs the question, what exactly is the agent of regulation? Below in the Preliminaries section, we argue that Brown and Goldstein's experimental data present evidence that suggests an answer: LDL-derived cholesterol, that

is, LDL that has recently entered the cell via the receptor pathway, may somehow be different from other endogenous cholesterol and it is this cholesterol which effects regulation. (We note that a somewhat similar idea appeared in Yuan *et al.* (1991),[21] but only to describe the substrate for esterification.) That is, even though fluid-phase pinocytosis can introduce exogenous LDL into the cell, LDL entering via this pathway does not appear to affect the regulatory actions[11 6], and can thus almost be ignored vis-à-vis regulation. Lysosomally-hydrolyzed cholesterol may differ from other endogenous cholesterol in perhaps being oxidized or oxygenated to a higher degree (although we know of no definite chemical evidence to prove this), and may thus be capable of much more potently instigating the cell's regulatory mechanisms. It also appears that after residing within the cell for probably one day or more, the LDL-derived cholesterol begins to revert to the much less (regulatorily) active form that is the majority of the cholesterol present within the cell.

After a brief summary of the work in the first half of this thesis and a literature review of previous modeling efforts related to the regulatory processes, our treatment below begins with a number of preliminaries that will be important bases for what follows. Amongst these is a fuller discussion of this issue of (lysosomally-) hydrolyzed cholesterol being the active agent as well as of how the cell-division kinetics affect, enter into and are handled by our modeling. In addition, the Preliminaries detail the make-up and architecture of the LDL particle and the numerical methods employed in the data-model comparisons.

The first regulatory process that we tackle is the *de novo* synthesis of cholesterol. Endogenously generated free cholesterol is the end product of a series of reactions beginning from the substrate Acetyl-CoA. Although complex and long, this pathway has a rate-limiting step, the production of mevalonate, a cholesterol precursor, which requires the action of an endogenously-generated enzyme, 3-hydroxy-3-methylglutaryl Coenzyme A reductase (abbreviated, HMG-CoA Reductase). For a review, see.[109] Basically, given a dearth of exogenously supplied cholesterol, cells produce this enzyme and, by its action, synthesize cholesterol *de novo*. In the presence of exogenous cholesterol, the cells, via a feedback mechanism, interfere with the production of this enzyme; enzyme attrition shuts down *de novo* synthesis.

For *de novo* synthesis, as well as for each of the processes discussed below, a fuller description of the qualitative as well as the quantitative features of the experiments done to investigate this system will open the discussion. A summary of experiments directly relevant to the modeling will follow directly and lead into the proposing of kinetic models. Considering the paucity of kinetically useful experimental data available, we will generally endeavor to neglect most intermediate species. Our models will be, again, of the well mixed variety (i.e., ordinary differential equations) and again based on the data for human fibroblast. As in the earlier part of this thesis, the modeling below has the following basic outline: 1. Identify the proper regulatory agent. 2. Propose a model for the action of the enzyme and for regulatory action of the agent described in 1, while assuming that processes that proceed on

much faster time scales are quasisteady and those on a slower time scale are constant. 3. Compare the model with experimental data in order to evaluate the model's parameters. 4. Test the model against other experimental data.

One final note about HMG CoA reductase and, in fact, the other enzymes under consideration is in order: The assay for HMG CoA reductase provides an enzyme *activity* rather than a concentration. Whereas the activity is actually the relevant biochemical quantity, kinetic models usually work in terms of concentrations. We shall at first treat this and like activities as if they were a particular concentration unit, and later use our models to show that such a tactic is justified, i.e., that the models as applied to the assay procedure result in values for the activities that are proportional to the respective enzyme's concentration at the beginning of the assay.

After *de novo* synthesis, we shall briefly investigate the processes of non-lysosomal hydrolysis of cholesteryl esters, typically the hydrolysis of cholesteryl esters that had been packed away, i.e., esterified, at some earlier time of cholesterol oversupply. This esterification of excess free cholesterol is the subject of the succeeding section. The enzyme or enzymes that catalyze esterification are acyl-CoA:cholesterol acyltransferase (abbreviated ACAT), which is a membrane-bound enzyme localized in the endoplasmic reticulum of the cell.[89] One of the most intriguing facts about ACAT is that although LDL-derived cholesterol appears to be significantly more potent than ordinary cellular cholesterol at activating ACAT, ACAT itself seems to *act* indiscriminately on LDL-derived as well on a sizable

fraction of the endogenously found cholesterol.[60] Our model will detail and propose an explanation/mechanism for this observation.

Before moving on to the next regulatory process, which acts on yet a slower time scale, we will have to account for the fate of the cholesterol introduced by either the LDL-receptor pathway or by *de novo* synthesis. In non-hepatic human cells *in vivo* it is known that cholesterol is used in the production of new membrane, particularly in dividing cells.[5] Other cholesterol escapes from the cells when so-called cholesterol acceptors such as HDL,[84] to which cholesterol can attach, are present in the medium. We lump such processes into a gross "efflux" process and construct a simple model to account for it.

This brings us to the final regulatory process, the regulation of receptor number, probably the most crucial one for determining the sink capacity of endothelial cells in the artery wall. Since this process acts on the slowest time scale of all of the known regulatory processes and since it both directly affects the concentration of the active agent and, at the same time, is affected by it, effective modeling of the total receptor number requires adequate models for the faster processes described above. This is the subject of section IX.E. The thesis then presents a summary, together with a number of model predictions and comparison with other experiments and with the models of previous investigators. This section will also attempt to draw conclusions, touch upon the highlights and point to the significance of this work.

## VII. Previous Work

## VII.A. Literature on the Modeling of Regulation of the Cellular LDL Pathway

Whereas the relatively "clean" (as far as performing and interpreting experiments) LDL receptor-binding, uptake and degradation seems to have inspired a number of prior modeling efforts (see the literature review in section II above), only one group seems to have taken on the task of modeling the regulatory processes. One can speculate as to the reasons: 1. Modeling of regulation requires as a prerequisite a good and robust model of the cholesterol supply processes just mentioned. 2. It is not obvious what the active agent of regulation is, and any modeling based upon a reasoned guess in this direction without direct proof is risky. 3. It is much harder to find data that apply to one regulatory process and cleanly excludes the others. The regulatory processes are, by nature, coupled and almost require simultaneous, rather than sequential modeling. This, in itself, is a daunting possibility. 4. The regulatory processes are less well understood and therefore require more *chutzpah* to model. In our case, as summarized in the sub-section II.B, we have a model which answers item 1. In the text below, we describe how we deal with items 2. and 3. And, item 4 refers to a quality whose dearth has never been problematic.

The one previous modeling effort that we are aware of is that of Yuan *et al.*,[21] already discussed in section II. As noted there, their work assumed that the LDL concentration in the medium determined the receptor number and that each of the processes that contributed to the overall cholesterol balance by

either increasing or decreasing cholesterol levels did so via a very simple, algebraic, often non-kinetic form. We shall return in the final discussion section to evaluate our work and to compare it with Yuan *et al.*'s models.

## VII.B. Brief Review of Our LDL Receptor-Mediated Uptake Model

In the first part of this thesis we developed a model for the LDL binding to its specific receptors and its subsequent internalization and degradation. Before continuing to model the cell's regulatory actions, we briefly review the main points of this earlier work, since the regulation considered below begins with LDL's receptor-mediated uptake and its catenated break-down that delivers lysosomally-hydrolyzed cholesterol to the cells' endogenous cholesterol pools. As a result the processes described by our earlier models play a crucial role in the interpretation of the regulatory data that we analyze forthwith.

Recall that normal cells express surface receptors which can specifically bind cholesterol from the surrounding medium, even when the medium's cholesterol concentration is very low. These receptors seem to be quite mobile when they first appear on the cell's surface, but they lose their mobility when they bind to the coated pits that occupy 1-2% of the cell's surface. These coated pits transfer their contents, including LDL receptors both with and without bound LDL particles, into the cells via endocytosis. Free receptors quickly separate and return to the surface and the lysosome degrades the internalized LDL's protein and hydrolyzes its cholesteryl esters.

We began by examining the (Boston model's) picture that presented kinetic steps for LDL-receptor binding, internalization and degradation; we found that while being consistent with smooth muscle cell data, their model could not satisfactorily account for human fibroblast data. In particular, it failed to account for the tail of the binding curve of a pulse-chase experiment and only could fit experimental results corresponding to step changes in (labelled) LDL concentrations with a coated pit invagination rate that differed from the experimentally measured value by a factor of three. In contrast, the model that we suggested distinguished between receptors in coated pits and those not in coated pits and allowed for different rates of receptor attachment to coated pits depending upon whether or not the receptors were LDL-laden or not. Back-of-the-envelope estimates based on the data as well as more sophisticated parameter estimation schemes yielded rate constants consistent with the suggestion that LDL-bound receptors not in coated pits are much slower to become coated-pit bound than LDL-free receptors and that essentially one set of rate constants seems to explain a large amount of data, including experiments of three qualitatively different types.

Before leaving this section, we briefly present this model and take it as a given for representing the rate at which LDL-cholesterol is delivered to the cells. Whether or not one accepts that its interpretation in terms of cellular-level events is absolutely correct, and we naturally lean in that direction, the model does seem to account for this delivery reasonably accurately under the various usual experimental conditions.

Let $R^p$, R, $L^p$and $L^a$ represent LDL-free receptors in and out of coated pits and LDL-bound receptors in and out of coated pits, respectively. Let L represent the medium' LDL concentration and $L^i$ and $L^d$, internalized, receptor-free LDL and its degraded protein component, respectively. The model in equation (2) in terms of these quantities is a well-mixed one (that is, ordinary differential equations), assumes that the concentration of coated pits remains time-invariant and relies on mass action kinetics.

$$
\begin{array}{l}
L + R^p \underset{}{\overset{1}{\rightleftarrows}} L^p \overset{2}{\rightleftarrows} L^i + R \\
\qquad\qquad\quad \uparrow\downarrow o \\
L + R \underset{}{\overset{1}{\rightleftarrows}} L^a \\
L^i \overset{3}{\rightleftarrows} L^d \\
R \underset{2}{\overset{9'}{\rightleftarrows}} R^p
\end{array}
\qquad (2)
$$

## VIII. Preliminaries

Before embarking on a detailed modeling effort for the various regulatory processes at play in the cellular LDL pathway, there are a number of fundamental issues that we feel are prerequisite. Among them are the question as to the effect of cell division kinetics on the kinetic modeling, some details about the LDL particle itself and identification of the most likely candidate for the regulatory agent responsible for triggering the processes under consideration below.

## VIII.A. Cell Division Kinetics

Non-confluent human fibroblasts divide until they experience contact inhibition. When they are closely packed, or in the so-called confluent state,[54] they are almost non-dividing. *In vivo*, they actually achieve an even slower pace of division called quiescence. In sparse (low cell density), *in vitro* cell cultures, human fibroblast cells divide exponentially, experiencing so-called exponential or logarithmic growth. As the cell density increases, even under the condition of sufficient exogenous nutrients supply, cell growth rate is gradually retarded and after late logarithmic growth phase, cells reach confluence due to contact inhibition.

Even though cells may be viewed as a heterogeneous collection of discrete entities, as they really are, the stochastic nature of cell growth allows one to employ a specific growth rate $\mu$ (defined below) to describe the growth of the total cell population in a continuous manner. Likewise, the total cell mass as well as their total contents of DNA are assumed to vary continuously with time.

If one examines experimental data (J.L. Goldstein *et al.*[55] - fig. 9) for the total cell population's (V) growth with time, one sees the clear exponential regime between day 1 and day 8. The simplest cell expansion model is a first order one:

$$\frac{dV}{dt} = \mu V \qquad (20)$$

where $\mu$ is the constant representing the specific growth rate. For rapidly growing cells, the figure shows that specific growth rate $\mu$ is approximately 0.01 / hour. For nearly confluent cells, it must be smaller. Since it takes a fibroblast cell about 18 hours to divide[54], the rate of doubling is (ln 2)/18~.04/hr. Thus even for cells undergoing exponential (days 1-8) growth only about one quarter of the cells are dividing at any given time.

As long as the cells remain in exponential growth with a $\mu$ that does not change, one may assume that the dividing cell fraction remains constant. As a result, it is reasonable to assume that the average cell composition, and in particular the average DNA per cell and the average protein mass per cell, remains time-invariant. Thus it is only the analogous *total* per-dish quantities, rather the per-cell ones which vary with time. In addition, when reactions occur in this context and concentrations of reactants and/or products are expressed in per-unit-cell-protein-mass units, the situation is completely analogous to that which occurs in a non-constant density chemical reactor.[56] There, concentrations are generally expressed in per-unit-volume units and a change in the density of the reaction mixture upon reaction results in a diluting or a concentrating of the reacting mixture. This is easy, but sometimes necessary to account for, as we shall see below. So, we see that cell proliferation does not affect the evolution of average cellular concentrations except via a diluting kinetic term resulting from an increase of the total cell mass.

As we saw, the dilution rate is relatively small, even for quickly multiplying cells. In fact, if one is interested only in processes taking place on time time scale of minutes to hours (as

in Part One), then the contribution due to $\mu$ is small and can easily be neglected. However, when processes involving growing cells have a characteristic time of days, such as the regulation of the total receptor tally, accounting for dilution may become quite significant. In order to do this, we look at a reacting substance whose concentration P is in per-cell units. The change in the total moles of the substance is given by $(d/dt)(VP)=VdP/dt+PdV/dt$. The rate of reaction is $(1/V)(d/dt)(VP)$, which is then set equal to the rate expression deriving from the proposed mechanism. Recalling (20), this leaves one with

$$\frac{dP}{dt} = - \mu P + \text{kinetic expression.} \qquad (21)$$

## VIII.B. The LDL particle and its Stoichiometry

Low density lipoprotein (LDL) are the prime source of cholesterol for cells such as fibroblasts. It is their receptor mediated uptake which can trigger the regulating processes that are the subject of this modeling effort. (Another lipid carrying molecule that specifically binds to and is internalized by the LDL receptors and can therefore trigger regulation is very low density lipoprotein (VLDL).[57] ) Due to its importance, a few words about the make-up of LDL are in order.

A particle of LDL contains about 1500 esterified cholesterol molecules, 500 unesterified cholesterol molecules and one large protein molecule, apoprotein B-100. The mass of apoprotein B is, at 0.4 - 0.6 million daltons ($5x10^5$daltons[26]) per one mol

of LDL, enormous. The unit of LDL concentration of medium is usually expressed as $\mu$g LDL protein mass/ml.

It is important to know 1 ng LDL protein corresponds to about 5 pmol cholesterol in LDL particles. There are a number of ways to estimate this quantity, first by dividing total cholesterol particle number per LDL particle by the protein mass per LDL particle and converting it into units of pmol/ng protein mass. A second estimated comes from the fact that a 1 $\mu$g cellular cholesterol increase due to LDL uptake corresponds to 500 ng of LDL protein.[58] Finally, we shall now demonstrate how Figures 10a-d implies a stoichiometry of about 6 pmol cholesterol/ng protein.

After 48 hours of LDL-free, LPDS incubation (to up-regulate the cells' receptor number), Goldstein *et al.*[82] transferred their cells to medium containing 10 $\mu$g/ml of doubly labelled LDL, one label for the protein component and one for the cholesteryl esters. The label for the cholesterol tags approximately 1/3 of the LDL's total cholesterol. During the course of the experiment, Goldstein examined the total LDL taken up by the cells (that is, the bound plus the internalized) and found (see Figures 10a-d) that it had a ratio of labelled-cholesterol to labelled protein of about 2 pmol LDL cholesterol/ 1 ng LDL protein. (They determined that essentially none of the cholesteryl esters comprising the internalized portion of the internalized fraction had been hydrolyzed and later reesterified.) About the same value described the ratio of the corresponding degraded LDL product, labelled free cholesterol to labelled degraded protein. Taking into account the factor of 3 mentioned above yields a

stoichiometric ratio of about 6 pmol LDL cholesterol/ ng LDL protein.

It is worth noticing that this same ratio seemed to hold both before and after the system, and in particular the LDL uptake, had reached steady state. This suggests that the rate constants for lysosomal hydrolysis and for LDL-protein degradation are similar. At this stage we allow them to be distinct and generalize the model from (2) to

$$\begin{aligned} L^p &\overset{2}{\dashv} L^i + \zeta\, L^{i'} + R \quad \text{where } \zeta \approx 5 \text{ pmol/ng} \\ L^i &\overset{3}{\dashv} L^d \\ L^{i'} &\overset{3'}{\dashv} C^{hy} \end{aligned} \tag{22}$$

It will turn out later (Chapter IX) that the best fit values for these rate constants are very close to one another. In that case, one could replace reactions 2, 3 and 3' with $L^p \overset{2}{\dashv} L^i + R$, $L^i \overset{3}{\dashv} L^d + \zeta C^{hy}$.

## VIII.C. $C^{hy}$ : The Active Agent in Cellular Regulation

As stated earlier, the internalized LDL is incorporated into endocytotic vesicles (endosomes) that fuse with lysosomes. Within the lysosome the protein component of LDL rapidly degrades to free amino acids, which dissolves in the culture medium.[36 59] Lysosomal acid lipase hydrolyzes LDL's cholesteryl ester component.[60] The resulting unesterified cholesterol makes its way

to the cellular compartment where it mainly associates with the cell's membranes.[53] It seems that the accumulation of unesterified cholesterol in the cell regulates the activities of two microsomal enzymes:

a) It suppresses 3-hydroxy-3-methylglutaryl coenzyme A reductase (HMG CoA reductase), causing a reduction of *de novo* cellular cholesterol synthesis.[60]

b) It activates acyl-CoA:Cholesteryl acyltransferase, an enzyme that facilitates the reesterification of cholesterol.[61] [62]

It also suppresses the LDL receptor number.

What is agent of this regulation? Is it the total cholesterol concentration of the cell? The total cholesterol concentration does not vary much. During 6 hours incubation in medium containing 25 $\mu$g protein/ml LDL, the total free cholesterol changes by only 16% (control=24 $\mu$g/mg protein). When the medium contains 5 $\mu$g protein/ml LDL, it remains essentially unchanged after 6 hrs (Fig. 11a). During this time, however, the HMG CoA reductase activity rapidly decreases by approximately 95% for 25 $\mu$g LDL protein/ml and by 80% for 5 $\mu$g LDL protein/ml (Fig. 11b). Certainly at least for the 5 $\mu$g LDL protein/ml experiment, the rapid and continuous 80% decrease of HMG CoA reductase activity cannot be due to a cellular free cholesterol increase. So, we rule out the total cholesterol concentration as the regulatory agent. Can it be the exogenous LDL cholesterol level, as assumed in [21]?

In contrast to LDL taken up by receptor mediated LDL pathway (high affinity process), LDL taken by the bulk phase pinocytosis process does not regulate cholesterol metabolism in

fibroblast since it "does not appear to be capable of expanding the nonlysosomal cellular compartment. Rather, this sterol is excreted into the culture medium.[35]" One can, for example, infer this from the experimental observation that both regulated HMG CoA activity (Fig. 12a) as well as bound and internalized LDL saturated with increasing medium LDL concentration, but LDL bulk phase pinocytosis (nonspecific uptake) increased linearly with LDL medium concentration.

With both of these obvious candidates excluded, we venture to propose that some form of exogenously-derived LDL-cholesterol taken up via the receptor pathway might be the regulatory agent. In fact, Goldstein *et al.* themselves pointed to this possibility when they stated that the reductase activity is suppressed by cholesterol supplied via receptor mediated endocytosis of low density lipoproteins[9]. But, can this cholesterol really be different? Consider the experimental facts. During the 6 hrs over which the experimental down-regulation of HMG CoA reductase described above occurred, the roughly equal initial numbers of receptors in the dishes exposed to 25 and 5 $\mu$g/ml LDL introduced ~2250 pmol/mg protein (~1 $\mu$g cholesterol) and ~900 pmol/mg protein (~0.5 $\mu$g cholesterol) of LDL-derived hydrolyzed cholesterol (fig. 12b). Even though the hydrolyzed LDL-cholesterol concentration is negligible compared with the total cellular free cholesterol concentration, the fractional change of accumulated amount of hydrolyzed LDL-cholesterol over the time course of these experiments is of the right magnitude to explain the rapid and drastic regulatory effect.

How might this LDL-derived cholesterol chemically differ from normal, "garden variety" cholesterol? It is well known that

oxygenated derivatives of cholesterol such as 7-ketocholesterol, 7$\beta$-hydroxycholesterol, and 25-hydroxycholesterol are very powerful regulatory agents[63]. Several studies have shown that they can influence reductase protein's degradation and synthesis.[64] [65] Hence oxysterols may be natural regulators of reductase activity, thereby controlling the biosynthesis of sterols in intact cells.[63] Gupta even suggested that intact cells might need to convert hydrolyzed LDL-cholesterol in order to experience any regulatory effect at all.[66] Also relevant is the fact that oxygenated sterols are present in horse serum,[67] in the lysosomes of cells from patients with Wolman's syndrom,[68] and in normal human aorta.[69] A rat liver enzyme, cholesterol 25-hydroxylase, produces 25 hydroxycholesterol from cholesterol.[70]

In contrast, carefully purified cholesterol does not affect the activity of HMG-CoA reductase in various cell lines, including human fibroblasts,[71] mouse liver cells,[72] and mouse lymphocytes.[73] Thus it seems plausible to presume that LDL-derived cholesterol may, for a certain time after receptor-mediated entry into the cell, have a chemically different character from other cellular cholesterol and, as such, be the active regulatory agent.

We shall presume this to be the case and denote LDL-derived hydrolyzed cholesterol by $C^{hy}$. As such, it will be necessary to distinguish between $C^{hy}$ and other cholesterol and to keep track of the time evolution of the latter's concentration, for it is

this that will enter the kinetic models for the regulatory processes.

In this paper we treat all free cholesterol entering via high affinity LDL pathway, whether as hydrolyzed LDL-cholesteryl ester or as LDL-cholesterol, equally as cellular process regulating agent. Yuan et al[21] also introduce a hydrolyzed LDL-cholesterol species, but only as the substrate of cholesterol esterification.

## VIII.D. Numerical methods

As discussed in Section III.3 above, comparison of a model with experimental data in order to test the form of the model and to determine the so-called best fit values for these parameters involves numerical methods. The analysis sets up an error function that is a norm of the deviation from the data of the model's predictions for a given set of parameters. The various data points are weighted in a Bayesian manner in this function. The method then minimizes this complicated function with respect to the choices of the parameters involved. We refer the reader to Section III.3 for a more detailed discussion of the techniques employed for these tasks. We just mention here that we employed the computationally expensive simulated annealing techniques in practically all of the fits below rather than the Bremermann's optimizer because of the generally better final answer that it yields.

## IX. Models of Individual Cellular Regulating Processes.

Below we go through each of the important sets of processes involved in the cellular cholesterol regulation and determine models for each process. We then subject those models to known experimental data in order to verify their form and to determine the appropriate rate parameters. We begin with the *de novo* synthesis of cholesterol which takes place in the absence of exogenous sources.

### IX.A. De Novo Synthesis

#### IX.A.1. Qualitative Discussion of *de Novo* Synthesis

The cholesterol balance in cells is maintained by the coordinate regulation of the endogenous pathway of cholesterol synthesis and the exogenous pathway of cholesterol delivery.[74] Cells primarily obtain cholesterol from the receptor-mediated endocytosis of cholesterol-carrying low density lipoproteins (LDL) in the extracellular environment. When sufficient cholesterol is delivered via the LDL receptor, the cell suppresses the activity of HMG CoA reductase thereby shutting off cholesterol synthesis. This avoids overproduction and excess accumulation of cholesterol.[75]

A series of over 20 enzymatic reactions comprises the endogenous synthesis that produces cholesterol from the substrate

acetyl CoA. One of the early step in the pathway of cholesterol synthesis and, in fact, its rate limiting step is the conversion of HMG CoA to mevalonate. 3-hydroxy 3-methylglutaryl coenzyme A (HMG CoA) reductase catalyzes this rate-limiting step and the cholesterol-induced shut off of the de novo synthesis acts by interfering with this enzyme.

In the absence of LDL, animal cells maintain high activities of this enzyme, thereby synthesizing mevalonate for the production of cholesterol as well as nonsterol products. When LDL is present,HMG-CoA synthase and reductase activities decline by more than 90%, and the cells produce only the small amounts of mevalonate needed for the nonsterol end-products. If excess mevalonate is supplied externally together with LDL, the residual activity of HMG-CoA reductase is abolished and mevalonate production terminates.[76]

### IX.A.2. Experimental Facts

Brown *et al.*[77] showed that upon administering cyclohexamide, a potent inhibitor of protein synthesis, to confluent human fibroblasts, HMG CoA reductase activity exhibits a first order decay with a half life of about 2.7 hours. This corresponds to a decay rate of 0.24/hour.

An important question is whether cholesterol exerts this regulatory effect within cells by direct allosteric inhibition of HMG-CoA reductase or simply by synthesis inhibition. Sterol in the form of whole serum, LDL, HDL, and in a solution containing ethanol and lipoprotein-deficient serum (LPDS) was added to cell

free extracts. None of these solutions produced any direct inhibitory effect. They concluded that LDL-cholesterol must reduce HMG CoA reductase activity in normal fibroblasts by inhibiting the synthesis of new enzyme molecules; this inhibition produces a rapid fall in enzyme activity because of the enzyme's very rapid degradation.

What is the strength and timing of this regulation? Recently Goldstein *et al.*[76], Nakanish *et al.*[78] and Luskey *et al.*[79] and others investigated molecular level regulation of HMG CoA reductase using agents such as compactin and lovastin. These inhibitory agents compete with the substrate (HMG CoA) of the mevalonate synthesis step for the enzyme's binding sites. In cultured human fibroblasts or in chinese hamster ovary cells, they block the synthesis of mevalonate and trigger adaptive reactions that yield a 200 fold increase in reductase protein within a few hours.[78 80] This shows that enzyme synthesis is very fast, taking only hours. On the other hand, the 200 fold increase in enzyme concentration reverses within hours upon incubating the compactin-treated cells with large amounts of mevalonate (10 mM) or with smaller amounts of mevalonate together with LDL.[78 80 81]

The major regulation of *de novo* synthesis, as Goldstein *et al.* originally determined, is at the transcriptional level. Induction of transcription produces a large increase in m-RNA levels. However, even when sterols are at saturating levels, the cell continues to transcribe reductase m-RNA at about one-eighth of its maximal rate.[78] Hence LDL alone suppreses the enzyme by only eight fold. Goldstein *et al.* used the term Sterol regulatory

element-1 (SRE-1) to describe the part of the promoter of the reductase gene that actively represses transcription in the presence of sterols.

Once formed, the m-RNA translates its message to form the protein enzyme. A nonsterol product in the mevalonate pathway can inhibit this translation. Absence of this product, as in the experiment that gave a 200-fold enzyme increase, resulted in a five-fold increase in the rate of translation. In addition, both sterol and nonsterol agents can directly contribute to reductase degradation. However, regulation of degradation is minor compared with transcriptional regulation: the absence of sterol and nonsterol agents, as in the experiment that gave a 200-fold enzyme increase, can slow enzyme degradation by at most a factor of five.

In summary, we see that full reduction of enzyme activity requires both a sterol and a mevalonate-synthesized nonsterol metabolite and acts on transcription, translation, and degradation; transcriptional regulation is, nevertheless, the most important.

### IX.A.3. Models for the Regulation of the Enzyme's Activity.

As discussed in the preliminaries, we take the regulating agent for cellular processes to be hydrolyzed LDL cholesterol even though there is also nonsterol metabolite feed back regulation on enzyme action. This greatly simplifies the modelling of the *de novo* synthesis processes and the fitting of the corresponding rate constants because it allows one to take the time evolution of $C^{hy}$ as an input; the result of *de novo* synthesis

does not then feed back onto the $C^{hy}$ evolution. Thus one can model *de novo* synthesis without simultaneously considering the details of the other processes beyond the dynamics of $C^{hy}$. We also restrict our attention to modeling only the most important (transcriptional) regulatory process.

One can now propose a kinetic model with the steps mentioned above:

| | |
|---|---|
| $D \overset{1}{\rightarrow}{}^{e} D + Q$ | the transcription of m-RNA (Q) from DNA (D) |
| $Q \overset{2}{\rightarrow}{}^{e} Q + E$ | the translation of enzyme (E) |
| $Q \overset{3}{\rightarrow}{}^{e} 0$ | the degradation of m-RNA (Q) (23) |
| $E \overset{4}{\rightarrow}{}^{e} 0$ | the degradation of enzyme (E) |
| $D + m\ C^{hy} \underset{\leftarrow}{\rightarrow} (D.C^{hy}_{m})$ - (*) | the transcription regulation via m $C^{hy}$ molecules |
| $E + C^{hy} \overset{5}{\rightarrow}{}^{e} 0 + C^{hy}$ | the direct sterol-induced enzyme degradation |

where 0 means "out of the system" of species whose concentrations vary with time, e.g., the monomer pools whose concentrations are not monitored and are assumed to be "in excess." Note that these presumed time-independent monomer concentrations are lumped into rate constants 1 and 2 above, which accounts for their *apparent* violation of mass conservation. Our model assumes that transcriptional regulation proceeds via the reversible binding of

m hydrolyzed LDL cholesterols to the DNA transcriptional binding sites, where the integer m still needs to be determined. To keep the model simple, we require this reaction to be in equilibrium, with equilibrium constant K. One may consider this a reaction with molecularity m+1 that, for $m \geq 1$ results from the equilibrium reactions $DC_i^{hy} + C^{hy} \rightleftarrows D(C^{hy})_{i+1}$ with equilibrium constant $K_i$ $(i=0,\ldots,m-1)$, where $K = \prod_{i=1}^{m} K_i$ and $K_m >> K_i$ for $i=1,2,\ldots,m-1$. In effect, these assumptions correspond to the assumption that at equilibrium the concentrations of the partially block states ($DC_i^{hy}$, for $i=1,2,\ldots,m-1$) are negligibly small with respect to those of D and of $DC_m$. Alternatively, one can just regard m as a phenomenological parameter. As a result, a balance on the conserved total gene *concentration* $D_t$, a presumed time-invariant quantity (since the total amount of gene is assumed to have the same specific growth rate as that of cell population - see the Preliminaries) gives

$$D_t = D + DC_m^{hy} \quad \text{and} \quad D = D_t/(1+K(C^{hy})^m).$$

Recall that the concentration $C^{hy}$ of hydrolyzed LDL cholesterol is independent of the *de novo* synthesis process and derives from its own rates of production and destruction.

Let $\eta = k_1 D_t$ and $\mu$, as before, be the cell's mass expansion rate per unit cell mass. Then the kinetic equations corresponding to mechanism (23) are

$$\frac{dQ}{dt} = \frac{\eta}{1 + K(C^{hy})^m} - (k_3^e+\mu)Q \qquad (24)$$

$$\frac{dE}{dt} = k_2^e\, Q - (k_4^e+k_5^e C^{hy}+\mu)E$$

**IX.A.4. Simplified Kinetic Model.**

Bailey and Ollis write, "The more closely a kinetic description represents the actual chemical events which occur, the more robust is the kinetic model; i.e., the model is more likely to give good results when applied to conditions different from those used to evaluate the model and determine its parameters. For protein synthesis and enzyme synthesis, our knowledge of the pertinent mechanisms permits formulation of kinetic models at the level of molecular events and interactions," i.e. a material balance on m-RNA transcribed from a particular gene and one on the intracellular concentration of the translation product.[106] Although the kinetic description of model (23) is close to actual chemical events of HMG CoA reductase synthesis, it is neither clear that adequate modeling of the experimental observations of *de novo* synthesis requires such a detailed model nor is it clear that there are sufficient such observations to confidently indicate values for so many undetermined parameters. Actually, $C^{hy}$ can directly increase the rate of HMG CoA reductase degradation by up to a factor of four to five and can only accomplish this when in collaboration with

cellular nonsterol metabolites. It is unknown how $C^{hy}$ and nonsterol metabolites collaborate with each other to increase the rate HMG CoA reductase degradation and observations of cellular concentrations of nonsterol metabolites during such regulation are unavailable. Moreover, there are no observations of messenger RNA (Q) concentration. Thus we attempt to derive and to work with a simplified version of (23). First, we kinetically lump the m-RNA balance into an effectively direct synthesis of the enzyme from its gene. The simplified kinetic model thus becomes:

$$\begin{aligned} &D \overset{1^e}{\downarrow} D + E \\ &D + m\, C^{hy} \underset{\leftarrow}{\overset{\rightarrow}{}} (D.C_m^{hy}) \\ &E \overset{2^e}{\downarrow} O \end{aligned} \tag{25}$$

with corresponding kinetic equations

$$\frac{dE}{dt} = \frac{\eta}{1 + K(C^{hy})^m} - (k_2^e+\mu)E \tag{26}$$

with $\eta$ and $\mu$ as above.

### IX.A.5. Determining the Rate Constants of Rate Limiting Step

#### IX.A.5.a Preliminary Crude Modeling of the Hydrolyzed Cholesterol Concentration Trajectory

Modelling based on historic data has the inherent disadvantage that the data were taken neither with the models nor, frequently, with kinetic analysis in mind. Thus, the data is often incomplete, as far as kinetic analysis is concerned. Also the amount of data appropriate for kinetic analysis might amount to just a small fraction of the total data available. In the case of *de novo* synthesis, the data that simultaneously tracks the hydrolyzed LDL-cholesterol concentration and the transient HMG CoA reductase activity (e.g., at various time-invariant LDL concentration) is limited, although not absent. In order to analyze enzyme activity data that do not include simultaneous $C^{hy}$ measurements, it thus becomes necessary to first predict the transient hydrolyzed cholesterol concentration under relevant experiment conditions, such as a time-invariant LDL concentration in the medium, since this information is needed in the above model. One can refine these predictions by comparison with the limited data available for that evolution.

Our first inclination is to devise a temporary, crude model for the time evolution of $C^{hy}$ in which we take the number of receptors to remain constant (i.e., to not be regulated by $C^{hy}$ over the time scale of the experiment) and where reesterification is negligible. Instead we would account for the depletion and down-regulation of the uptake of $C^{hy}$ by invoking a simple, first order efflux rate which will thus end up having a significantly larger rate constant than the true efflux rate. Also, since degradation to normal C occurs over days (see Fig. 28), this process is not important for the short time scale regulation of *de novo* synthesis. Another reason to neglect it is that the

reported data do not distinguish between $C^{hy}$ and LDL-derived cholesterol that has decayed to normal cholesterol. We would combine this temporary model with the already-determined model from Part One for LDL uptake to test the HMG coA reductase regulation model and to determine its parameters. We will, however, later develop a more sound model instead of this crude one once we have been able to kinetically account for other processes that contribute to the $C^{hy}$ dynamics.

There are two sets of data which appear initially to be relevant to such a temporary model. The first set (Figures 12a and b[35]) is of the total amount of hydrolyzed LDL-derived cholesterol and the HMG coA reductase activity at six hours after cells were tranferred from an LDL-free, LPDS based medium into one with the indicated amount of labelled LDL. However, as already noted, in order to use such data for model testing and parameter estimation, one needs the $C^{hy}$ trajectory for this six hour period. Thus, we turn to the second set of data is (Figure 13) which displays the time evolution of the LDL-derived cholesterol after medium transfer from LDL-free, LPDS-based medium to one with 10 $\mu$g/ml LDL. Interestingly, the values of Fig. 12b for L=10 $\mu$g/ml and Fig. 13 for t=6 hours are both about 500 pmol/mg. However, this is not good news, as we now explain.

A careful examination of the experimental procedure reveals an important difference between the way in which the two experiments were prepared. In the former, the medium transfer occurred after 48 hours LPDS incubation while in the latter it happened after only 24 hours. The corresponding number of receptors derives from the total binding (surface bound plus internalized)

labelled LDL after the indicated time under the same experimental conditions. Ref. [82] (our Fig. 10a) does just that and yields a value of about 1000 ng/mg cell protein typically corresponds to about 200 - 250 (for the total number of LDL receptors, as expressed in its usual units of ng LDL bound/mg cell protein. On the other hand, the difference in total binding between the two experiments (cf., Figs. 10a and 13 - open circles) is about a factor of 5, indicating that the total receptor tally there is probably only about 40 - 50 in the same units. Thus, assuming that the other rate constants (in particular, the hydrolysis rate constant) are not affected by the difference in LPDS preincubation time and that the label and the cholesterol contents of both batches of LDL used were the same, there seems to be an inherent inconsistency between these two data sets in that one fifth of the receptors seems to lead to the same amount of hydrolyzed LDL-derived cholesterol after six hours. As such, explaining both of these curves with one model having the same parameters but different total receptor tallies is hopeless.

(We note one possible explanation for the above paradox. It follows from a note that the authors make, that essentially all of the label in the cholesteryl esters represented unhydrolyzed labelled cholesteryl ester from the LDL. That is, no appreciable esterification occurred, although after 6 hours one would normally expect it to have been very significant (see Fig. 12c). This might, on average, explain why the system that should have one fifth the total number of receptors has the same tally of free, labelled cholesterol after 6 hours as does the other system.)

Instead, we make a crude assumption: That the form of the time evolution of $C^{hy}$ in Figure 13 is similar to the form that it would take at other medium LDL concentrations and that the major difference would be one of scale. Thus, as input to the testing procedure for the HMG coA regulation model we shall opt to simply use, for each value of the medium LDL concentration for which Figs. 12a and b present data, the Figure 13 curve scaled by the ratio of the ratio of Figure 12b's value at the LDL concentration of interest to its value at L=10 $\mu$g/ml. It is also worth noting the appeal of this procedure since Figure 13 seems essentially linear between 2 and 12 hours. So a curve fit of that data can just be piecewise linear, with a smoothing at either end. It will turn out that the more sound model developed in the later sections that will be independent of these crude assumptions about the $C^{hy}$ trajectory, will thus be able to generate predictions for it. In fact, it will give predictions that qualitatively agree with the crude, to some extent directly-data-based assumptions.

### IX.A.5.b Best Fit Rate Constants for Simplified Model of HMG-CoA Reductase Regulation

With a form for the hydrolyzed cholesterol trajectory in hand we can proceed to determine the best fit parameters for the simplified *de novo* cholesterol synthesis model based upon the data from Fig. 12a. We note here, as in the Preliminaries, that the units of enzyme are typically not those of concentration, but rather those of activity, i.e., of the average amount of

mevalonate that the said amount of enzyme produces per hour in a specific assay. At this point, we take this measurement of enzyme just as one would a concentration. We will return to this point when discussing the action of the enzyme.

We repeat the assumptions that are in force for the regression: 1) The activity of the enzyme is at the steady state value corresponding to LPDS incubation at the beginning of the experiment and is thus equal to $\eta/k_2^e$. ii) The number of receptors, which is assumed to be a slow variable, remains constant over the course of the experiment. iii) Degradation of recently lysosomally-hydrolyzed cholesterol to endogenous free cholesterol ($C^{hy \to C}$) is not appreciable during the 8 hours of the experiment.

In order to perform a best fit analysis, the user must supply upper and lower bounds for the parameters. In particular, $k_2^e$, which Brown and Goldstein estimate to be 0.24/hour, requires an upper bound which we choose to be 1/hour. The meaning behind this choice is simply that we are attempting to model a complex regulatory process by only accounting for the dominant effect and, as such, its parameter may in part reflect what has been neglected: As we noted earlier, $C^{hy}$ only when in collaboration with cellular nonsterol metabolites, can directly increase the rate of HMG CoA reductase degradation by up to a factor of four to five. It is unknown how $C^{hy}$ and nonsterol metabolites collaborate with each other to increase the rate HMG CoA reductase degradation and there are no observations of the time evolution of the concentrations of these nonsterol cellular metabolites.

This simplified model also neglects the direct inhibition of enzyme synthesis in favor of the dominant gene-level regulation. Thus we allow for an upper bound that is four to five times the estimated value.

The results of the best fit on Figure 12a are $\eta$=201 pmol/min./mg cell protein/hr, $k_2^e$=1/hr, K=7.1x10$^{-6}$ pmol$^{-2}$, m=2. Note that m=2 corresponds to requiring two molecules of $C^{hy}$ to interfere with transcription. Fig. 12a shows the best fit curve.

Let us now test this model by comparison with data on similarly 24 hr-LDL-starved cells from another study (Fig. 15a). The experiment[53] follows the time course of HMG CoA reductase activity over a period of eight hours after transfer of the cells from an LDL-free LPDS medium to a medium containing 5 or 25 $\mu$g/ml LDL in LPDS. Note that the although the initial conditions of both this study and the one used for the best fit procedure should both be the same steady state value $\eta/k_2^e$, experimentally there is some variation (.6 vs .7). In order for a fair comparison of the prediction with the data we choose to align the initial values first, in particular, by adjusting $k_2$ to be $\approx$ 0.8/hr. We choose $k_2$ rather than $\eta$ since the model's simplicity lumped the acceleration of degradation, even for saturated LDL concentrations, into $k_2$. Otherwise, there is nothing adjustable for this prediction. It also employs the crude $C^{hy}$ trajectories discussed above. The agreement, as fig. 15a shows, is excellent.

### IX.A.6. Modeling of the Enzyme's Action

Since the reaction that produces mevalonate is the rate limiting step in *de novo* cholesterol synthesis, we do not distinguish between mevalonate (M) and its end product, cholesterol (C). The rate expressions thus contain only mevalonate to represent the cholesterol that has been produced *de novo*. For the overall model it will be of interest to be able to predict the total amount of cholesterol synthesized *de novo*. Let us abbreviate the substrate, Hydroxymethylglutaryl CoA (HMG CoA) by H and the enzyme reductase by E. As we did earlier, we choose to use the same symbol to denote a species name in the context of describing reactions and its concentration in the rate equations.

For simplicity, we assume a simple Michaelis Menten form for the enzyme's action

$$\frac{dM}{dt} = \frac{k\,HE}{H+K_m} \tag{28}$$

where Ref.[4] gives a value of 5 $\mu$M for $K_m$. This then couples to equation (26) for the regulation of enzyme activity. In principle, one would solve this latter equation for E(t) and then plug into the former equation. However, since, as we noted earlier, the enzyme is usually quantitated not by its concentration but rather by the average amount of mevalonate that it produces per minute in assay, the values of H and of E are not usually available individually. In the overall model that interests us, the amount of cholesterol synthesized *de novo* over time scale longer than a few hours, where E will have already reached quasisteady values, is the relevant quantity. For such time scales one can set dE/dt = 0 in (26) and plug into (28). The

resulting expression for dM/dt is just the time rate of change of cholesterol due to *de novo* synthesis, or

$$\left.\frac{dC}{dt}\right|_{de\ novo} = \frac{\beta}{1 + K(C^{hy})^2}; \text{ where } \beta := \frac{kH}{H+K_m}\frac{n}{k_2+\mu}. \qquad (29)$$

In (29), $\beta$ corresponds to the maximum *de novo* synthesis rate, i.e., the rate corresponding to $C^{hy}=0$, of about 27 pmol/mg cell protein/hr. This value is the acetate-incorporation rate divided by the number of acetates per cholesterol, i.e., 400 acetate pmol/mg cell protein/hr[6] ÷ 15 mole of acetate/1 mol of cholesterol[83 6]).

A word of caution is in order before leaving this subsection. Recall that our model of *de novo* synthesis is based on data for cells in late logarithmic growth phase, i.e., nearly confluent cells. Physiologically, transcription and translation efficiency may be functions of cell density, i.e., they may be included in what's generally referred to as contact inhibition. In fact, the maximally induced HMG co-A reductase activity of human fibroblasts in logarithmic growth phase is more than three times that of confluent human fibroblasts (Fig. 16a and b). Our model also glossed over the contribution of cellular nonsterol metabolites to translation and neglected the degradation of enzyme by $C^{hy}$. Actually, the concentration of these nonsterol metabolites may change for long-time experiments. Therefore, even though our model does quite well for data on the order of hours, there are still too many factors of unknown importance for long time studies (i.e., many days or longer) that are not included, to extrapolate the model to such long times.

## IX.A.7. Estimation of the Rate Constant for the Degradation of $C^{hy}$ to C

With the models just derived for *de novo* synthesis in hand, we have the opportunity to crudely estimate the rate of $C^{hy} \rightarrow C$ at which $C^{hy}$ loses its ability to affect cellular regulation. Since the best fit constants above suggest a fast (hours) HMG CoA reductase activity degradation in the presence of $C^{hy}$ and some experiments (e.g., Fig. 16a and b) show a rather slow (1 day) recovery of the maximal HMG-CoA activity upon transfer of cells from an LDL-rich environment to LPDS, one can postulate that the degradation rate of the regulatory agent (i.e lysosomally hydrolyzed LDL cholesterol) limits the recovery process of the HMG CoA reductase and that it thus endows its time scale on the whole recovery process of HMG CoA reductase.

If one, at this stage, lumps the efflux of $C^{hy}$, another processes which depletes $C^{hy}$, together with $C^{hy}$ decay, the processes which govern the time evolution of $C^{hy}$ are esterification, hydrolysis and decay, which we symbolically represent in (30).

$$\begin{array}{cc} C & CE \\ \uparrow & \uparrow \\ C^{hy} & \underset{\leftarrow}{\rightarrow} \; CE^{hy} \end{array} \qquad (30)$$

Upon transfer to from an LDL-rich environment to an LDL-free LPDS medium, the uptake of LDL is restricted to the LDL

already bound to cell receptors before transfer; as we saw earlier, this value decays in about ten minutes. If one restricts attention to time scales much longer than ten minutes, then one may neglect new LDL supplied $C^{hy}$. In addition, if $CE^{hy}$ degrades to CE at the same rate at which $C^{hy}$ degrades to C, then the loss of regulation-active lipid is simply

$$\frac{d(C^{hy}+ CE^{hy})}{dt} = -k ( C^{hy} + CE^{hy}). \qquad (31)$$

If one notes that the time scale for esterification and non-lysosomal hydrolysis is hours and that of the decay of $C^{hy}$ and $CE^{hy}$ is much longer, one can crudely assume that the former two processes conspire to provide a time-invariant ratio of $C^{hy}$ to $CE^{hy}$. This simply leads to an exponential time course $C^{hy}(t)=C_o^{hy}\, e^{-kt}$ for $C^{hy}$.

For day-long time scales, *de novo* synthesis is quasi-steady at the values dictated by the "instantaneous" $C^{hy}$ concentration. Combination of the expression for the time evolution of $C^{hy}$ with the quasi steady expression for E in terms of $C^{hy}$ for *de novo* synthesis leads to

$$E = \frac{\eta/(k_2^e+\mu)}{1+K(C^{hy}(t=0))^2\, e^{-2kt}} \qquad (32)$$

The best fit value for k, the decay rate constant of $C^{hy}$, is about 0.092/hr. The curve in Fig. 16a is the crude estimate, equation (32), with this k.

## IX.B. Non-lysosomal Hydrolysis

### IX.B.1. The Rate Limiting Step of Nonlysosomal Hydrolysis

When there is adequate exogenous cholesterol, fibroblasts continuously esterify and accumulate cholesteryl esters to maintain the cellular level of free cholesterol essentially constant (cholesterol homeostasis). Alternately, they hydrolyze cholesteryl esters when there is too little exogenous cholesterol to meet cell's need for free cholesterol. Under prolonged conditions of high exogenous LDL, these cells drastically regulate their receptor tally and thereby the amount of cholesterol that they take up and must store in esterified form. As a result, fibroblasts are not observed to store large amounts of cholesteryl esters under normal conditions. Below focus on the process of non-lysosomal hydrolysis, whose rate-limiting step is promoted by a neutral nonlysosomal cholesterol esterase.[84]

### IX.B.2. Experimental Facts:

Goldstein *et al.*[82] asked whether, in addition to hydrolyzing exogenously derived cholesteryl esters, lysosomal acid lipase was also the enzyme that hydrolyzed endogenously esterified cholesteryl esters. To investigate this, they incubated normal

and mutant cells that were deficient in acid lipase with LDL in the presence of $^{14}C$ oleate in order to label the fatty acid moiety of endogenously esterified cholesteryl esters (Fig. 17). They then switched the cell medium to one that contained no LDL and further incubated them either in the presence or in the absence of chloroquine, which potently inhibits the lysosomal hydrolysis of exogenous cholesteryl esters. The cholesteryl $^{14}C$ oleate clearly shows first order decay (Fig. 17) where one half of the cholesteryl $^{14}C$ oleate disappears in 12 hours in normal cells and in 8 hours in the mutant cells. In contrast to chloroquine's potent inhibition of the hydrolysis of the exogenous cholesteryl esters, it had no inhibitory effect on the hydrolysis of endogenously synthesized cholesteryl $^{14}C$ oleate in either the normal or in the mutant cells.

Thus lysosomal acid lipase, although essential for the hydrolysis of incoming cholesteryl esters contained in LDL, does not appear to be critical to the hydrolysis of cholesteryl esters synthesized within the cell. More over, the the hydrolysis of the endogenously esterified cholesteryl esters is a process distinct from lysosomal hydrolysis of exogenously derived cholesteryl esters. Its kinetics appear to be first order. We propose the simple first order mechanism CE → C to account for nonlysosomal hydrolysis; it implicitly assumes that the concentration of free non-lysosomal cholesterol esterase is essentially time independent.

### IX.B.3. Determination of the Rate Constant for Non-lysosomal Hydrolysis

Since the experiment in Fig. 17 follows the decay of *initially loaded* $^{14}C$ labeled cholesteryl ester due to non-lysosomal hydrolysis, the change of labeled $^{14}CE$ concentration is due solely to hydrolysis, or

$$\frac{d^{14}CE}{dt} = - k\ ^{14}CE. \qquad (33)$$

The data analysis is simple in this case due to the log linear decay in Fig. 17. A simple estimation of $k \approx (\ln 2)/t_{\frac{1}{2}}$ gives $k \approx 0.001/min$.

## IX.C. Cholesterol Reesterification

### IX.C.1. Qualitative Aspects of the Reesterification processes

When normal fibroblasts are deprived of cholesterol by being incubated in the medium without LDL or any other exogenous cholesterol source, then $^{14}C$ oleate is not incorporated into cellular cholesteryl ester to any detectable degree[15], even though the cholesterol synthesis rate in the normal cells reaches its maximal value under such condition. On the other hand, when LDL is added to these cholesterol-deprived fibroblasts, the rate of $^{14}C$ oleate incorporation into cellular cholesteryl $^{14}C$ esters increases more than 500-fold within 6 hrs.[61] ACAT, a microsomal

enzyme or set of enzymes which is known to be nontranscriptionally regulated, catalyzes this reesterification of free cholesterol, triggered by hydrolyzed, LDL-derived cholesterol.[9]

There was two questions that one would naturally ask here. First, is cholesterol $C^{hy}$ derived from receptor-mediated LDL uptake the only agent that can activate ACAT activity? Second, does ACAT esterify only the cholesterol that activates it, or can ACAT, once activated, esterify other endogenous cholesterol as well? With regard to the first of these questions, Shireman *et al.*[58] incubated receptor-negative (i.e. homozygote familial hypercholesterolemic (FH) cells) and normal LDL receptor-positive cells with $^{3}H$ cholesterol labeled LDL. In addition to its participation in receptor-mediated uptake in normal cells, LDL can diffusively exchange its cholesterol, and in this case its $^{3}H$ cholesterol, with the cell's plasma membrane; this provides a second route for introducing LDL-derived cholesterol into the cells. However, determination of the $^{3}H$ cholesteryl ester's radioactivity indicated no detectable ester formation in the FH cells, even after 24 hrs. In contrast, in the receptor positive cells, appreciable radioactivity was present after 24 hrs. incubation in cholesteryl ester. Thus diffusional biflux of free cholesterol between cells and LDL in the medium does not appear to activate ACAT.[58]

As for the second question, Goldstein *et al.*[60] clearly showed that activated ACAT esterifies not only $C^{hy}$ but also endogenous cholesterol. Interestingly, however, some (up to about 1/3) but not all of the endogenous cholesterol seems to participate in the reesterification. Although many experiments have

shown such results, the mechanism regulating the fraction of the total cholesterol available for reesterification remains a mystery. In the next section, we propose a model for this regulation which we call "dilution kinetics." In essence, it suggests that hydrolyzed cholesterol initiates the reesterification process by activating endogenous cholesterol to join the cytosolic cholesterol pool available for reesterification.

The mechanism by which ACAT acts to esterify cholesterol is unknown. In fact, since ACAT is an integral membrane protein, sensitive to the nature of its environment, even its purification has proved very difficult. The kinetic mechanism by which ACAT esterifies cholesterol might be simple Michaelis-Menten kinetics, it may be allosteric, requiring the its binding to multiple substrates,[86] or it might be even more complicated. In the absense of large amounts of data specific to this question, we will opt in section IX.C.3. below, for the *simplest* model consistent with the available data.

## IX.C.2. Modeling of the Re-esterification Processes

### IX.C.2.a. Dilution Kinetics Model

An important question to ask is whether or not the intracellular cholesterol pools available for reesterification are isolated from the cell surface membrane cholesterol. In this context, it is interesting to note some experimental observations regarding cellular content of the agent sphingomyelin. Cellular degradation of sphingomyelin by the enzyme sphingomyelinase exerts a dramatic effect on the distribution of cell cholesterol between the cell surface and its intracellular membranes. Within 90 minutes after sphingomyelin hydrolysis begins, about 30% of the cell's total unesterified cholesterol transfers from the plasma membrane to intracellular membranes.[87] This mass movement of cholesterol away from plasma membranes presumably results from a decreased capacity in sphingomyelin-poor cells of the plasma membranes to solubilize cholesterol.[88] In addition, the total cellular mass of cholesteryl ester is significantly higher in sphingomyelin-depleted fibroblasts 3 hours after exposure to sphingomyelinase than in untreated fibroblasts. The sphingomyelin depleted cells also showed a reduction in the rate of endogenous synthesis of cholesterol.[87] These results are consistent with a rapid movement of cholesterol from sphingomyelin-depleted plasma membranes to a putative intracellular regulatory pool of cholesterol and thus suggest that these locations are not metabolically isolated from one another.[87]

It seems that an increase in $C^{hy}$ and a sphingomyelin depletion have the common effects of decreasing *de novo* cholesterol

synthesis and of increasing cholesterol esterification. sphingomyelin depletion also causes a rapid redistribution of a fraction of the cell's cholesterol. These facts suggest a a simple mechanism for the regulation of cholesterol esterification: By controlling the supply of substrate to the esterifiable cholesterol pools, $C^{hy}$, the cholesterol that recently entered via the high affinity pathway, might cause movement (or, kinetically, the conversion) of cholesterol from a pool that is not amenable to esterification (let $C^{u}$:-unavailable cholesterol) to one ($C^{*}$) that is, i.e., $C^{hy} + C^{u} \rightarrow C^{hy} + C^{*}$. Both $C^{hy}$ and $C^{*}$ then comprise the cholesterol $C^{a}=C^{hy}+C^{*}$ available for esterification. Note that $C=C^{u}+C^{a}=C^{u}+C^{*}+C^{hy}$. In the absence of exogenous cholesterol, this pool remains empty and esterification does not occur. Finally, cholesterol in this pool can relax back to the unesterifiable pool, or $C^{*} \rightarrow C^{u}$.

It is our intention here neither to restrict the identification of esterifiable and non-esterifiable cholesterol pools to the plasma and intracellular membranes nor to limit the inter-pool exchange mechanism to being diffusional rather than reaction, pool-type conversion or some combination. Our aim here is only to propose a mechanism capable of accounting for the observed management of available and unavailable cholesterol together with the observed strong sensitivity of the esterification process to small changes in $C^{hy}$. We also aim to suggest evidence that makes our dilution kinetics model biologically plausible.

The sphingomyelin data suggest that the inter-conversion between pools is fast and, in particular, at least as fast as

esterification. Thus, it seems reasonable, for simplicity and to reduce the number of free parameters, to assume that the two reactions that manage the available cholesterol supply rapidly equilibrate. Let the subscript eq denote, "equilibrium value." Define an equilibrium constant M for the reaction pair $C^{hy} + C^{u} \rightarrow C^{hy} + C^{*}$ and $C^{*} \rightarrow C^{u}$ as $M := C^{*}_{eq}/(C^{hy}_{eq}C^{u}_{eq})$. This allows us to express the concentration of cholesterol $C^{a}$ available for reesterification as an algebraic function of the total endogenous cholesterol C and the hydrolyzed cholesterol $C^{hy}$ concentrations, *vis.*,

$$C^{a} = C^{hy}\,\frac{1 + MC}{1 + MC^{hy}}\,. \qquad (34)$$

Thus this model rapidly effects a magnification of $C^{hy}$, typically present only as a small fraction of the total endogenous cholesterol, into a significant esterification substrate as or before one observes regulatory effects.

Although there is scant direct evidence as yet to support this model, it provides, as we shall see, a unified explanation of a number of observations about this system.

### IX.C.2.b. Model for the Action of ACAT: Re-esterification

It is natural to ask if the action of ACAT proceeds via a straight-forward Michaelis-Menten mechanism. If F represents a presumed time-invariant fatty acid concentration and $E_4$ represents ACAT, then such a mechanism would be

$$C' + E_4 \underset{\leftarrow}{\overset{\rightarrow}{}} (C'.E_4) \overset{F}{\rightarrow} CE + E_4 \qquad (35)$$

or whether it is allosteric, e.g.,

$$\begin{aligned} C^a + E_4 &\underset{\leftarrow}{\overset{\rightarrow}{}} C^a.E_4 \\ C^a.E_4 + C^a &\underset{\leftarrow}{\overset{\rightarrow}{}} C^a.E_4.C^a \\ C^a.E_4.C^a + F &\rightarrow (C^a.E_4) + CE, \end{aligned} \qquad (36)$$

with regard to the substrate cholesterol. At first glance, the S-shaped curve (Fig. 18 representing the labelled cholesteryl ester formed after incubation with LDL (60 $\mu$g/ml.) for the time indicated on the abscissa followed by one hour incubation with $^{14}$C-oleate) might suggest an allosteric mechanism. However, the almost three hour delay before labelled oleate shows a significant incorporation into cholesteryl ester may simply be due to the induction time of endogenous $C^{hy}$ from the LDL in the medium and not necessarily to a complex esterification mechanism. Thus, in the absence of a compelling reason to choose a more complex model, we opt for the simple Michaelis Menten explanation of the esterification process. We now combine this model with the model for cholesterol pool management in order to compare with experiment and to determine the rate parameters.

### IX.C.3. Determination of Rate Constants for Esterification

#### IX.C.3.a. Estimate of a 1/M

Before proceeding to properly fit the model's parameters, we reexamine Goldstein J.L. *et al.*'s evidence[60] for the existence of esterification-accessible and non-accessible cholesterol pools to estimate the proposed equilibrium constant M. Goldstein *et al.* incubated cholesterol-starved cells in 10 $\mu$g/ml labelled LDL (the LDL's cholesterol linoleate, about one third of its total cholesterol content, contained a $^{3}H$ label) and labelled $^{14}C$ oleate. After 12 hours (Figs. 19a,b), about 3x2200-6600 pmol LDL-derived cholesterol and 3200 pmol $^{14}C$ oleate-labelled cholesteryl esters, 3x250-750 pmol of which were reesterified and LDL-derived, resulted per milligram cell protein. Clearly, some LDL-derived cholesterol caused endogenous free cholesterol to esterify, but a complete dilution of incoming LDL-derived cholesterol with cellular free cholesterol ($\sim 10^5$ pmol/mg cell protein) would have resulted in an LDL-derived esterified fraction of 6600/100,000~1/15, rather than the observed value of 750/3200~1/4.3.

Due to the decay of $C^{hy} \rightarrow C$, not all of the LDL-derived cholesterol, say $C^L$, remains $C^{hy}$. In terms of $C^L$, one can calculate the fraction of cellular cholesterol available for esterification as about $C^a/C = (C^L/C)/(C^L/C^a) \approx 4.3/15 \approx 0.3$. This rough estimate clearly neglects the fact that in the early part of the 12 hour period the fraction of the total endogenous cholesterol that was LDL-derived was much less than the final value; however, during this induction period esterification had not yet been induced and thus very little esterification took place. In addition, one can estimate M by equating the model expression $(1+MC)/(1+MC^L)$ for the inverse of the fraction of the available

cholesterol that is LDL-derived with the measured value of 4.3. This gives $1/M \approx 22{,}000$ pmol.

### IX.C.3.b. Estimation of the Rate Constants for Esterification

We now appear to be in a position to combine the dilution kinetics model for esterifiable cholesterol management with the model for the action of the enzyme ACAT and to use the experimental data to determine the rate constants. Let's begin by examining a typical experiment[35] (Fig. 12c). One transfers cells that have been preincubated for 48 hours in LPDS to a medium containing graduated amounts of LDL. After five hours incubation, one adds a fixed amount (0.1 mM) of radioactive $^{14}$C-oleate to the medium and measures the $^{14}$C-oleate incorporated into the cholesteryl esters formed over the next 60 minutes. Clearly, an interpretation of *these* experiments requires more than just a model for the esterification process. The rate expression for usual esterification, as written in the previous section, implicitly includes the concentration of oleate F (for fatty acid) as part of its rate constant, i.e., $k_8 = k_{80}F$. Since we presume that the typical situation is one where fatty acid for use in esterification is in an ample, fixed, time-invariant supply, it is reasonable to normally include it in $k_8$. However, in experiments like the one just described, labelled fatty acid, $^{14}$F, is *not* present in excess, even though the total F may be; $^{14}$F is supplied to the medium and must transport into the cell before participating in the production of labelled cholesteryl ester C$^{14}$E. Thus the rate of the transport process of $^{14}$F couples to

the esterification kinetics for the interpretation of the said experiments and we must therefore model these processes together.

With all of this said, let's consider a time dependent experiment which can tell us something about this transport. Fig. 20[98] preincubates cells for 17 hours in LPDS plus LDL, adds 0.1 mM $^{14}$C-oleate and finds the the incorporation of labelled oleate into cholesteryl ester is quite linear for at least the first four hours. (The experiment in Fig. 20 chose 0.1 mM of labelled oleate because the precursor experiment found radioactive oleate incorporation plateauing at this concentration and higher concentrations leading to only marginally higher and probably artifactual values.) The expression for the evolution of $C^{14}E$ is simply:

$$\frac{dC^{14}E}{dt} = \frac{k_{80}{}^{14}F\ C^a}{k_7+C^a} - k_h C^{14}E. \qquad (37)$$

We shall assume that after 17 hours in LPDS/LDL, $C^{hy}$ has either reached a quasisteady value or has at least become a very weak function of time, varying little over the four hours of the current experiment. Thus one can lump the factors in the first term on the right of this equation into a time-invariant (at least for the four hours in question) factor $\eta = k_{80}C^a/(k_7+C^a)$ times $^{14}F$, with $C^a$ as given in the previous section. For $^{14}F(t)$ we simply assume that fatty acid transport proceeds simply via a mass transfer coefficient multiplied by a (presumed time-invariant) medium concentration, which integrates simply to $^{14}F = {}^{14}F_0(1+\gamma t)$. The resulting expression is

$$\frac{dC^{14}E}{dt} = \eta^{14}F_0(1+\gamma t) - k_h C^{14}E. \qquad (38)$$

From the figure, $C^{14}E$ is linear with time, i.e., $C^{14}E=\beta t$, for $\beta=3$ (nM/mg protein)/hr. and $dC^{14}E/dt=\beta$. Thus, $\eta F_0=\beta$ and $\gamma=k_h$. We shall use this $^{14}F$ transport expression to interpret all of the experimental data involving labelled oleate added to the medium. Let us return to Fig. 12c[35] to do just this.

Recall that in Fig. 12c, cells preincubated for 48 hours in LPDS and then for 5 hours in LDL receive 0.1 mM labelled oleate; the figure displays the labelled cholesteryl ester formed during the succeeding hour. Using the previous equation with the expression $C^a=C^{hy}(1+MC)/(1+MC^{hy})$ to describe this curve should, with the aid of the parameter fitting scheme described in the numerical methods section, allow a least squares fit for $k_7$ and $k_{80}$. This method, however, needs a value for M, a quantity for which only an estimate is as yet available. One can either take M equal to this estimate or fit it simultaneously with $k_7$ and $k_{80}$. An alternative procedure is to note that Figure 12b accompanying Figure 12c provides a simultaneous measurement of $C^L$, which bounds $C^{hy}$ from above. In fact, for the 5-6 hour period after the introduction of the cells into the LDL-containing medium during which the experiment takes place, the saturated value of $C^L$ is about 2700 pmol/mg. A conservative estimate for $MC^{hy}$ follows as $2700/22{,}000 \approx 0.12$. Thus, the denominator of $C^a$ is dominated by 1 *for this experiment* and the overall expression reduces to

$$\frac{dC^{14}E}{dt} = \frac{k_{80}{}^{14}F\ C^{hy}}{k_7/(1+MC)+C^{hy}} - k_h C^{14}E. \qquad (39)$$

Appendix I gives an error analysis for this approximation.

The best fit values for $k_{80}F_0$ and $k_7/(1+MC)$ are 90 (pmol/min)/mg cell protein and 9654 pmol/mg cell protein, respectively. The curve in Figure 12c is the best fit plot. This still leaves us with the task of estimating $k_{80}$.

Since $k_{80}$ and $F_0$ always appear multiplied together, it is unnecessary to try to separate out individual values for $k_{80}$ and $F_0$. We choose rather to estimate the biologically relevant $k_8$ corresponding to the *endogenous fatty acid supply*, as opposed to the labelled supply in the above-mentioned experiments, and then use an independent piece of data to check the reliablity of the calculation. Table I of ref. 82, notes that the 35% of endogenous cholesteryl ester is cholesteryl oleate. If the non-lysosomal hydrolysis rate is the same for all fatty acid cholesteryl esters, then the ratio of the values of $k_8$ for the endogenous and the labelled fatty acid pools should, as an independent check, yield a value for this percentage well. Alternately, since the $k_8$ value for the endogenous fatty acid pool is only known to within a factor of three, one can obtain an independent estimate of it from the labelled-pool's value and the table's reported percentage. The result is ~260 pmol/mg/min. Fig. 22a[9] shows the evolution of intra-cellular reesterified cholesterol after three days LPDS incubation followed by incubation in 10 $\mu$g/ml LDL. The figure shows that the cholesteryl ester level goes through a maximum at about 24 hours and then

slowly decreases over the next three days as, and presumably because, the receptor number down-regulates.

An estimate for $k_8$ follows simply from balancing the rates of reesterification and non-lysosomal hydrolysis (dCE/dt=0 - see Equation (37). CE and F replace $C^{14}E$ and $^{14}F$) at 24 hours. From the earlier sections we may assume that $C^{hy}$ at 24 hours ranges between 1000 and 3000 pmols/mg protein. Taking an approximate value of M as 1/22,000 pmol/mg protein gives a value of 144-342 pmol/min./mg for $k_8$ (as opposed to the value 90 pmol/min./mg determined above for the labelled pool), which comfortably includes the predicted rate constant, 260 pmol/mg/min. Alternately, one could have used the other values to estimate $C^{hy}$ and found that it lies within the given range.

## IX.D. Cholesterol Efflux and Cholesterol Depletion from Cells

### IX.D.1. Introduction

The LDL receptor pathway and bulk fluid phase pinocytosis both deliver exogenous cholesterol to the cells. So can the diffusive transfer of free cholesterol from lipoprotein particles to the celluar membrane. When there is a dearth of exogenous cholesterol, *de novo* processes synthesize cholesterol to augment and to maintain endogenous levels. All of these processes increase cellular cholesterol. Cellular esterification of free cholesterol and the hydrolysis of cholesteryl esters just interchange these two forms and do not affect the aggregate amount of cholesterol and its esterified form. Thus cells that do not

produce steroid hormone or bile acid (e.g., human fibroblasts) clearly need a mechanism for eliminating or depleting cholesterol in excess of that needed for the synthesis of membrane. These processes amount to the (typically diffusive) efflux of free cholesterol molecules to extracellular acceptor particles in medium.

Before discussing these processes in detail, it is important to recall that a major use for cholesterol is the production of new membrane for cells undergoing mitosis. For dividing cells, such as those in sparse cell culture, this use is very significant. However, once cells such as fibroblasts (which tend to form monolayers) reach a number density such that they touch, their mitotic processes undergo a contact inhibition and cell division proceeds in tandem with cell death. *In vitro* this stage is called confluence whereas *in vivo* in, for example, the endothelial cells of the arterial endothelium, it is called quiescence. An important distinction between confluence and quiescence is that the rate of cell turnover is much lower in quiescent cells.

At first blush, one might suspect that membrane synthesis as needed for the production of new cells could account for cholesterol depletion. However, as noted in the Preliminaries Section III.A and briefly reviewed here, the units in which experimental results are reported are, uniformly, per-unit cell protein mass units. Thus, as described in that section, the kinetic formalism resembles that used in the study of non-constant density chemical reactors. Here we only reiterate the upshot of this discussion: that the specific growth rate term $\mu:=(1/V)(dV/dt) \sim 0.01/hr$ for rapidly dividing cells, V being the total cell protein mass, enters into the kinetic formalism in order to account for such

processes; and, that an explicit depletion, i.e., efflux is still necessary in order to close the mass balance.

With this said, let's proceed to the mechanics of cholesterol efflux. Even though its aqueous solubility is small (its critical micelle concentration is about $3x10^{-8}$ M), cholesterol manages to transfer to and from cell membranes by virtue of the presence of so-called cholesterol acceptors (such as various lipoprotein molecules, e.g., HDL) in the medium. In the presence of these acceptors, the aqueous solubility of cholesterol is still sufficient to account for the observed flux of cholesterol between different lipoprotein particles, or between lipoproteins and cell membranes[10]. The overall process involves desorption of free cholesterol from the membrane, diffusion of cholesterol in the aqueous phase between cell membrane and acceptor particles (HDL) and, finally, adsorption on or attachment to these particle. Phillips *et al.*[91]suggested that the rate of dissociation of cholesterol from the plasma membrane into the surrounding aqueous milieu may control the rate of loss of cholesterol from the cell when the acceptor is in excess. Interestingly, specific HDL binding to the cell surface does not seem to enhance or facilitate cholesterol efflux.[92]

Of the so-called promoters or acceptors, the most potent known example of which is lipoprotein deficient serum. The maximum saturated efflux rate occurs at LPDS concentrations greater than 1.5 mg protein/ml.[93] Luckily, most of Brown and Goldstein's *in vitro* studies, upon which we base much of our kinetic analyses, employed a basic medium that contained more than a saturable LPDS protein concentration. Thus, for the data that we analyze and, in principle, for *in vivo* situations as well, efflux

is not limited by the acceptor's concentration in the medium, but by only the desorption of cholesterol from the plasma membrane.

In addition to the notion of cholesterol acceptors, there is a vast literature debating and describing the details of the efflux mechanism. Our goal here is a modest one: not to become efflux experts, but rather to construct a simple model which closes the cholesterol mass balance for a pulse initial input of labeled cholesterol and accurately models the basic efflux measurements. This model will play an important role in the regulation of the active agent (see Section VIII.C) $C^{hy}$, constituting its efflux/depletion.

### IX.D.2. Experimental Facts Important for Modelling Cholesterol Efflux

To study cholesterol efflux, Rothblat and Phillips[94] loaded human fibroblasts with $^{3}$H-cholesterol (by preincubating them with $^{3}$H-cholesterol-labeled LDL ($^{3}$H C-LDL) for 48 hours) and then incubated them in medium saturated with the acceptor HDL. Measurement of the fraction of the initial labelled cholesterol charge remaining in the cells as a function of time of incubation shows an exponential (linear in a semi-log plot), i.e., first order, region lasting about 19 hours, until about 35% of the initial charge remains. The decay rate of about 0.02/hour then changes to a slower efflux[94] in the 24-72 hour range. This slowing is attributed neither to lateral cholesterol redistribution between different regions of the plasma membrane nor to the "flip flop" of cholesterol across the cells' plasma membranes. Lateral

redistribution along the plasma membrane (which contains about 90% of the cell's total free cholesterol) is fast[95]; cholesterol flip-flop is not rate limiting for the removal of cholesterol from cells.[96]

Which cellular processes then are related to efflux? To show that efflux appears to have nothing to do with the LDL receptor, Wu *et al.*[97] conducted the cholesterol efflux experiment with normal human fibroblasts and with homozygous FH cells. Both cell lines showed similar efflux rates at 6 hours incubation under various acceptor conditions. Also, chloroquine, which inhibits lysosomal function, does not affect efflux, suggesting a mechanism independent of the lysosomes.[93]

Finally, we note that cellular cholesteryl esters decreased in a log-linear fashion for up to 72 hours in the above experiment. In addition, almost all of the cholesterol and cholesteryl ester (>90%) that was lost from the cell by efflux appeared in the efflux medium as free cholesterol, indicating that hydrolyzed cholesteryl esters also participated in efflux.[93]

### IX.D.3. Kinetic Modeling of Efflux

Based on the the above-mentioned experimental facts, a natural guess for an efflux model is simply CE → C → O, i.e., free cholesterol transfers via a first order process out of the cell while cholesteryl ester hydrolyzes to free cholesterol which can then also efflux; this would account for the two time scales noted above, since upon depletion of available free cholesterol, the rate of cholesterol hydrolysis would come to dominate the effective overall efflux rate. Unfortunately, certain facts speak

against this interpretation: In the above experiment, labeled CE was negligible, compared with labeled C and labeled C remains large even after 3 days of efflux.

Next, one might imagine that $C^{hy}$ somehow controls efflux, with a higher concentration of $C^{hy}$ raising the efflux rate: $^{3}H$-cholesterol LDL preincubation leads to an initial charge of $C^{hy}$, which decays (and effluxes) as the experiment proceeds. However, as noted in the last section, efflux measurements show no difference between normal human fibroblasts and homozygous FHs, the latter having no $C^{hy}$.

Thirdly, one can imagine that *two* efflux pools exist: Once the faster efflux pool is depleted, the slower efflux pool dominates. However, rapid lateral redistribution of the efflux pool in plasma membrane would cause the remaining $^{3}H$-cholesterol not to show the log-linear decay behaviour described in the last section.

The only simple model that doesn't seem to contradict this list of experimental facts is biflux. For initial short times, one only observes the forward reaction, the efflux $C \rightarrow C_m$, where $C_m$ is the cholesterol concentration of the medium; at long times, the reverse reaction, influx, becomes important and one observes $C \underset{\leftarrow}{\overset{\rightarrow}{}} C_m$.

### IX.D.4. Estimation of the Rate Constants for Efflux

#### IX.D.4.a. The Efflux Rate Constant

Given the model just arrived at, we estimate the rate constant $k_e$ for efflux from several independent sets of data. As shown below, these various estimates agree with one another.

Golstein *et al.*[82] (Fig. 13) pre-incubated human fibroblasts in LPDS for 24 hours, transferred them to medium containing LPDS (2.5 mg/ml protein concentration) and 10 $\mu$g protein/ml of labeled cholesterol linoleate ($^3$H CL-LDL) and measured the time evolution of the $^3$H-labeled free cholesterol concentration in the cells. They found that no detectable amount of $^3$H-labeled hydrolyzed cholesterol formed during the first 8 hours of the incubation, had effluxed from the cells into the medium, and less than 10% thereafter.

If one assumes that dissociation from the membrane surface is the limiting step in efflux (since the acceptor is in excess) and if one neglects diffusive influx of the already effluxed $^3$H-labeled hydrolyzed cholesterol (due to its dilution in the medium) for the, say, first twelve hours of the experiment, the total label lost via efflux over these twelve hours is simply the integral of the efflux rate ($k_e C^L(t)$) over time t from zero to twelve hours, with $C^L(t)$ given from the data. Setting the ratio equal to 0.1 and solving for $k_e$ gives about 0.02 /hr. Since we have neglected influx, this value is, in principle, a bit low.

Let's now return to Clair *et al.*'s experiments and use it to calculate the rate constants for our efflux model. Recall that the efflux of labelled cholesterol from loaded cells was initially first order and later slowed. If one focuses on the labeled cholesterol and cholesteryl esters only, then according

to our model, cholesterol is effluxing to the medium and cholesteryl ester is hydrolyzing into cholesterol. In addition, some residual hydrolyzed cholesterol may still be esterifying some of the endogenous cholesterol. Initially, the concentration $^3C_m$ of labeled cholesterol in the medium is zero and, since the influx rate $k_i\,^3C_m$ is proportional to $^3C_m$, the influx is unimportant in the early phase. Thus, our model for the early dynamics is simply

$$\frac{d(C^3E+{}^3C)}{dt} = -k_e\,^3C. \tag{40}$$

Integration gives

$$(C^3E + {}^3C)_{t=12} - (C^3E + {}^3C)_{t=0} = -k_e\int_0^{12} {}^3C\,dt. \tag{41}$$

Short time data for $C^3E$ and $^3C$ allows evaluation of the integral as well as the left side of the equation. The resulting value for $k_e$ is 0.02/hr, very close to the last estimate.

For longer times, the concentration $^3C_m$ builds up and influx becomes important. One must now keep track of the concentration $^3C_m$ as well. Thus instead of equation (25), one writes

$$\frac{d(C^3E+{}^3C)}{dt} = -k_e\,^3C + k_i\,^3C_m; \tag{42}$$

$$\frac{d^3C_m}{dt} = A(k_e\,^3C - k_i\,^3C_m). \tag{43}$$

Note that the units of $^3C$ are pmol/mg cell protein whereas those of $C^3E$ are pmol/ml. This requires the units of $k_i$ to be (ml/mg cell protein)/hr and there to appear a conversion factor A with units total cell protein/culture medium volume. Integration and rearrangement gives

$$(C^3E + {}^3C)_{t=0} - (C^3E + {}^3C)_{t=\tau} - k_e\int_0^\tau {}^3C\, dt = - k_i\int_0^\tau {}^3C_m\, dt. \quad (44)$$

Since the total label is conserved, in principle, data for $^3C(t)$ and $C^3E(t)$ allow calculation of $^3C_m(t) = A\,(C^3E(0)+{}^3C(0)) - (C^3E(t) + {}^3C(t))$. Figure 14 shows a plot of the left side of this equation vs the integral on the right, with the points corresponding to different values of $\tau$. The slope of the least squares line through the data gives $k_i \sim 0.25$ ml/hr/mg protein where A is assumed to be 0.1 mg protein/ml.

If one simply phenomenologically uses the model from equation (40) rather than (42) to fit the late time data and calculates an effective $k_e$ for that data, one gets 0.0005/hr. Interestingly, if one notes that *de novo* synthesis incorporates 15 moles of acetate into one mole of synthesized cholesterol and assumes that the minimum level of total cellular free cholesterol is ~20$\mu$g/mg protein, then this effective value of $k_e$ for long times balances quite closely the *de novo* synthesis rate (see section IX.A.6) for LPDS incubation; the maximum value of this rate is ~.01 $\mu$g cholesterol/mg cell protein[6 83] (see section IX.A.6).

It is also worth noting that these data present us with an opportunity to independently check the rate constant $k_h$ for non-lysosomal hydrolysis determined in section IX.B.3.. In particular, the $^3C$ and $C^3E$ data, together with the model $C^3E \rightarrow {}^3C \underset{\leftarrow}{\rightarrow} {}^3C_m$ that neglects esterification (and thus the earliest data points) gives $k_h \sim 0.0009$/min, which is (embarrassingly) close to the earlier value of .001/min. from section IX.B.3.

Let us take a moment to recall our overall goal, to model the kinetics of the overall regulatory processes and hence of the cellular cholesterol pathway. As discussed in the preliminaries, a quantity which we have called $C^{hy}$ seems to be the active agent in the regulation and it is therefore incumbent upon us to model all of the processes that contribute to the dynamics of the $C^{hy}$ concentration carefully. It was with this in mind that we began to crudely model cholesterol and, in particular, $C^{hy}$ efflux. As such, we believe that for these purposes, influx is rarely significant and can be dropped from the model. There are at least two reasons for this. First, the rate constant for the degradation $C^{hy} \rightarrow C$ of $C^{hy}$ is about three to four times as fast as the estimated efflux rate constant. Thus long before $C_m^{hy}$ gets large enough to make $C^{hy}$ influx appreciable, most of it would already have been destroyed. Second, if $C^{hy}$ is really an oxidized form of cholesterol, then the natural presence of antioxidants in the *in vivo* medium[107] would reduce the concentration $C_m^{hy}$, and hence the influx rate, to zero. Thus in the remainder of this work we

neglect cholesterol influx; instead, we simply work with the simple efflux model $C^{hy} \rightarrow 0$, with $k_e = 0.02/hr$.

## IX.E. The Regulation of Receptor Number

### IX.E.1. Overall View

Cultured human fibroblasts typically derive cholesterol for membrane synthesis from plasma low density lipoproteins contained within the culture medium.[53] As we have seen, the cellular uptake of LDL-cholesterol follows a series of processes in which LDL first binds to a specific cell surface receptor[98], then internalizes by endocytosis to the lysosome where lysosomal enzymes hydrolyze its protein and cholesteryl ester components.[59]

The study of fibroblasts from patients with the homozygous form of Familial Hypercholesterolemia[99] that lack functional LDL receptors has aided the analysis of the events mediated by the LDL receptor enormously. These mutant cells cannot bind, take up, and degrade the lipoproteins with high affinity[99] and therefore neither suppress 3-hydroxy-3-methylglutaryl coenzyme A reductase activity[100] nor activate acyl-CoA:cholesteryl acyltransferase in the presence of LDL.[36 62]

The overall result of incubating normal fibroblast cells having functional receptors with LDL is to increase the cellular content of free and esterified cholesterol.[53] Since the LDL receptor's *raison d'etre* is to introduce plasma LDL's cholesterol into cells, one might expect LDL binding activity to be suppressed when the cells have accumulated enough cholesterol.[36] In fact, when fibroblasts grow continuously in LDL-containing

medium, the cells down-regulate their LDL receptor tally so ao to take up only enough cholesterol necessary for new membrane synthesis and to replace sterol lost via membrane turnover.[9] Typically, the number of receptors expressed upon long-time incubation at high LDL concentrations is less than 10% of the maximal number that the cells are capable of synthesizing.[9]

### IX.E.2. The Cell Biology of Receptor Synthesis and Degradation

Closely following and largely quoting from Ref. [102], we relay a bit about the cell biology of receptor synthesis and degradation:

The transcription of the structural genes for LDL receptors leads to the export from the nucleus of an mRNA species that encodes the complete sequence of amino acids required to form the receptor protein. The rate at which these new mRNA blueprints appear in the cytosol is the main controlling part of the up- and down-regulation of the receptor number in the body's cells.[102]

The LDL receptor is synthesized in the rough endoplasmic recticulum (ER). It is likely that free cytosolic ribosomes begin to translate the mRNAs that encode the LDL receptors, synthesizing hydrophobic signal sequences that permit the docking of the relevent ribosomes on specific sites of the rough endoplasmic recticulum. Translocation to the Golgi apparatus, either by membrane flow from the recticulum or, more likely, by a system of directed vesicular transport occurs soon thereafter. In the complex enzymatic processing factory of the Golgi plates and vesicles, chemical and configurational modification, processes that are closely associated with the net movement of the receptor

molecules to their functionally important positions on the cell surface, occur.[102]

As is well known, the LDL receptor is sometimes degraded. However, unlike the EGF system where the lysosome degrades a substantial fraction of the receptors that are internalized, the LDL receptor appears to separate from its ligand in the endosome and to quickly recycle to the cell surface. The enormous organizational and structural complexity of the entire Golgi-endoplasmic recticulum-lysosome region makes it likely that there may be other places where the receptor molecules is degraded. The secondary lysosome (the endosome) exposes the bulky and protease-sensitive ligand binding domain of the receptor to the cathesins and other lysosomal peptidases; it is thus a likely seat of degradation.[102] All that is certain, though, is that the necessity for effective regulation of receptor number means that degradation must occur at a rate that is appropriate for the transition from one steady value of the receptor number to another. It is not known whether the susceptibility of receptor molecules to available proteases or the rate at which receptors are partitioned into the degradation compartment controls the receptor degradation rate.[102]

### IX.E.3. Experimental Facts

As already noted many times, prolonged incubation of fibroblast cells with LDL results in a drastic down-regulation of the receptor number. In general, a maximal number of LDL receptors is reached after actively growing fibroblasts have been incubated for 48-72 hours in the absence of LDL and this number

decreases by more than 90% in the presence of LDL.[9] To investigate this phenomenon further, Brown and Goldstein[101] incubated human fibroblasts in LDL-free LPDS and then added the potent protein synthesis inhibitor cycloheximide; a first order decay in receptor number with a half-life of about 25 hours[1] ensued, thereby kinetically characterizing the LDL-free receptor degradation processes. A similar decay occurred upon incubation with 10 $\mu$g/ml LDL and no cycloheximide, after a short induction period of about two hours. Thus LDL seems to shut off receptor production and to allow simple receptor attrition. Interestingly, addition of chloroquine, a lysosomal inhibitor, in addition to LDL leads to no decay in receptor number. Chloroquine's lysosomal interruption would not only interfere with any receptor degradation that took place there, but it would also obstruct the delivery of the LDL-derived regulatory agent $C^{hy}$. Apparently, the interference with degradation is more important than the lack of $C^{hy}$ on the receptor tally and thus on the processes that replenishing the receptors normally lost to attrition. What are these replenishing processes?

Hybridization studies in cultured cells of the mRNA responsible for the production of the receptor protein have shown that the presence of sterols in the culture medium markedly reduces the amount of this mRNA.[104] Thus the feedback regulation of the

1. Experiments involving the insulin receptor suggest that cycloheximide may interfere not only with receptor synthesis but also with receptor decay, thus leading to an overestimate of the decay time.[103] However, these experiments are limited to the insulin receptor. The half-life of the LDL receptor is sometimes actually given as about 30 hours,[102] even longer than the 25 hours stated here. Thus for LDL receptor, we neglect this effect.

LDL receptor protein[74] is a molecular level suppression of receptor m-RNA concentration, which we take to be a suppression in its synthesis.

Let us now examine the kinetics of receptor turnover a bit more carefully. Recall that cycloheximide incubation without LDL, which presumably totally shuts off receptor production, led to a first order receptor decay characterized by a half-life of about 25 hours; this corresponds to a decay constant of 0.028/hr. On the other hand, incubation of cells initially expressing their maximum receptor tally with 10 $\mu$g/ml LDL leads to a first order decay with a half-life of 15-20 hours[9], or a decay constant of 0.036-0.048/hr. Fibroblasts whose receptor numbers had been down-regulated by 24 hour incubation with 10 $\mu$g/ml LDL exhibited a 14 hour half-life (decay constant $\approx$ 0.051/hr) upon addition of cycloheximide to the medium (Fig. 21[101], solid triangles). At saturating concentrations of LDL, e.g., 50 $\mu$g/ml as in Fig. 22b, the decay rate is the inverse of the measurement time multiplied by the natural logarithm of the ratio of the final and initial receptor tallies, or ln(145/25)/24(hr)=0.07/hr., which gives a half-life of 9.5 hours. Using (0.6 $\mu$g/ml) 25-hydroxycholesterol, a form of cholesterol that is more potent than LDL-derived cholesterol in instigating regulation, in ethanol caused a 50% decrease about every 10 hours[101] (Fig. 23) in one experiment and a decay rate of ln(140/27.6)/25(hr) = 0.065/hr (a half-life of ~10.7 hours) in another (Table 1 of ref. 101). These values are both quite similar to that obtained upon incubation with 20 $\mu$g/ml LDL (Table 1 of ref. 101), which had a half-life of 11 hrs and a decay constant of ln(140/29.3)/25(hr) = 0.063/hr. As one can see from this collection of data (plotted in Figure 25), the half-lives seem to get shorter, i.e., the decay constants seem to

increase, as the LDL concentration increases up to saturation levels and these half-lives are shorter than the cycloheximide-induced, presumably non-receptor producing and purely decaying half-life. In addition, the fact that four days incubation with either 10 or 50 $\mu$g/ml LDL results in similar receptor tallies (Figs. 22a and b) suggests that receptor production is already turned off at some value less than or equal to 10$\mu$g/ml.

These facts suggest that $C^{hy}$ may, in addition to interfering with receptor mRNA production, also actively participate in a post-translational receptor destruction process such as $C^{hy}+R \rightarrow C^{hy}$, although such a process would still be less important than mRNA inhibition and attrition. Such an additional minor regulation would only affect the dynamics of receptor number decay during the first few days and hardly impact the long time receptor value. At long times R would be small. So too would $C^{hy}$, since the receptor tally would be low. Thus the rate of this reaction would be negligible. In fact, a close (and possibly wishful) examination of individual experimental curves seems to be consistent with or even to suggest something like this, despite the small number of data points per curve. For example, Fig. 24 (LDL but no chloroquine) follows the receptor number as a function of time after introduction of LDL into the medium and seems to be multi-exponential. At first, little changes as the cell takes up LDL and breaks it down into $C^{hy}$. As the $C^{hy}$ level increases, the receptor synthesis rate should quickly shut off and a pure attrition process would lead to a straight line semi-log plot. The rate of decay, however, seems to initially increase in parallel with the increase in $C^{hy}$ and

then to slow as the concentration of R and of $C^{hy}$ gradually decrease to their steady, low levels. This is quite consistent with a process such as $C^{hy}+R \rightarrow C^{hy}$ in addition to attrition and interferable synthesis. Fig. 25 shows the half-life of the receptor number under different medium LDL concentrations.

One can even roughly estimate the magnitude of this alternate degradation process by comparing the cycloheximide degradation rate with the one realized at 10 μg/ml LDL. The difference in degradation constants is 0.051/hr-0.028/hr=0.023/hr. After a few days LDPS incubation, followed by one day of 10 μg/ml LDL incubation, one may assume that the $C^{hy}$ level is about 3000 pmol/mg cell protein. Thus, the rate constant for this latter process is about $.023/3000 \sim 10^{-7}$ mg cell protein/pmol/min. In $R + C^{hy} \xrightarrow{5r} C^{hy}$ as written, one assumes that $C^{hy}$ is not consumed. However, even if one allowed $C^{hy}$ to be consumed here, the effect on the overall model and its calculations would be completely negligible: i.e., $k_5^r \sim 10^{-7}$ mg cell protein/pmol/min, R (pmol/mg protein) = R (ng/mg protein) + LDL protein mass per particle + Avogadro # x $10^{12}$. Even if one took the maximum R as 200 ng/mg protein, $k_5^r R \sim 10^{-8}$/min.

## IX.E.4. Kinetic Modeling of Regulation of the LDL Receptor Tally

Since the major part of the LDL receptor tally's regulation is, as with *de novo* synthesis, gene-level control, one can assume that the kinetic mechanisms for both processes take similar

forms. Unlike HMG CoA reductase, however, where both[76] of $C^{hy}$ and non-sterol metabolites are reported to be regulating agents, it seems that $C^{hy}$ is the only regulating agent for the receptor tally. Also unlike HMG coA reductase, where the level of the active agent $C^{hy}$ played a major role in regulating the enzyme's activity but where the enzyme played no role in setting the concentration of the active agent, the LDL receptor and $C^{hy}$ both interact with and influence each other's concentration. As a result, the kinetic equations for LDL receptor tally regulation are much more complicated than those for HMG CoA reductase activity. In particular, unlike in the HMG co-A reductase case where one assumed that R remained constant and that one could roughly estimate the concentration of $C^{hy}$, here one must write the coupled balances for the time rates of change of both R and $C^{hy}$. Let us now write out this model[2], including the mRNA (Q) step:

| | |
|---|---|
| $D \xrightarrow{1r} D + Q$ | transcription of m-RNA |
| $Q \xrightarrow{2r} Q + R$ | translation of receptor |
| $Q \xrightarrow{3r} 0$ | degradation of m-RNA |

2. For general protein synthetic processes, Bailey and Ollis[106] suggested a kinetic model composed of two ordinary differential equations describing the time rates of change of the m-RNA and the protein. Our model includes theirs.

| | |
|---|---|
| $R \xrightarrow{\downarrow r} O$ | receptor attrition (45) |
| $D + m\, C^{hy} \rightleftarrows (D.C_m^{hy})$ - (*) | transcriptional regulation |
| $R + C^{hy} \xrightarrow{\downarrow r} C^{hy}$ | degeradation by $C^{hy}$ |

In (45), D, Q and R are gene, m-RNA and receptor concentrations, respectively and O, as in the past, denotes "out of the system" or the concentration of some species or pool whose concentration is in excess or otherwise time-invariant. We leave m, the number of $C^{hy}$ needed to coordinate D, as a free parameter to be determined by the fitting procedures. In this way, a high value of m will correspond to a higher sensitivity of the receptor kinetics to $C^{hy}$.

Let's review what's known about the molecular basis of transcription inhibition for the receptor mRNAs. A piece of the receptor gene that is called the sterol regulatory element-1 or SRE-1 enhances transcription if and only if sterols are absent. High level transcription requires reinforcement from the enhancing protein that binds to the SRE-1. In fact, high level transcription driven by the promoter of the LDL receptor gene requires activation at not only the SRE-1 site but also at two relatively weak binding sites for the general transcription factor Sp1. Inactivation of these enhancing proteins in the presence of sterols or blocking of their binding sites by sterols would account for the sterol mediated decline in transcription of

the LDL receptor.[76] Our kinetic model expressed this inactivation as the rapid and reversible binding of m molecules of $C^{hy}$ to the active gene D to form a deactivated form denoted as $D.C_m^{hy}$.

Conservation of total gene $D_t$ (see the Preliminaries Section XIII.A for a discussion of mitotic effects) says that the sum of the active and deactivated forms must remain time-invariant, or,

$$D_t = D + (D.C_m^{hy}). \tag{46}$$

Assuming that activation and deactivation proceed rapidly allows one to require these reactions to be in equilibrium (with equilibrium constant $K_r$) over the time scales of the variation in receptor number. This gives

$$D = \frac{D_t}{1+K_r(C^{hy})^m}. \tag{47}$$

The model above has four dependent variables, D, Q, R and $C^{hy}$. One can eliminate D from the kinetic equations by using the equilibrium assumption in the last equation, and one obtains $C^{hy}$ by coupling this model to the models from the earlier sections which all contribute to the $C^{hy}$ balance. As a result, the two kinetic equations resulting from the receptor regulation part of the model are:

$$\frac{dQ}{dt} = \frac{k_r^1 D_t}{1 + K_r(C^{hy})^m} - (k_3^r+\mu)\, Q \tag{48}$$

$$\frac{dR}{dt} = k_2^r Q - (k_4^r + k_5^r C^{hy} + \mu) R,$$

where the superscript r denotes the receptor regulation mechanism and $\mu$ is the cell mass expansion rate per unit cell mass discussed in Section XIII.A.

To reduce the number of unknowns in the equations, let $X = k_2^r Q$, $B = k_1^r k_2^r D_t$:

$$\frac{dX}{dt} = \frac{B}{1 + K_r (C^{hy})^m} - (k_3^r + \mu) X \qquad (49)$$

$$\frac{dR}{dt} = X - (k_4^r + k_5^r C^{hy} + \mu) R.$$

At the steady state (subscript o) that obtains under LPDS incubation,

$$X_o = B/(k_3^r + \mu_o) = (k_4^r + \mu_o) R_o \qquad (50)$$

$$R_o = X_o/(k_4^r + \mu).$$

Solving for B in terms of the maximum receptor number $R_o$ gives

$$B = (k_3^r + \mu_o)(k_4^r + \mu_o) R_o. \qquad (51)$$

**IX.E.5. Combined Model for the Cellular LDL Pathway in Human Fibroblasts**

In this subsection, we combine all of the models for the subprocesses into an overall model for the cellular cholesterol pathway. As such, it includes 1) the receptor mediated LDL binding, internalization, and the lysosomal hydrolysis of LDL-cholesterol; 2) reesterification; 3) nonlysosomal hydrolysis; 4) efflux/depletion; and 5) receptor number regulation. As noted, items 1)-4) all enter into the hydrolyzed cholesterol balance and therefore are needed in order to complete the model to follow the LDL receptor tally's dynamics. We note here that in contrast to the simplifying assumptions made in the analysis of the *de novo* synthesis processes, where it was necessary to have a crude estimation for the hydrolyzed cholesterol concentration, we have a much more detailed hydrolyzed cholesterol balance here. In addition, whereas in the analysis of the esterification processes we worked under the assumption (valid for the particular experiment analyzed at that point) that $1/M >> C^{hy}$ in order to simplify the expression for the cholesterol available for esterification, we use the full expression (equation (34)) here. The overall model, as collected from the preious sections, is:

$$L + R \rightarrow L^a \qquad \text{LDL Binding, Uptake \&}$$

$$\downarrow \quad , \quad R \underset{\leftarrow}{\overset{\rightarrow}{\rightleftharpoons}} R^P \qquad \text{Degradation}$$

$$L + R^P \rightarrow L^P \rightarrow L^i + \zeta\, L^{i'} + R, \quad L^i \rightarrow L^d, \quad L^{i'} \rightarrow C^{hy}$$

Esterification

$$C^{hy} + C^{u} \rightarrow C^{hy} + C^{*} \quad \backslash$$
$$C^{*} \rightarrow C^{u} \quad / \text{ (In Equilibrium, M)} \qquad (52)$$

$$C^{a} + E_4 \underset{\leftarrow}{\overset{\rightarrow}{}} (C.E_4) \rightarrow CE + E_4$$

$C^{hy}$ Decay & Efflux

$$C^{hy} \rightarrow 0, \quad C^{hy} \rightarrow C^{u}$$

Non-Lysosomal Hydrolysis

$$CE^{hy} \rightarrow C^{hy}$$

$$CE \rightarrow C$$

In (52), M is the equilibrium constant defined above Equation (34) and the available cholesterol is defined in Equation (34). For incubations in 10 $\mu$g/ml LDL, the *total* cellular cholesterol content is known to vary only slightly with time; we shall take it to be time-invariant under those conditions.

**IX.E.6. Determination of Rate Constants**

It is now incumbent upon us to determine the as yet unknown rate constants for the receptor number regulation based upon experimental data and the known values for the rate constants of the various processes that we have determined throughout the previous sections of this paper. However, due to the crude models for $C^{hy}$ that we, out of necessity, made in order to investigate

those earlier models for the sub-processes, the rate constants determined there should be considered as reasonable approximations to some more accurate set of values. As such, in our rate constant determinations below, we will not only allow the new rate constants for the receptor number regulation processes be fit, but we shall also allow those of the previously determined rate constants whose estimation relied on those crude approximations to vary. The difference shall be that, given reasonable estimates for these previously determined rate constants, their allowed variability (that is, the upper and lower bounds on each unknown parameter that the optimization program requires) will be much more circumscribed than the receptor tally regulation's rate constants. As a result, it will be necessary to go back and to recheck some of the experiments used earlier to determine those rate parameters in the context of the crude approximations and to see that the overall model with the modified parameters fits those data equally well (e.g., Fig. 27).

We now proceed to find such a set of rate constants from a particular set of experiments and then use the overall model together with this set of rate constants to predict the results of other experiments; we then see how these compare with the data from those experiments. The predictions (or post-dictions) have no adjustable quantities. As we shall see, the results are surprisingly good considering the fact that so many processes contribute to the overall mechanism.

### IX.E.6.a. Regression for Growing Cells in an Unsteady, Step Experiment in a Medium containing 10 $\mu$g/ml LDL[9]

The experiment whose results we shall use to arrive at parameter values begins with growing human fibroblasts, preincubated for 3 days in LPDS and further incubated in LPDS and 10 $\mu$g/ml LDL (Figs. 22a and b). Since growing cells that are incubated for 48-72 hours without LDL express their maximal number of LDL receptors,[9] one can assume that upon addition of LDL in the experiment in question, the receptor number and its associated mRNA were at their steady values. From (51), one sees that the initial condition is $X_o = (k_4^r+\mu_o)R_o$. This inference about the initial condition is important because it reduces the number of unknown parameters.

The initial specific growth rate $\mu_o$ is about 0.01/hr (Fig. 9). Since an estimate for $R_o$ follows immediately from the initial data on receptor number, and since one already has a value (0.028/hr) for $k_4^r$ from sub-section IX.E.3, one can estimate $X_o$. These estimates for $R_o$ and $\mu_o$ will serve as very good starting values for the fitting procedure, which will determine "best" values for these quantities as well. Also, even though $\mu$ and $\mu_o$ seem to differ slightly, we shall take them as being equal to one another.

Experimental data for the time evolution of the total cellular free cholesterol concentration are not available for times ranging over a period of a few days. However some data for final cholesterol concentrations do exist for human fibroblasts preincubated for 24 hours in LPDS-containing medium followed by one day in LPDS and various concentrations of LDL. They show that the total cellular free cholesterol concentration in medium

containing less than about 10 $\mu$g/ml LDL is essentially identical to the value (about 40 $\mu$g/ml, Fig. 26) for the incubation in LPDS without LDL. Although the experiment under discussion here lasted for 4 days, one may still guess that the total cellular free cholesterol concentration remains almost time-invariant since it used a medium containing 10 $\mu$g/ml LDL. This is the main motivation for choosing these experimental data for the parameter determination to follow.

Before continuing, we note that the parameters for receptor mediated LDL uptake ($k_1$, $k_2$, $k_3$, $k_o$, $k_o'$, $\alpha$) are fixed and already known (see chapter V., VII.B. and Table 3).

Fig. 22a shows the best fit curves of $^{125}$I-LDL binding activity (the receptor tally) and the total cellular cholesteryl ester. Table 3 provides the best fit values and the previously estimated values of those rate constants for which such estimates already existed. It is satisfying to note that although almost all of the best fit values are very similar to the earlier estimates, the fit to the data is excellent, passing almost directly through the data. Using these parameters, one can generate the corresponding curves for the total cellular and LDL-derived cholesteryl esters. The ratio of these two values at 12 hours of incubation in medium with 10 $\mu$g/ml LDL gives about 4. This ratio is amazingly consistent with what Goldstein *et al.*[98,60] measured using $^{14}$C-oleate and $^{3}$H-CL LDL tracers (see section IX.C.3).

As just stated, almost all of the best fit parameter values are consistent with previously estimated values, where available. The only exceptions are $k_7$ and M, and these are also within a

factor of two of the earlier estimates. Note that the fitting procedure gives m, the number of $C^{hy}$ needed to coordinate D as equal to 3.

### IX.E.6.b. Predictions

Brown and Goldstein repeated the experiment[9] used for the fitting procedure under experimental conditions identical to those in the last sub-section, except that the LDL concentration in the medium was 50 $\mu$g/ml instead of 10 $\mu$g/ml. Using the parameters just determined, we shall now predict the time evolution of the receptor tally and the cholesteryl ester content and compare them with the experimental results. There is at least one major distinction between the LDL-10 and the LDL-50 cases, the total free cholesterol content of the cells during and after incubation. Since the total cholesterol content affects the amount available for esterification and, hence, the amount esterified, errors in this estimation will lead to errors in the cellular content of cholesteryl esters as a function of time, although the receptor tally's dynamics should remain practically unchanged. For this approximation, we defer to the following experiments of Brown *et al.*[53]

After 24 hours preincubation in medium containing LPDS, human fibroblasts were further incubated for one day with various LDL concentrations. The result (Fig. 26) shows a cellular free cholesterol that first increases and then saturates. For an LDL concentration of about 50 $\mu$g protein/ml ($\approx$ 80 $\mu$g cholesterol/ml), the cellular free cholesterol increased by about 50% relative to

cells incubated in LPDS without LDL. Thus, to generate predictions for LDL=50 μg protein/ml LDL in LPDS, we begin by assuming that the total cellular free cholesterol (smoothly) increases by 50% after one day and by 100% after times much longer than one day.

The resulting prediction of $^{125}$I-LDL binding activity (Fig. 22b), i.e., receptor tally, is very close to the experimental data, but that of the cellular cholesteryl ester is consistently lower than the experimental data beyond one day of incubation. This is probably due to one or more of the following: First, the estimation of the total cellular content of free cholesterol is probably significantly off, thereby leading to an erroneous cholesteryl ester prediction, as just described. Second, lysosomal hydrolysis of the large amount of LDL that enters initially probably leads to high endogenous concentrations of fatty acids which can increase the rate of esterification. Moreover, lysosomal hydrolysis of the LDL taken up by fluid phase pinocytosis[36] can probably contribute to a higher endogenous concentration of fatty acids even after the receptor tally is fully suppressed; this might explain the low prediction after 1 day. Third, M might be larger than its best fit value thereby resulting in more activated and hence more available cholesterol for esterification. Finally, the best fit value for the degradation of $C^{hy}$ may be too large, although this seems unlikely since the sum of the "best" values for the degradation and the efflux of $C^{hy}$ is almost exactly equal to the value estimated earlier.

Fig. 22c shows a prediction for the same experiment done with an LDL concentration of 2 μg/ml. Although it does not appear

that anyone has yet performed this experiment, the prediction has the interesting feature that after an initial decrease in the receptor tally, the number of receptors recovers slightly on about the third day and moves toward a presumably steady value which is higher than the minimum achieved at 2.5 days. What appears to be happening is that the initially up-regulated receptor number infuses a large amount of LDL, and thus of $C^{hy}$, into the cell. The high $C^{hy}$ acts to decrease the receptor tally quickly over the first two days, which then drastically slows the introduction of new $C^{hy}$ just at a time when the $C^{hy}$ begins to show appreciable decay. With less $C^{hy}$ around, the receptor tally can recover a bit and find a (higher) steady balance with the hydrolyzed cholesterol.

### IX.E.7. Prediction for Receptor Relaxation Kinetics: The Shock of Medium Transfer on Growing Cells

Fig. 28a[101] shows data and the corresponding predictions for a completely different type of experiment. The authors incubated cells in late logarithmic growth phase for 18 hours in LPDS medium containing 2 $\mu$g/ml, 10 $\mu$g/ml and 100 $\mu$g/ml LDL, respectively, in order to down-regulate receptor numbers and to create various cellular inventories of $C^{hy}$. They then transferred the cells to LDL-free LPDS medium and observed the recovery of the receptor tally for the next fifty four hours. After an initial spike in some of the data during the first two hours following

medium shift, all three dishes showed a recovery of receptor number. After fifty four hours, though, there was still a significant difference between the three dishes, with the dish previously incubated with 100 $\mu$g/ml LDL having about 30% fewer receptors than the one previously incubated with L-2 $\mu$g/ml. The initial shock was most noticeable in the control experiment where the dish was simply transferred from one LDL-free medium to another. We do not pretend to have any sort of deep understanding of this phenomena. We do, however, suggest a couple of crude, admittedly arbitrary phenomenologies to describe it, so that we can subtract it out or otherwise correct for its effect and predict the results of such experiments.

Let $R_o(t)$ be the dynamic receptor tally and $R_o^s$ be the maximum receptor number achieved after transfer of growing cells from one LDL-free LPDS medium to another (i.e., the upper curve);thus, $f(t):=R_o(t)/R_o^s$ is the the scaled shock function. In this view, $R_o^s$ is the maximum number of receptors that the growing cells can express upon shock after they have acclimated to the LDL-free LPDS medium's environment, i.e., after they have been incubated in that medium for a few days and therefore have probably depleted some or much of the medium's nutrients and secreted reaction products into it. The main assumption in this phenomenology is that the time evolution of f(t) also applies *instantaneously* to fibroblasts even as they acclimate to new conditions. Thus, *even after a change in medium LDL concentration*, f(t) is assumed to give the time-evolution in response to

shock of the fraction $R(t)/R^S(t)$ of the maximal number of receptors $R^S(t)$ expressible upon shock. When the medium's LDL concentration is changed, it is this maximal total $R^S(t)$ which we assume can vary with time as the cells acclimate and, it is $R^S(t)$ (and similarly $X^S(t):=X(t)/f(t)$) to which we assume equations (49) and (50) apply, rather than directly to R(t) and X(t) as written. We recognize that this phenomenology is quite arbitrary, but it stems from the rather fast rise in receptor number just after medium transfer. On the other hand, since we do not claim any understanding of the shock phenomenon, it may very well turn out that another phenomenology is more appropriate. One such possibility is to add $[R_o(t)-R_o(t=0)][R(t=0)/R_o(t=0)]$, the deviation of the time evolution of the receptor tally in the LPDS→LPDS transfer from its initial value, scaled by the ratio of the initial values of the actual and of the LPDS experiments, to the model's (Equations (49) and (50)) predictions.

With the first phenomenology outlined above one can take equations (49) and (50), written now for $R^S$ and $X^S$, and substitute $R=fR^S$ and $X=fX^S$ in order to get the following equations determining the observed time-evolution of the shock-included receptor number R(t).

$$\frac{dX}{dt} = \frac{B}{1 + K_r(C^{hy})^m} - (k_3^r+\mu-\frac{d(\ln f)}{dt}); \qquad B=(k_3^r+\mu_o)(k_4^r+\mu_o)R_o(t\to\infty);$$

$$\frac{dR}{dt} = X - (k_4^r + k_5^r C^{hy} + \mu - \frac{d(\ln f)}{dt}) R. \qquad (53)$$

Clearly if f(t) were just a constant, these equations would just reduce to (49) and (50). In fact, for times greater than 30 hours after medium transfer, this appears to be the case.

We now fit the LPDS→LPDS curve to the very simple piecewise-linear function (see Figure 28b)

| | | |
|---|---|---|
| $f(t)=0.6+0.001663(/min)t$ | for $t \leq 4$ hrs. | (54) |
| $f(t)=1.04-0.00016(/min)t$ | for 4 hrs. $< t \leq 30$ hrs. | |
| $f(t)=0.75$ | for $t > 30$ hrs. | |

At the points where this simple function is not differentiable, we represent its derivative by the average of its left and right values. With either this phenomenology or the second one outlined above, our overall model, together with the best fit rate constants from Table 3 can generate predictions that one can compare with the data. These calculations begin by first simulating the evolution of the receptor tally, the lysosomally hydrolyzed cholesterol and its reesterified form during the 18 hour preincubation period before the start of the experiment and then continues through the period of the experiment. Figures 28c and d show the results for each of the two phenomenologies. We first comment on the modeling of the shock effect and reserve analysis of the balance of the curves' predictions for the Discussion Section V below. Both phenomenologies seem to work reasonably well, although in the LDL-10 and 100 curves they seem to overestimate the shock. This may be in part due to the crude, piecewise-linear fit of f(t), which leads to an overestimation of

its derivative near the maximum. The sharp kink in the predicted curves also results simply from the crude fit of f(t).

## V. Discussion

Human cells such as arterial endothelial cells and fibroblasts have a need to maintain adequate levels of cholesterol for use in membranes. This need is particularly strong and its value probably high in dividing cells that must constantly produce new membrane. The cells' primary source of cholesterol is exogenous LDL, via the LDL receptor pathway. It has been our goal in this thesis to mathematically model the processes that deliver LDL-cholesterol to the cells as well as those that regulate the delivery system and the internal cellular processes in order to maintain appropriate cholesterol levels. Aside from its intrinsic interest, a quantitative handling of the data can point to inconsistencies in qualitative models as well as being helpful in suggesting possible mechanistic adjustments. We saw an example of this in Part One of this thesis with regard to receptor uptake of cholesterol and binding to coated pits. An example from Part Two was the dilution kinetics model for esterification regulation that followed from an attempt to quantitatively account for the various historical experimental findings.

Another motivation for exerting the significant effort necessary to come up with a kinetic model for the complex cellular processes comprising the cellular LDL pathway is as a contributing part to a general theory of the early stages of atherosclerotic lesion formation. It is natural to presume that

the initial formation and growth of such lesions in the intimal region of the artery wall depends strongly on the evolution of the local lipid concentration there. This concentration derives from lipid transport from the lumen through the endothelium and into and out of the artery wall's media, as well as from lipid depletion due to receptor-mediated cellular uptake. In that sense, the models of the cellular pathway account for the sink terms in this overall balance.

As noted earlier, whereas there have been a few approaches to the modeling of receptor binding of LDL, migration to coated pits, internalization and recycling of the receptors to the surface, there has been, to the best of our knowledge, only one other attempt at modeling the regulatory processes, that of Yuan *et al.*[21] We have already thoroughly discussed the relationship of our model of the initial steps in the cellular LDL pathway, those of binding, internalization and degradation of LDL, with experimental data and with previous modeling efforts in Part One's discussion. In this discussion, therefore, we restrict our attention to the models in Part Two, contrast them in some detail with those of Yuan *et al.* and compare our model's predictions with available experimental results.

Both our work and that of Yuan *et al.* seek to model the cellular pathway, including the regulatory processes. The basic difference lies in approach and method. Yuan *et al.* aim only to describe processes that proceed on time scales of at least one-half-day; therefore, for each of the faster processes, they only carry out a curve-fit of one set of experimental results. These functional forms are chosen to conform to these curves' shapes, and do not derive from any sort of mechanistic model. The

process they do kinetically model is the control of the cell's receptor tally. The functions employed for the curve-fits take the dependent variable to be the *medium's* LDL concentration rather than any intracellular quantity. In fact, this is the major assumption that enables their procedure to arrive at a model: That one can consider the receptor number as being solely a function of the *medium's* LDL concentration. This allows them to *first* model the receptor tally's dynamics *independently of the other processes* and then use the result as an aid in determining quasi-steady state LDL binding, hydrolysis, efflux, *de novo* synthesis and esterification. Such an assumption affords an enormous simplification but, as they themselves admit, probably dooms any dynamic predictions.

In our approach, in contrast, we begin with Brown and Goldstein's experimental observations that intracellular quantities rather than the extracellular LDL concentration directly control receptor number. Whereas over very long time scales, all intracellular processes adjust to the extracellular LDL level and therefore find steady values commensurate with this external condition, modeling based only and explicitly on that level will only be applicable to the steady state. We felt that in order to *predict* the dynamics of, say, the receptor tally, one needs to know how the intracellular quantities are changing dynamically, since they control the receptor dynamics. In addition, it is our conviction that in order for one to be able to extrapolate a model much beyond the data from which it was derived and to apply it to different types of experiments, it must have mechanistic content. Therefore, we chose to take the receptor tally's controlling agent to be intra-cellular, in agreement with

experiment, even though this meant that the other, faster processes such as binding, internalization, esterification, *et cetera*, needed to be modeled *before* one could attempt to model the dynamics of the receptor tally. We did, though, take advantage of the separation of scales in order to assume that for the initial modeling of the fast processes the receptor number was essentially time-invariant during the relevant experiments. This allowed sequential, rather than simultaneous modeling. Unfortunately, as just mentioned, the receptor tally's dynamics come *last* rather than first in the sequence.

Our analysis began with a discussion of just what the intracellular controlling agent could possibly be. From a number of arguments based on the large amount of historical data from the Brown and Goldstein group, we concluded that the total cellular cholesterol could *not* fulfill this role. Circumstancial evidence seemed to point to LDL-derived cholesterol that had recently entered via the specific receptor pathway (a quantity similar to what Yuan *et al.* took as the substrate for esterification). In addition we found it prudent to properly account for cell population growth, whose influence on the kinetics, since concentrations tended to be expressed in terms of per-unit-mass-cell-protein units, turned out to be analagous to the kinetics in a non-constant density chemical reactor, with concentrations in per-unit-volume units. With these notes in mind, let's now consider the predictions of both models for various sets of data.

Both models rely, for the determination of the rate constants involved in receptor synthesis and decay, on the receptor number down-regulation experiment that occurred over a period of four

days following the transfer of growing cell from an LDL-starved environment to medium containing 10 μg/ml LDL. At such conditions, receptor synthesis is quickly all but shut down and an almost pure receptor decay ensues. Notice that our fit (Figure 22a) seems to rise slightly after three days: The vast amounts of $C^{hy}$ introduced early on at high receptor tally suppress receptor production. However, after a few days, these stores decay and are not as quickly replaced because of the reduced receptor number. This trend seems to be present in the data, although the absence of error bars in the data leave the significance of this data rise in doubt.

The first prediction is for almost the same experiment, but where the medium contains 50 μg/ml LDL rather than 10 μg/ml. Since receptor production is shut off here just as in the last figure and this figure is therefore very similar to the one from which the rate constants were determined, it is no surprise that both models (Figure 22a, b and Figure 29) do quite well. The decay in both figures is similar, although the L=50 case in our model is slightly faster due to the minor contribution of reaction 5 (see (45). We also include a prediction for an experiment not yet carried out (Figure 22c, LDL=2 μg/ml) where the upturn in receptor number after two and a half days is more pronounced.

The next case requiring some discussion is Figure 28, the receptor recovery described in Section IX.E.7 upon which the discussion of the shock to growing cells upon medium transfer

centered. We compare with Figure 30 from Yuan *et al.*[3] At first glance, both sets of curves seem to give qualitatively the right trends, although neither tracks the data exactly. A closer examination will reveal some important differences. Our figure's simulation begins 18 hours before the data were taken and tracks the system through the period of LDL incubation during which the cells build up a reserve of $C^{hy}$. This reserve then affects the later receptor dynamics. Thus the zero-time values in the figure are calculated and not assumed. The calculation then proceeds to the indicated time of the experiment. Thus these curves contain no information from the data as inputs other than the experimental conditions (which more or less determine a value for the total receptor number prior to LDL-incubation. Data for this determination are available from other sources.[11 105]).

In contrast, Figure 30 from Yuan *et al.* begins its simulation after transfer to LDL-free medium and takes the initial receptor number *as well as its initial derivative* from the experimental results. In addition, as in our case, the leveling off of the curves at long times and the value at which they level off is hard-wired into the system via the steady state condition and the choice of total receptor number for the upper (LDL-free preincubation) curve. Thus, these latter curves need to be scrutinized differently from those in Figures 30 since they have

3. It is curious that even though Yuan *et al.* note (and take corrective action for) the difference in the definitions of "binding" (used to assess the total receptor tally) between the experiments from which the rate parameters were fit and this one, they make no mention (or note of corrective action) of the fact that different LDL concentrations (10 and 25 μg/ml) were used for the assays in these two experiments.

a large amount of input from data themselves. Despite these inputs, the curves, particularly those for LDL=10 and 100 $\mu$g/ml, achieve their steady values much faster than do the data. On the other hand, due to the slow decay of the intra-cellular inventory of $C^{hy}$, the lower curves in our figure recover more slowly, as do the data.

It is worth examining our curves a bit more closely. They show a downward trend following medium transfer that is initially overwhelmed by (L=2) or cancelled by (L=10, 100) the shock effect, but still appears before recovery. This effect does not seem to be present in the data for times after the shock has dissipated (about one day), although the fact that the data for the lower curves seem flat may actually be a reflection of the cancellation just mentioned. Now the presence of such a dip would, *a priori*, seem reasonable, since at about 18 hours LDL incubation, the receptor number vs time plot (see Figure 22a ,b and c) has its sharpest downward slope. One would expect medium transfer to reverse this trend, although not instantaneously. That is, since memory of LDL incubation is clearly present in the persistence of a difference in receptor number for the L=10 and 100 cases even at three days, it is conceivable that this memory should manifest itself in the short term as well; however, due to the shock of medium transfer, this effect might be cancelled or masked. One way out of the dilemma that the data fail to dip is to suggest that our value for the decay constant for $C^{hy} \rightarrow C$ or for efflux may be a bit low. If it were higher, then the curves would begin to recover before the shock of medium transfer subsided and would track the curves much better. On the other hand,

Figure 28e shows what would the model would predict if the washing procedure during medium transfer somehow depleted the cell's $C^{hy}$ and $CE^{hy}$ reserves. Even though this would raise the curves and brings them closer to the data, the curves would merge to their steady values (and with one another) much more quickly than do the data; this fact shows the important role of these initial reserves.

In our model, the cholesterol esterification values that correspond to the LDL receptor down-regulation experiments appear on the same curves as the receptor number's dynamics. The agreement for L=10 $\mu$g/ml is not significant since we used this curve for parameter determination. At L=50 $\mu$g/ml, our prediction is low (about 50% at the worst point), although it has the right shape. This situation is somewhat similar to the situation of Yuan *et al.*, whose curves were consistently a factor of four or more below the data. This might be attributed to the fact that their model neglected the participation of endogenous free cholesterol in the reesterification process. The order of magnitude of this participation is about a third of the total cellular free cholesterol when one incubates human fibroblasts in the medium containing 10 $\mu$g/ml LDL for 12 hours.[60]

The next curves are the predictions of the cholesteryl ester concentration after one day incubation with various concentrations of LDL (Figure 31, our model; Figure 32, Yuan *et al.*'s). Since these experimental conditions lead to essentially steady behaviour, Yuan *et al.*'s model does quite well, as does ours.

Finally, due to its importance in the modeling of LDL infiltration into the arterial intima where atherosclerotic lesions begin, Yuan *et al.* predict the quasi-steady hydrolysis rate as a

function of LDL medium concentration. Curiously they find (see Figure 33) the rate of hydrolysis going through a maximum and then a weak minimum before appearing to become independent of LDL concentration for LDL>~50 μg/ml. This independence at high LDL concentrations has been seen[6 11], but the predicted inversion has not been seen. The authors themselves doubt its significance. In contrast, our prediction (Figure 34) smoothly saturates (without extrema) to about the same (and experimental) value.

The final figures present predictions. Figure 35 predicts the LDL-receptor tally versus the medium's LDL concentration after 3 days of incubation of growing human fibroblasts in a medium containing various LDL concentrations.[105] As is evident, the match is quite good.

In summary, it appears that the set of models that we have developed is capable of representing and even predicting experimental data on the cellular LDL pathway reasonably well. This is actually surprising since the processes involved are quite complex and the quantitative data appropriate for kinetic analysis are limited. Along the way we modeled some processes in detail due to their importance to our overall modeling effort and because there experimental results' complexity seemed to require more than a simple model; others, such as efflux, we modeled with drastic simplifications. In the process, we proposed a number of new and, we believe, interesting trial models for some of the regulation processes, that seem to fit the available data well and to offer explanations for some of their paradoxes. A primary example of this is the dilution kinetics model for cholesterol esterification control. It should be emphasized, however, that without explicit experiments designed to specifically test our

proposed models, neither the extent of their validity nor the accuracy of the mechanistic guesses can be ascertained. At this point, one can only justify their use by virtue of their being able to account for and to "predict" historic data.

There is one more point worth addressing before concluding this work. In this modeling effort we were forced to consider cells that were in various stages of growth, from sparse cultures, to cells in late logarithmic growth to those that are almost confluent. Clearly the cholesterol needs of cells in these different stages of growth are different from one another. One way in which they manifested these differences in our models was through the specific growth rate $\mu$ which entered most of the rate equations. It seems plausible that even some of the rate constants may vary with the degree of confluency. In particular, it would seem reasonable that growing cells would tend to down-regulate receptor number only at higher exogenous LDL concentrations than would confluent or quiescent monolayers. There might also be differences in esterification pools and in efflux. We have thusfar shied away from such *Ansätze* due to the paucity of data; allowing for these distinctions would almost require a separate model fit for each available experiment, and thereby rob any model of its utility. Such a treatment must await the availability of more data.

Table 3

| Rate Constant | Eq.(#) | Best Fit | Previous Approximation |
|---|---|---|---|
| $k_1$ | (2) | 0.0056 ml/μg/min | |
| $k_2$ | (2) | 0.32/min | |
| $k_o$ | (2) | 0.03/min | |
| $k_o'$ | (2) | 0.4/min | |
| $R_o$ | (51) | 190 ng/mg cell protein | |
| $k_7$ | (37) | 59672 pmol/mg cell protein | about (1+MC)X9654 pmol/mg cell protein |
| $k_8$ | (37) | 237 pmol/mg cell protein/min | i) 144-342/min<br>ii) 260/min |
| $k_9$ | (33) | 0.0009/min | 0.0009-0.001/min |
| $k_{10}$ | ($C^{hy} \rightarrow C^{u}$) | 0.07/hr | 0.09/hr |
| $\frac{1}{M}$ | (34) | 47599 pmol | about 22000 pmol |
| $K_r$ | (47) | $8.5 \times 10^{-8}$(mg cell protein/pmol)$^3$ | |
| $k_3'$ | (22) | 0.008/min | |
| $\mu$ | (21) | 0.008/hr | 0.01/hr |
| $k_5^r$ | (45) | 11.25 e-8 mg cell protein/pmol/min | $10^{-7}$mg cell protein/pmol/min |
| $k_3^r$ | (45) | 0.005/min | > 3 hrs[108] |
| m | (47) | 3 | |

The rate constants for receptor mediated LDL uptake LDL are taken as (see Table 1) $k_1 \approx 0.0056$ ml/μg/min, $k_2 \approx 0.3$/min, $k_o \approx 0.03$/min, $k_o' \approx 0.3$/min and reconfirmed. $\alpha$ is given as 0.41. $k_4^r$ is given as $4.62 \times 10^{-4}$/min from $t_{\frac{1}{2}} = 25$ hrs.

## Figures

Descriptions of experimental procedures are taken essentially verbatim from the original papers of M.S. Brown and J.L. Goldstein.

**Fig. 9**[34]: Growth rate of normal fibroblasts. Cells were initially plated (day 0) at a concentration of $1x10^5$ cells per dish in 3 ml of growth medium containing 10% fetal calf serum (final protein concentration, 6.3 mg per ml) and 50 $\mu$l of ethanol (o); 10% lipoprotein deficient fetal calf serum (final protein concentration, 4.7 mg per ml) and 50 $\mu$l of ethanol ($\Delta$). Fresh medium was added on Days 4 and 7 after plating. Cell number was determined at the indicated time by counting trypsinized cells from duplicate dishes.

**Fig. 10a, b, c and d**[82]: Time course of LDL metabolism in normal ($\bullet$,o) and mutant ($\blacktriangle$,$\Delta$) fibroblast monolayers incubated in the absence ($\bullet$,$\blacktriangle$) and presence (o,$\Delta$) of chloroquine. The cells were grown under standard conditions except that the grown medium was switched to 5% human LPDS on Day 5. After 48 hours in LPDS (Day 7), one group of cell monolayers received 2 ml of growth medium containing 5% human LPDS. 10 $\mu$g protein/ml of $^{125}$I-LDL (116 cpm/ng of protein) and either no chloroquine ($\bullet$,$\blacktriangle$) or 50 $\mu$M chloroquine (o,$\Delta$). After incubation at 37° for the indicated time, the amount of cellular binding (10a) and proteolytic degradation (10c) of the $^{125}$I-LDL were determined. A second group of cell monolayers was incubated on a different day but under identical conditions except that instead of $^{125}$I-LDL, the growth medium contained 10 $\mu$g of protein/ml of [$^3$H]CL-LDL. After incubation at 37° for the indicated time, the cellular content of [$^3$H]cholesterol linoleate (10b) and the cellular content of [$^3$H]cholesterol (10d) were determined. *Circles* refer to normal cells incubated either in the absence ($\bullet$) or presence (o) of chloroquine. *Triangles* refer to mutant cells incubated either in the absence ($\blacktriangle$) or presence ($\Delta$) of chloroquine.

**Fig. 11a and b**[53]: Fig. 11a and b correspond to experiment (E) and (C) respectively as described below. Manifestations of LDL-receptor interactions in normal with LDL at 5 ($\bullet$) and 25 ($\blacktriangle$) $\mu$g protein/ml for varying time intervals. Cells from one normal subject were plated (day 0) into 94 petri dishes (60 mm) at a concentration of $1x10^5$ cells/dish in 3 ml of growth medium containing 10% FCS. On day 8 the medium was replaced with 2 ml of fresh grown medium containing 5% human LPDS and either [$^{125}$I]LDL (120 cpm/ng protein, exps. A and B) or unlabeled LDL (exps. C-F) at a concentration of 5 ($\bullet$) or 25 ($\blacktriangle$) $\mu$g protein/ml. After incubation of 37° C for the indicated time, the following determinations were made. High affinity [$^{125}$I]LDL binding (A) and degradation (B): The medium was removed, its content of $^{125}$I-labeled, trichloroacetic acid soluble degradative products was measured, and the amount of $^{125}$I radioactivity bound to the cells was determined. High affinity binding and degradation were calculated by subtracting the amount of radioactivity bound or degraded in the presence of 395 $\mu$g protein/ml of unlabeled LDL from that bound or degraded in its absence. At both concentrations of LDL, the high affinity binding and degradation accounted

for more than 80% of the total radioactivity bound or degraded in the absence of the unlabeled LDL. HMG CoA reductase activity (C): Cells were harvested, cell-free extracts were prepared, and HMG-CoA reductase activity was determined. [$^{14}$C]oleate incorporation into cholesteryl esters (D): 30 min before each indicated time point, cell monolayers were pulse-labeled with [$^{14}$C]oleate (56 cpm/pmol) bound to albumin at a final oleate concentration of 0.1 mM. After 30 min. the cells were harvested and the content of [$^{14}$C]cholesteryl esters was determined. Cellular content of free (E) and esterified (F) cholesterol: Cells from two dishes were washed, harvested, pooled, and the content of free and esterified cholesterol was determined. In all experiments (A-F), each data point represents the mean of duplicate determinations.

**Fig. 12a, b and c**[35]: Fig. 12a and c are generated with the best fit parameters. Fig. 12a, b and c correspond to experiment (E), (D) and (F) respectively as described below. Manifestations of LDL-receptor interactions in normal (●) and homozygous familial hypercholesterolemia (▲) fibroblasts incubated with varying concentrations of LDL. Cell strains derived from explants of skin were maintained in monolayer culture and were set up for experiments (day 0) in 60 mm petri dishes at a concentration of $1x10^5$ cells per dish in medium containing fetal calf serum. On day 6, which was 48 hours before the experiment, the medium was replaced by medium containing 10 percent low density lipoprotein-deficient serum (5 mg of protein per milliliter). On day 8, the medium was replaced with 2 ml of fresh medium containing (A to C) $^{125}$I-labeled LDL (441 count/min per nanogram of protein). (D) [$^3$H]cholesteryl linoleate-labeled LDL (32,830 count/min per nanomole of cholesteryl linoleate. (E or F) unlabeled LDL. After incubation with LDL at 37°C for either 2 hours (A and B) or 6 hours (C and F), the indicated measurement were made. (A and B) Surface binding and cellular uptake of $^{125}$I-labeled LDL. Each cell monolayer was washed six times at 4°C with an albumin-containing buffer and a solution containing sodium heparin (10 mg/ml) was added to each dish. The dishes were then incubated at 4°C for 1 hour, the heparin-containing medium was then removed, and the amount of $^{125}$I-labeled LDL bound to the cell surface and hence accessible for heparin release was determined. The cells were dissolved in 0.1 *N* NAOH and the amount of $^{125}$I-labeled LDL that had entered the cell and was hence resistant to heparin release was determined. (C) Proteolytic hydrolysis of $^{125}$I-labeled LDL. The medium was assayed for $^{125}$I-labeled trichloroacetic acid-soluble degradative protein products that had been formed. (D) Hydrolysis of LDL-cholesteryl esters. The cellular content of unesterified [$^3$H]cholesterol formed from the hydrolysis of [$^3$H]cholesteryl linoleate-labeled LDL was measured. (E) Suppression of HMG CoA reductase activity. Cells were harvested, detergent-solubilized extracts were prepared, and enzyme activity was determined. (F) Stimulation of cholesteryl [$^{14}$C]oleate formation. One hour before the end of the incubation (that is, 5 hours after the addition of LDL), each cell monolayer was labeled at 37°C with 0.1 m*M* [$^{14}$C]oleate (21,000 count.min per nanomole) bound to albumin and the cellular content of cholesteryl [$^{14}$C]oleate was determined. In all experiments, each value represents the mean of duplicate incubations and measurements.

**Fig. 13**[82]: Non-specific LDL uptake is taken from the data of Figure 1 of ref. 11 and subtracted from total LDL uptake and hydrolysis.[82] Time course of LDL metabolism in normal (●) and mutant (▲) fibroblasts monolayers, relating cellular uptake of [$^3$H]cholesteryl linoleate-LDL, hydrolysis of the [$^3$H]cholesteryl linoleate. After 24 hours in human LPDS (day 7), each monolayer received 2 ml of growth medium containing 5% human LPDS, 0.1mM unlabeled oleate albumin, and 10 μg of protein/ml of [$^3$H]CL-LDL (83,406 cpm/nmol of cholesteryl linoleate). After incubation at 37°C for the indicated time, the cellular content of [$^3$H]cholesteryl linoleate and free [$^3$H]cholesterol was determined.

**Fig. 14**[93]: Ki is the best fit-influx rate constant.

**Fig. 15a and b**[53]: Prediction: See Figure 11a and b.[53] Fig. 15a and b[53] correspond to experiment (C) and (D) respectively.

**Fig. 16**[77]: The curve is generated with the best fit rate constants for normal nonconfluent cells. Figure 16a and b correspond to experiment (A) and (B) respectively, as described below. Changes in HMG-CoA reductase activity of normal nonconfluent and confluent cells after removal of fetal calf serum and after replacement of fetal calf serum with lipoprotein-deficient human serum. On Day 1, cells were seeded at a concentration of $2.5 \times 10^5$ per dish and grown in medium containing 10% fetal calf serum. For experiment (A), on Day 2 the medium was replaced with human LPDS (6 mg per ml). For experiment (B), on Day 6 the medium was replaced with human LPDS (6 mg per ml). After indicated time intervals extracts were prepared and HMG-CoA reductase activity was assayed.

**Fig. 17**[82]: Rate of hydrolysis of endogenously synthesized cholesteryl [$^{14}$C]oleate in normal (●,o) and mutant (▲,Δ) fibroblast monolayers incubated in the presence and absence of chloroquine.

**Fig. 18**[61]: Rate of [$^{14}$C]oleate incorporation into cholesteryl esters in normal cells as a function of duration of preincubation with LDL (o, 60 μg cholesterol/ml; ●, 150 μg cholesterol/ml) and nonlipoprotein cholesterol (Δ, 30 μg/ml;▲, 60 μg/ml). At the indicated time, [$^{14}$C]oleate (0.1 mM, 24,000 cpm/nmol) was added and the cells were harvested 1 hr later.

**Fig. 19**[60]: Time course of LDL metabolism in normal fibroblast monolayers. One group of cells was incubated with 10 μg of protein per ml of $^{125}$I-labeled LDL (340 cpm/ng of protein) and the amount of binding (●) and proteolytic hydrolysis (Δ) of the lipoprotein were determined as described. A second group of dishes was incubated with 10 μg of protein per ml of [$^3$H]CL-LDL (83,350 cpm/nmol of cholesteryl linoleate) and the amount of free [$^3$H]cholesterol formed (▲) was measured. A third group of dishes was incubated with 10 μg of protein per ml of [$^3$H]CL-LDL (83,350 cpm/nmol of cholesteryl linoleate) and 0.1 nM [$^{14}$C]oleate-albumin (19,550 cpm/nmol) and the incorporation of [$^{14}$C]oleate (■) and [$^3$H]cholesterol (□) into cholesteryl oleate was determined by thin-layer chromatography.

**Fig. 20**[61]: [$^{14}$C]Oleate incorporation into cholesteryl esters after incubation with LDL as a function of oleate concentration (A) and time (B) in normal (●) and mutant (o) cells. Cell monolayers were preincubated 17 hours in LPDS-medium containing LDL (Exp. A, 60 μg of cholesterol per ml; Exp. B, 150 μg of cholesterol per ml). In Exp. A, the indicated concentration of [$^{14}$C]oleate (2300 cpm/nmol) was then added and the cells were incubated for a further 3 hours before harvest. In Exp. B, [$^{14}$C]oleate (0.1 mM, 24,000 cpm/nmol) was added then cells were harvested at the indicated time. The cellular content of cholesteryl [$^{14}$C]esters was determined.

**Fig. 21**[101]: Effect of cycloheximide on $^{125}$I-LDL binding activity in fibroblasts monolayers after prior incubation either in the presence or absence of unlabeled LDL. On day 6, half of the dishes (Δ,▲) received 10 μg/ml of unlabeled LDL. After 24 hour (zero time), all monolayers were washed twice with 4 ml of PBS, after which 2 ml of medium containing either no cycloheximide (o,Δ) or 0.5 mM cycloheximide (●,▲) were added. At the indicated time, 10 μg/ml of $^{125}$I-LDL (70 cpm/ng) were added to duplicate dishes from each group and the cellular content of $^{125}$I radioactivity was determined 2 hour later. The mean content of total cellular protein (μg/dish) was (o) 230; (●) 190; (Δ) 216; (▲) 191.

**Fig. 22a and b**[9 105]: The curves of Fig. 22a are generated with the best fit parameters in table 3. The curves of Fig. 22b are predicted with the best fit parameters. Correlation of the time courses for suppression of $^{125}$I-LDL binding activity and accumulation of cholesteryl esters. On day 4 of cell growth (zero time), each dish received 2 ml of medium containing either 10 μg protein per ml of unlabeled LDL (22a) or 50 μg protein per ml of unlabeled LDL (22b). Every 24 hour throughout the experiment, the medium in each dish was replaced with fresh medium containing the indicated amount of unlabeled LDL. At the indicated time, the dishes were divided into two sets. In one set, the medium from each was removed and replaced with 2 ml of medium containing 25 μg protein/ml of $^{125}$I-LDL. After incubation at 37°C for 2 hr, the specific heparin-releasable $^{125}$I radioactivity was determined. A second set of dishes was washed, harvested and pooled, and their content of cholesteryl esters was determined.

**Fig. 22c**: Prediction[9 105] in the medium containing LDL 2 μg/ml. See Figure 22a and b.[9 105]

**Fig. 23**[101]: Suppression of $^{125}$I-LDL binding activity in fibroblast monolayers by 25-hydroxycholesterol and cholesterol. On day 7 (zero time), each dish received 2 ml of medium containing either 6 μl of ethanol alone (o) or 6 μl of ethanol containing 24 μg of cholesterol (●), 1.2 μg of 25-hydroxycholesterol (Δ), or 24 μg of cholesterol plus 1.2 μg of 25-hydroxycholesterol (▲). At the indicated time, 10 μg/ml of $^{125}$I-LDL (70 cpm/ng) were added to duplicate dishes from each group and the cellular content of $^{125}$I radioactivity was determined 2 hr later. The mean content of total cellular protein (μg/dish) was (o) 245, (●) 250, (Δ) 245, (▲) 241.

**Fig. 24**[101]: Feedback suppression of $^{125}$I-LDL binding activity in fibroblast monolayers by unlabeled LDL and its prevention by

chloroquine. On day 7 (zero time) the dishes were divided into 4 groups and received 2 ml of medium containing (o) no LDL, no chloroquine; (•) no LDL, 75 μM chloroquine; (Δ) 10 μg/ml unlabeled LDL, no chloroquine; (▲) 10 μg /ml unlabeled LDL, 75 μM chloroquine. At the indicated time, duplicated dishes containing 10 μg/ml of unlabeled LDL (Δ,▲) received an additional 10 μg/ml of $^{125}$I-LDL (60 cpm/ng) and duplicate dishes containing no LDL (o,•) received 20 μg/ml of $^{125}$I-LDL (30 cpm/ng). Thus during the labeling period, all dishes contained 20 μg/ml of $^{125}$I-LDL at a final specific activity of 30 cpm/ng. The cellular content of $^{125}$I radioactivity was determined after 1 hr incubation.

**Fig. 25**[101]: The estimated half life of LDL receptor with various LDL concentration in medium.

**Fig. 26**[53]: The cells were incubated in fresh growth medium containing 10% fetal calf serum. After 3 days, the medium was replaced with 2 ml of fresh growth medium containing 5% human LPDS. After 24 hours, the medium was replaced with 2 ml of fresh growth medium containing 5% human LPDS and the indicated concentration of LDL. After a further 24 hours, each cell monolayer was washed and harvested and the sterols contents were measured.

**Fig. 27**[35]: Prediction: The curve is predicted with the best fit parameters in table 3. See Figure 12c.

**Fig. 28a-e**[101]: Prediction: The curve is predicted with the best fit parameters in table 3. Effect of prior incubation with varying concentrations of unlabeled LDL on unlabeled LDL on $^{125}$I-LDL binding activity in fibroblast monolayers. On day6, cell monolayers were switched to 2 ml of medium containing the indicated concentration of unlabeled LDL: none, 2 μg/ml, 10 μg/ml, 100 μg/ml. After 18 hours (zero time), each monolayer was washed twice with 3 ml of PBS. At the indicated time, 10 μg/ml of $^{125}$I-LDL (76 cpm/ng) were added to duplicate dishes from each group and the cellular content of total cellular protein (μg/dish) was 317, 313, 314 and 335 respectively.

**Fig. 29**[21]: Prediction: See Figure 22a and b.[9,105]

**Fig. 30**[21]: See Figure 28a through e.[101]

**Fig. 31**[10]: The curve is predicted with the best fit parameters in table 3 except initial receptor conditions are given as 50% of steady state value in LPDS incubation. Initial condition of CE is given as 15 μg/mg protein. See Figure 26.

**Fig. 32**[21]: Prediction: See Fig. 26.[10]

**Fig. 33**[21]: The predicted rate of LDL hydrolysis at steady state.

**Fig. 34**: The predicted rate of LDL hydrolysis at steady state with the best fit parameters in table 3..

**Fig. 35**[105]: Prediction: The curve is predicted with the best fit parameters in table 3. Effect of prolonged incubation with varying amounts of LDL on $^{125}$I-LDL binding activity. On day 4 of cell growth, each dish received 2 ml of growth medium containing

10% calf lipoprotein-deficient serum and the indicated concentration of unlabeled LDL. Each 24 hour through experiment, the medium in each dish was replaced with fresh medium containing the indicated amount of unlabeled LDL. After 3 days of such treatment, on day 7 of cell growth, the medium was removed and replaced with 2 ml of medium containing 25 $\mu$g protein/ml of $^{125}$I-LDL (106 cpm/ng). After incubation at 37°C for 2 hours, the specific heparin-releasable $^{125}$I radioactivity was determined.

# Fig. 9

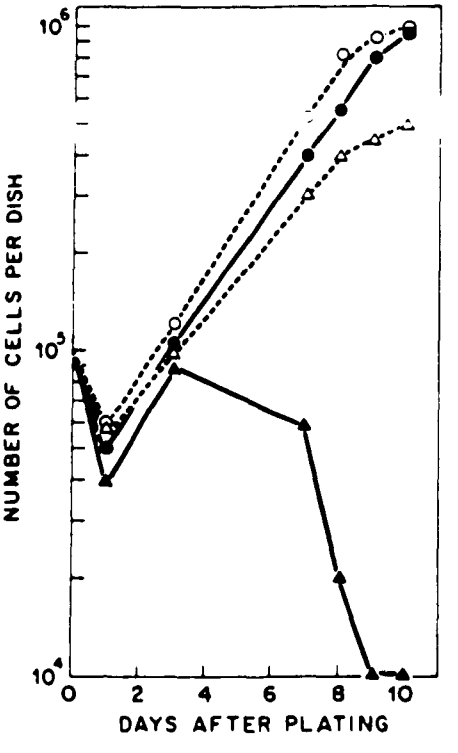


Growth rate of normal fibroblasts

**Fig. 10a**

**Fig. 10c**

**Fig. 10b**

**Fig. 10d**

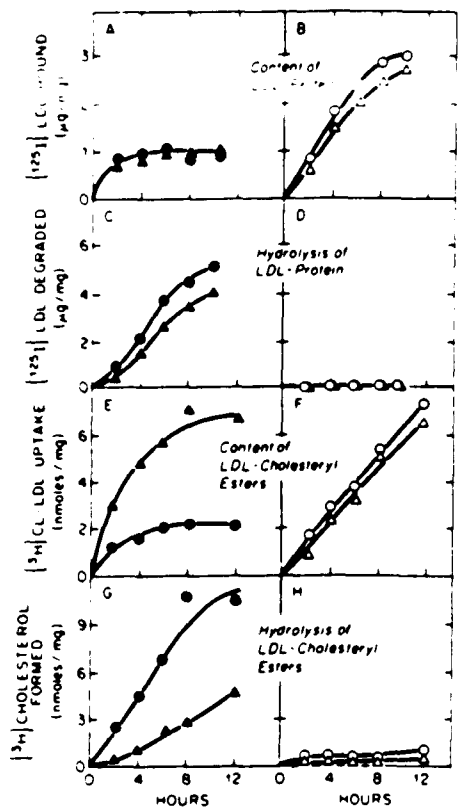


Time course of LDL metabolism in normal (●,○) and
t (▲,△) fibroblast monolayers incubated in the absence and
ce of chloroquine.

**Fig. 11b**

**Fig. 11a**

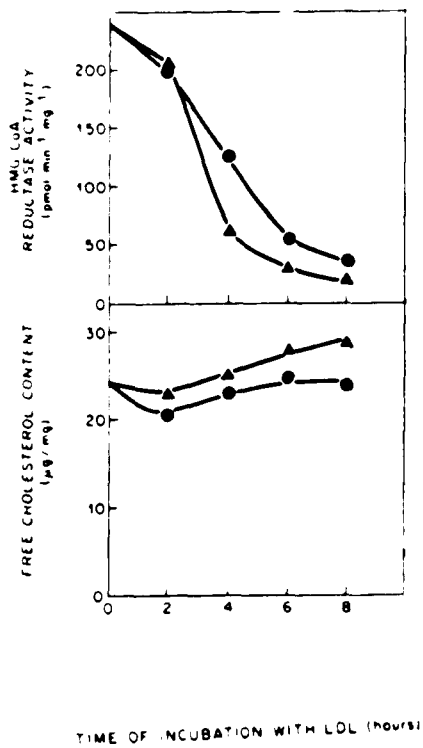

**Fig. 12a**

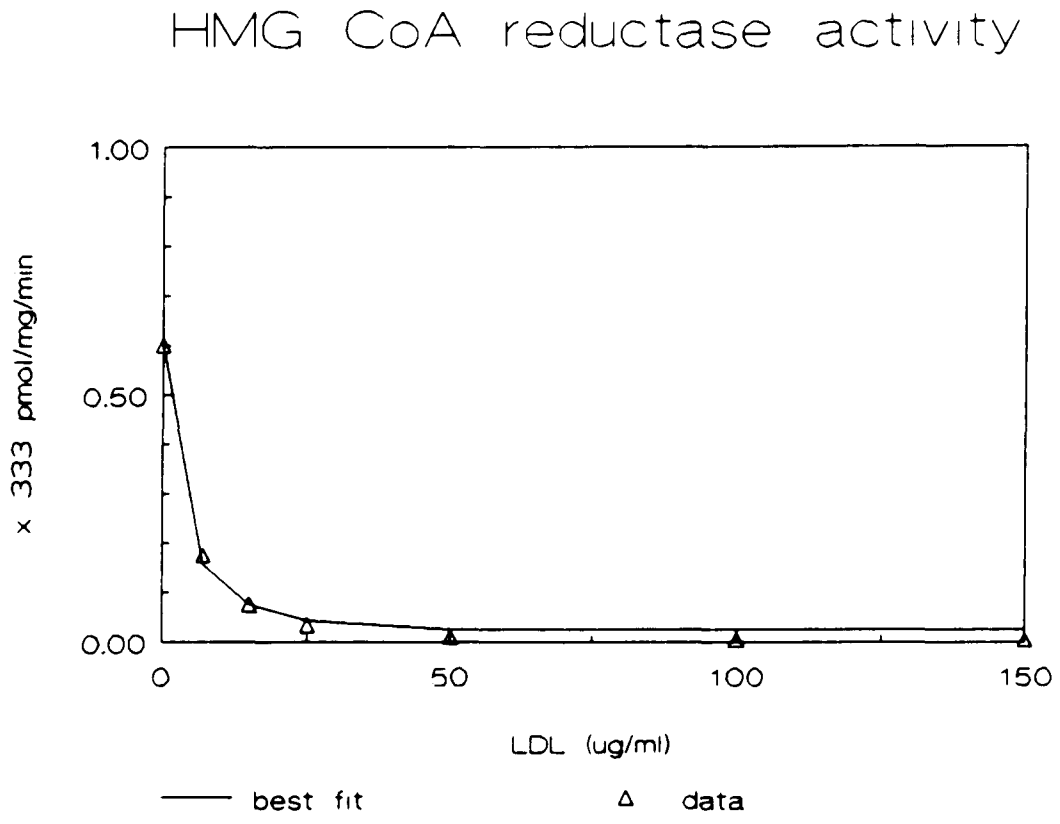
HMG CoA reductase activity
1.00
0.50
0.00
x 333 pmol/mg/min
0
50
100
150
LDL (ug/ml)
best fit
data

**Fig. 12b**

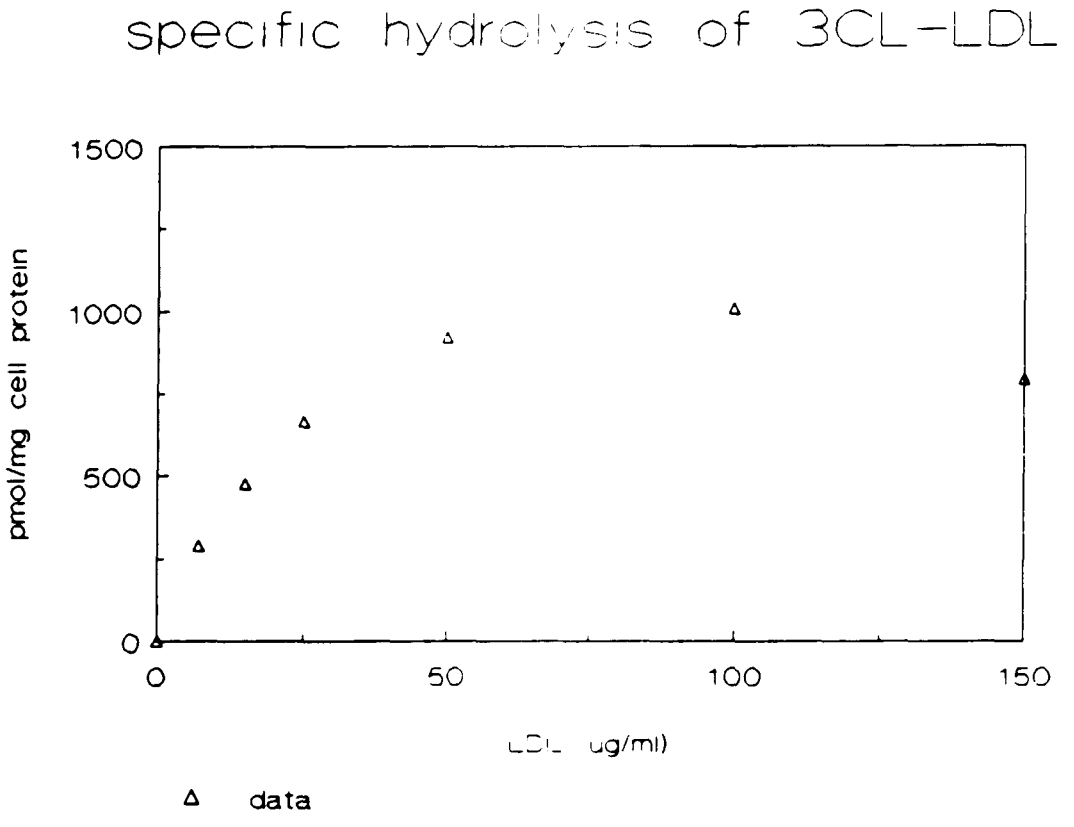
specific hydrolysis of 3CL-LDL
1500
1000
500
0
pmol/mg cell protein
0
50
100
150
LDL ug/ml)
data

**Fig. 12c**

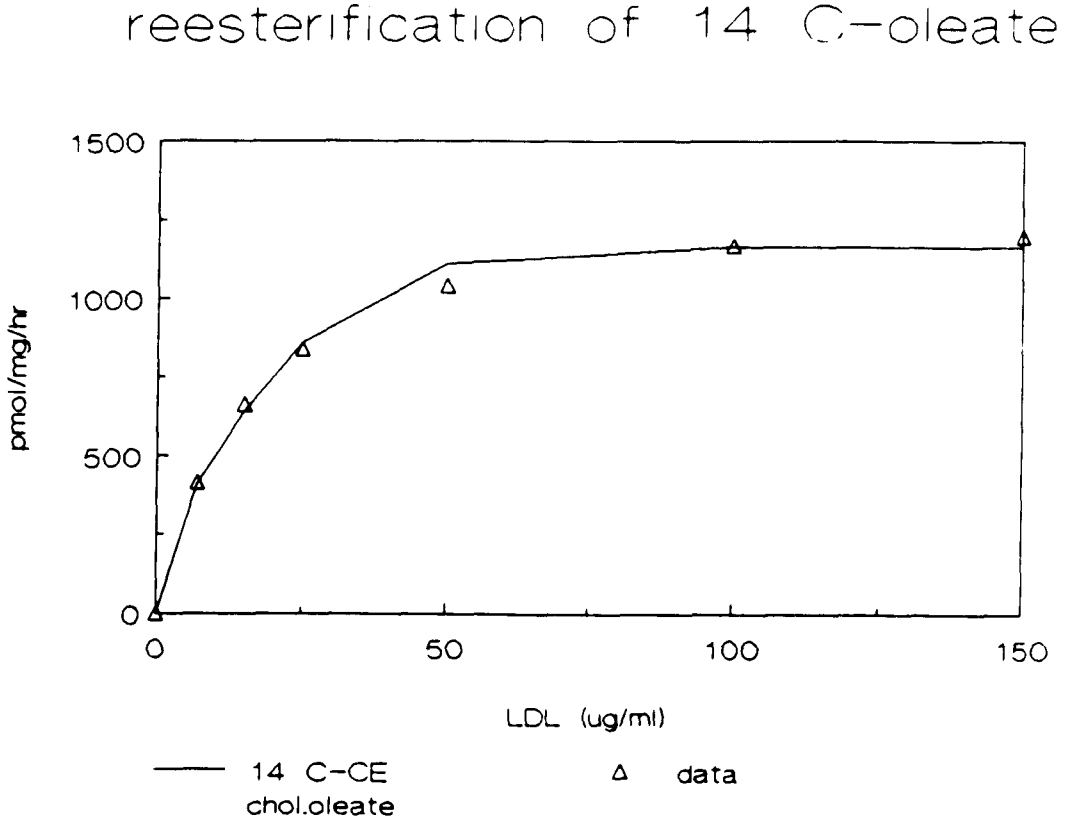
reesterification of 14 C-oleate
1500
1000
500
0
pmol/mg/hr
0
50
100
150
LDL (ug/ml)
14 C-CE chol.oleate
data

**Fig. 13**

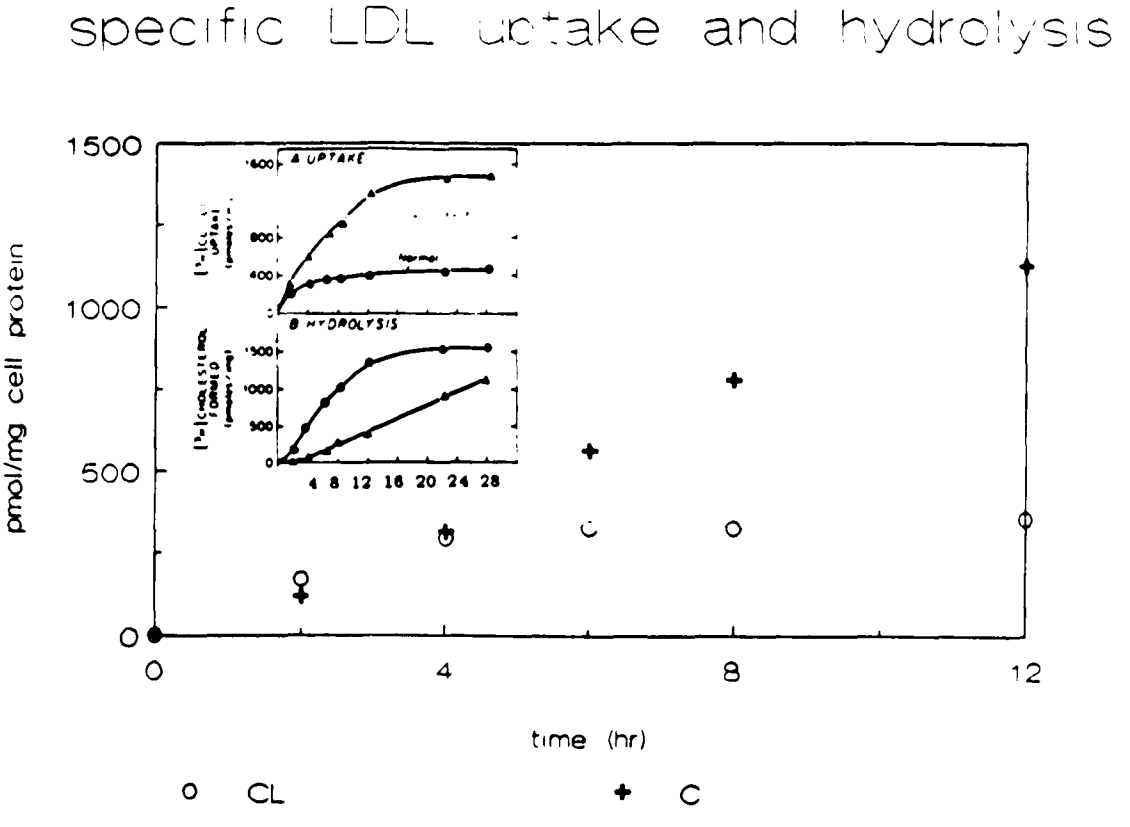
specific LDL uptake and hydrolysis
pmol/mg cell protein
1500
1000
500
0
0
4
8
12
time (hr)
A UPTAKE
B HYDROLYSIS
4 8 12 16 20 24 28
o CL
+ C

**Fig. 14**

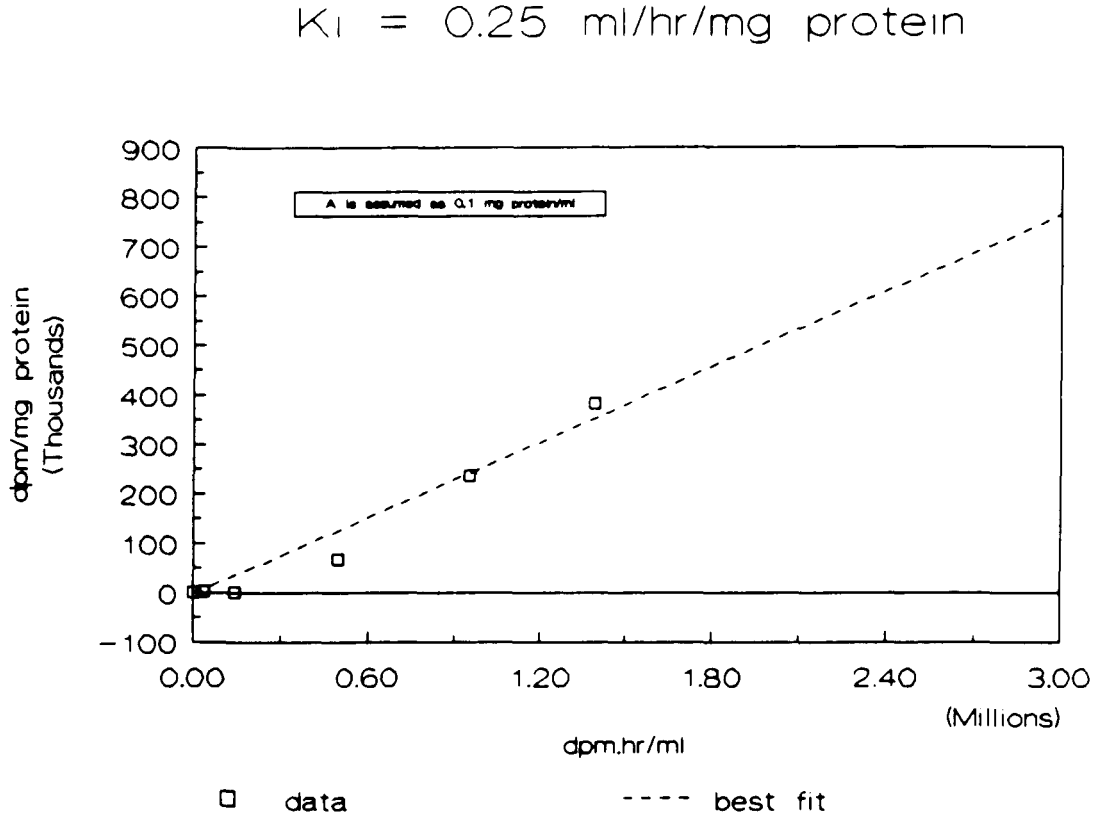
K1 = 0.25 ml/hr/mg protein
900
800
700
600
500
400
300
200
100
0
−100
dpm/mg protein
(Thousands)
0.00
0.60
1.20
1.80
2.40
3.00
(Millions)
dpm.hr/ml
data
best fit

**Fig. 15a**

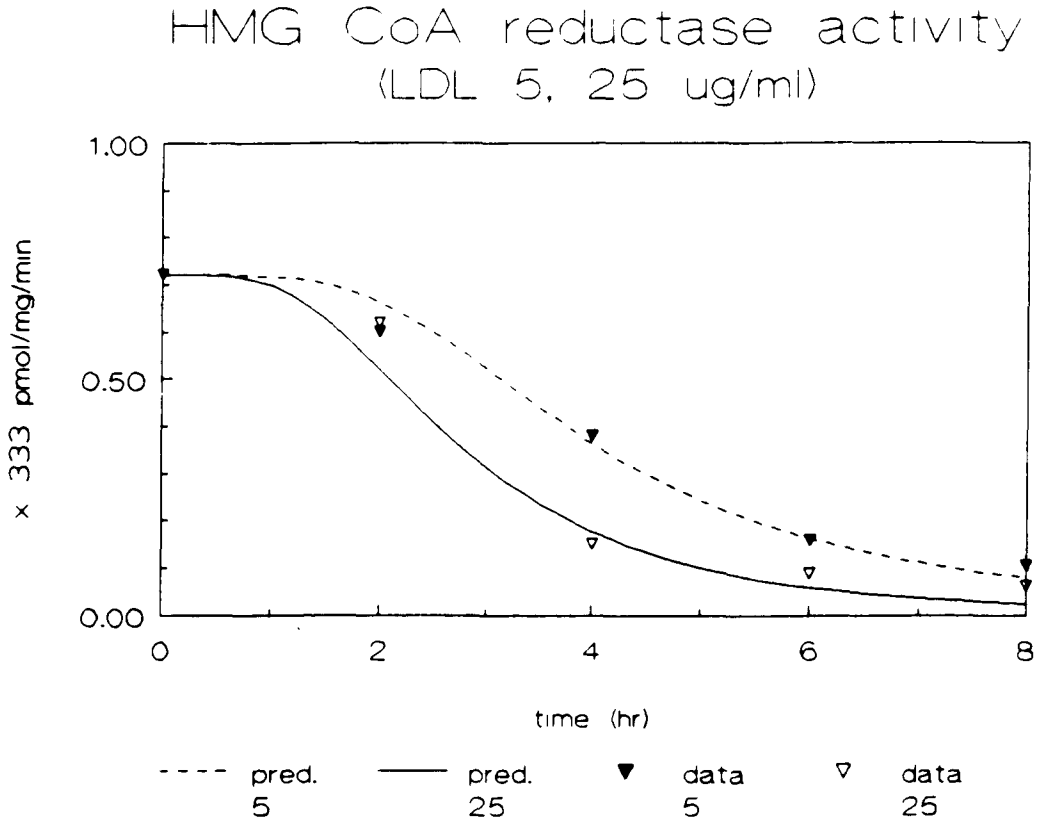
HMG CoA reductase activity
(LDL 5, 25 ug/ml)
1.00
0.50
0.00
× 333 pmol/mg/min
0
2
4
6
8
time (hr)
pred. 5
pred. 25
data 5
data 25

**Fig. 15b**

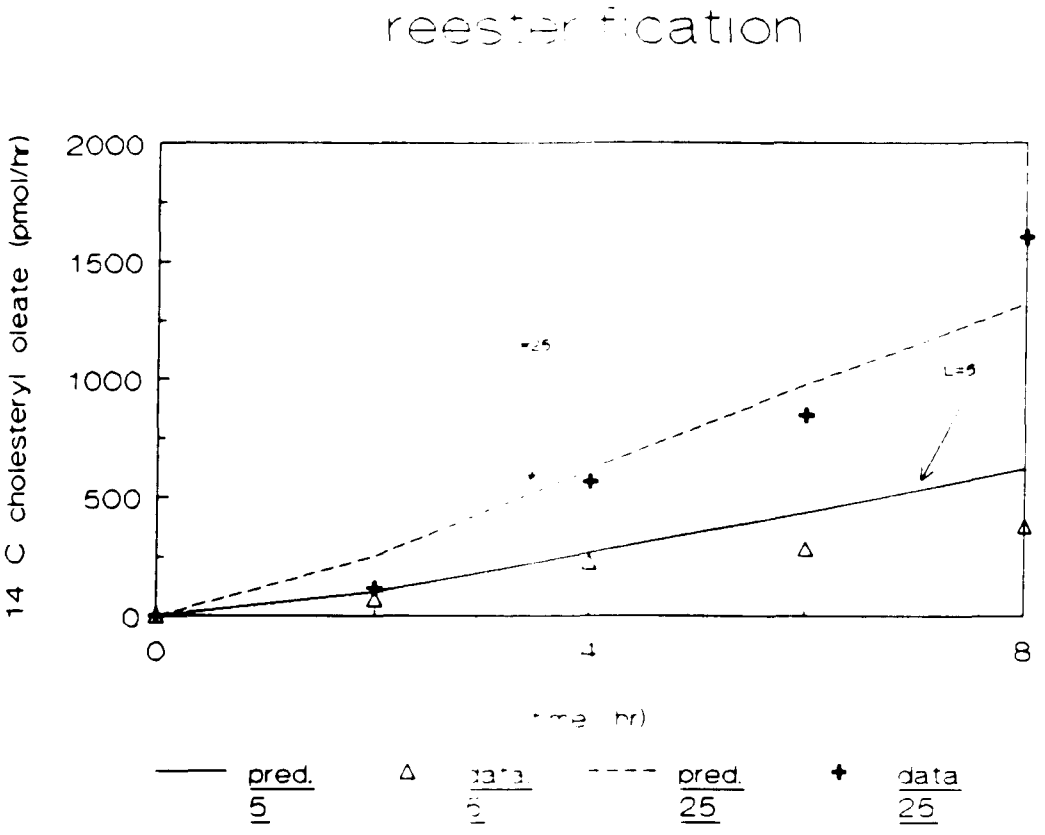
reesterification
14 C cholesteryl oleate (pmol/hr)
2000
1500
1000
500
0
0
4
8
pred. 5
data 5
pred. 25
data 25

**Fig. 16a**

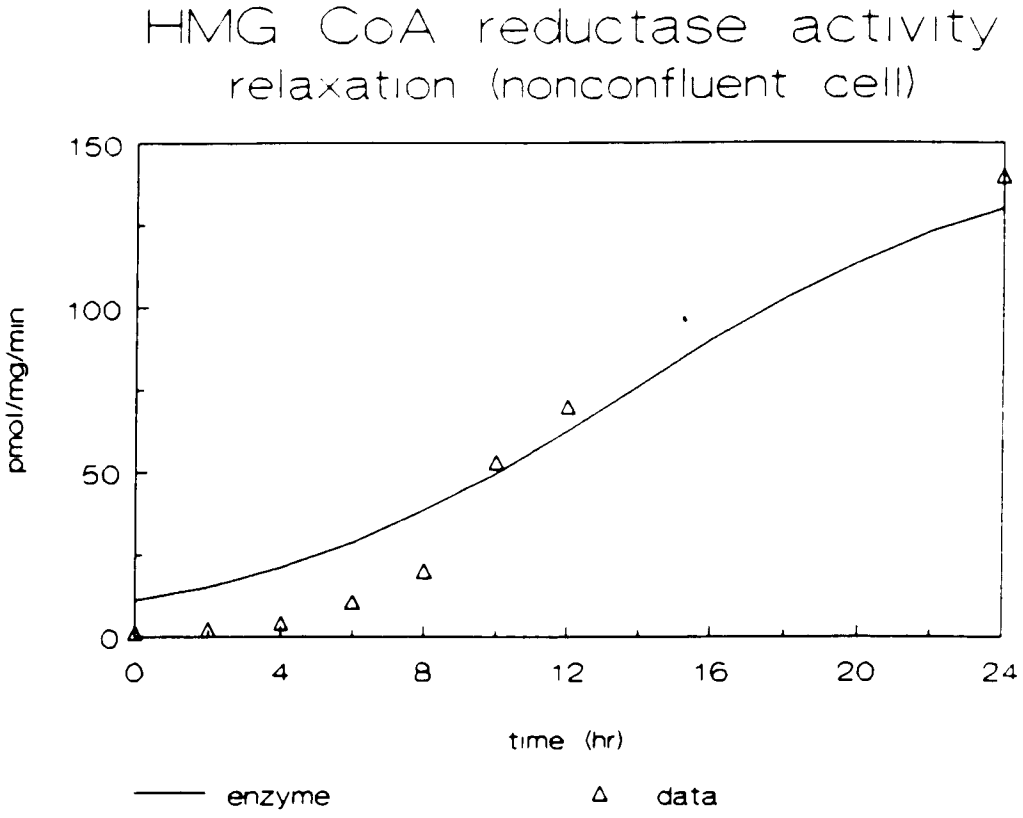
HMG CoA reductase activity
relaxation (nonconfluent cell)
150
100
50
0
pmol/mg/min
0
4
8
12
16
20
24
time (hr)
enzyme
data

**Fig. 16b**

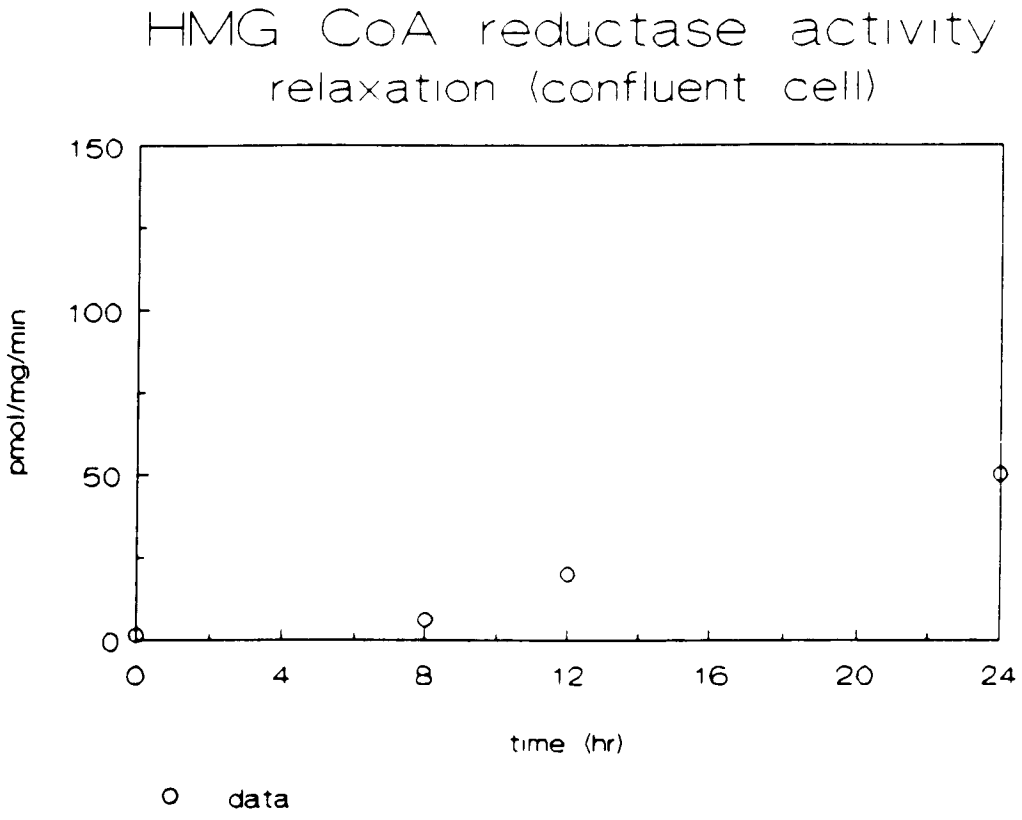
HMG CoA reductase activity
relaxation (confluent cell)
150
100
50
0
pmol/mg/min
0
4
8
12
16
20
24
time (hr)
data

# Fig. 17

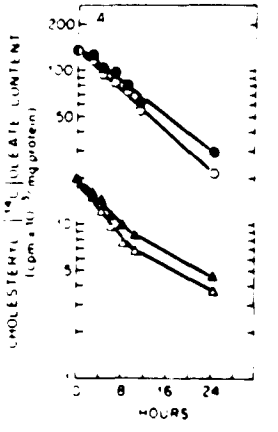


Rate of hydrolysis of endogenously synthesized cholesteryl [$^{14}$C]oleate in normal (●,○) and mutant (▲,△) fibroblast monolayers incubated in the presence and absence of chloroquine.

# Fig. 18

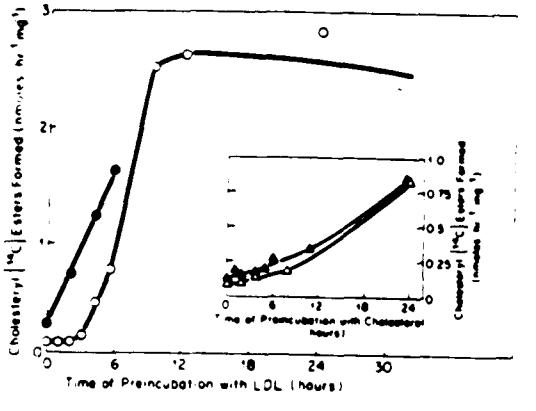


Rate of [$^{14}$C]oleate incorporation into cholesteryl esters in normal cells

# Fig. 19

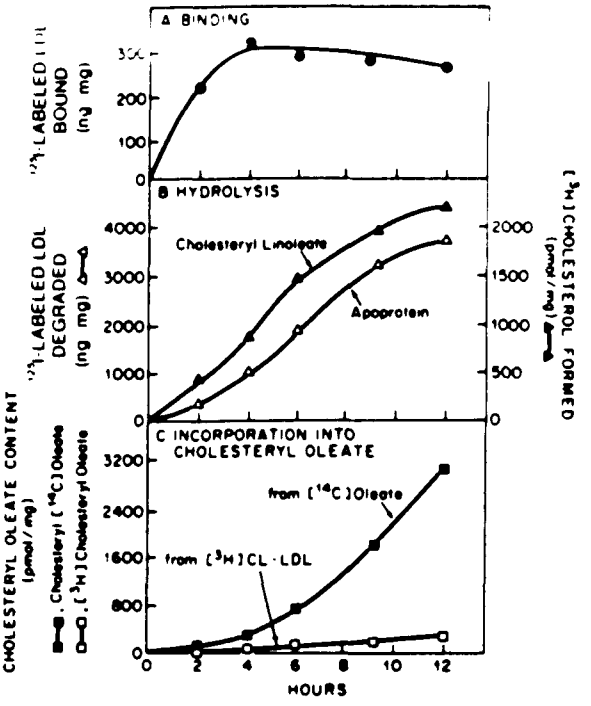


Time course of LDL metabolism in normal fibroblast monolayers.

# Fig. 20

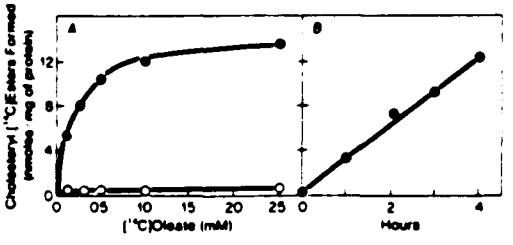


[14C]Oleate incorporation into cholesteryl esters after incubation with LDL as a function of oleate concentration (*A*) and time (*B*) in normal (●) and mutant (○) cells.

# Fig. 21

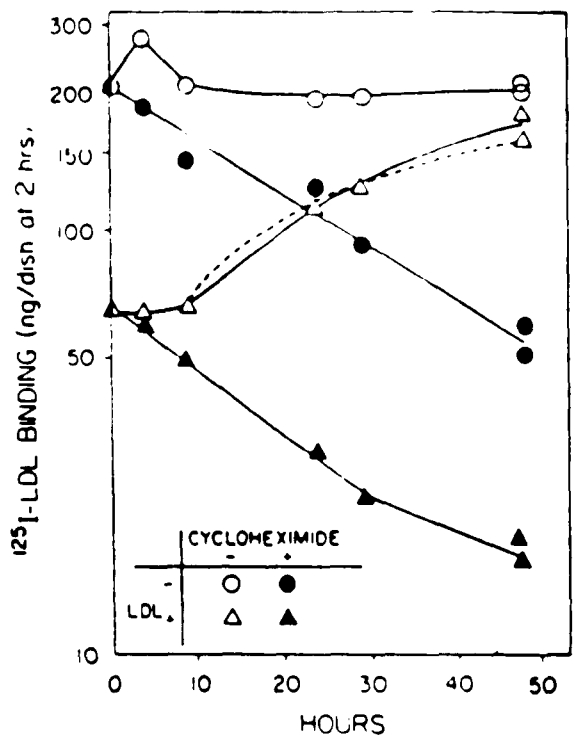


Effect of Cycloheximide on $^{125}$I-LDL Binding Activity in Fibroblast Monolayers after Prior Incubation either in the Presence or Absence of Unlabeled LDL

**Fig. 22a**

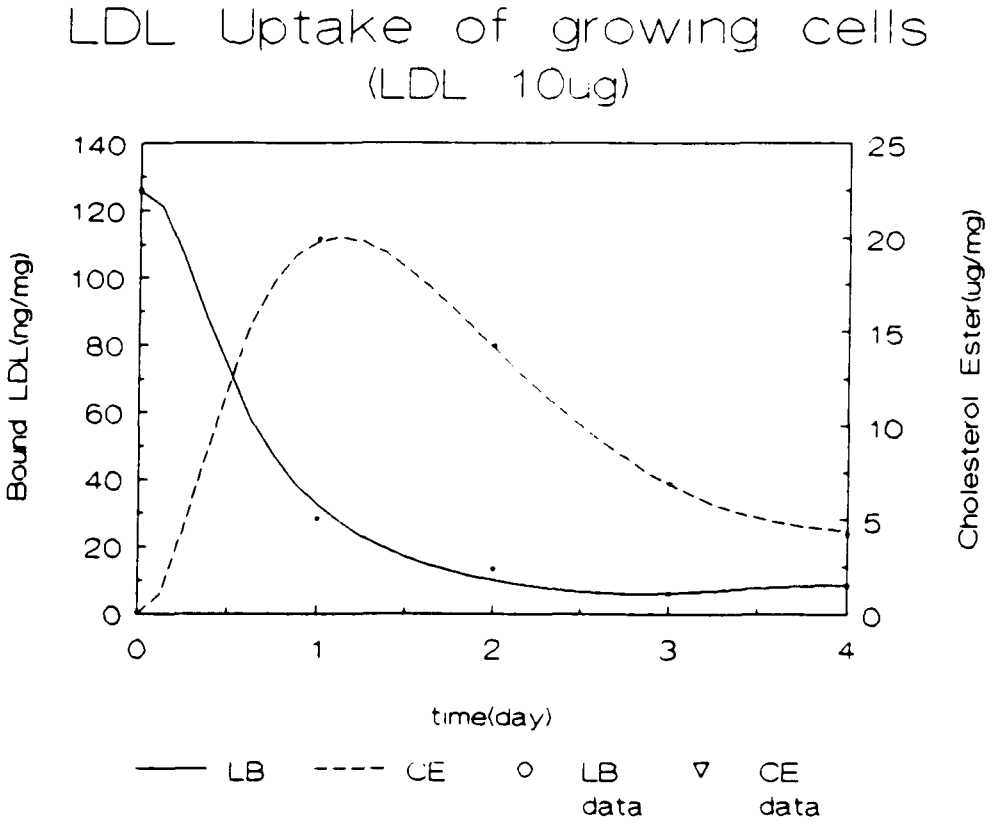
LDL Uptake of growing cells
(LDL 10ug)
Bound LDL(ng/mg)
Cholesterol Ester(ug/mg)
time(day)
140
120
100
80
60
40
20
0
25
20
15
10
5
0
0
1
2
3
4
LB
CE
LB data
CE data

**Fig. 22b**

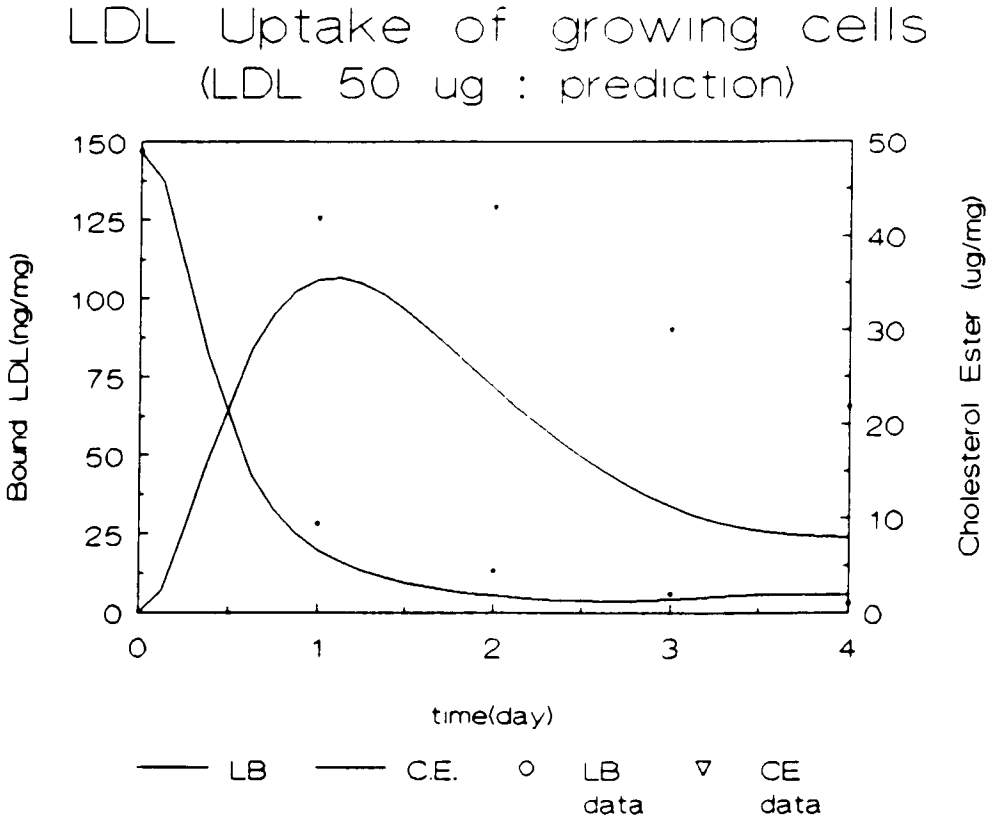
LDL Uptake of growing cells
(LDL 50 ug : prediction)
Bound LDL(ng/mg)
Cholesterol Ester (ug/mg)
150
125
100
75
50
25
0
50
40
30
20
10
0
0
1
2
3
4
time(day)
LB
C.E.
LB data
CE data

**Fig. 22c**

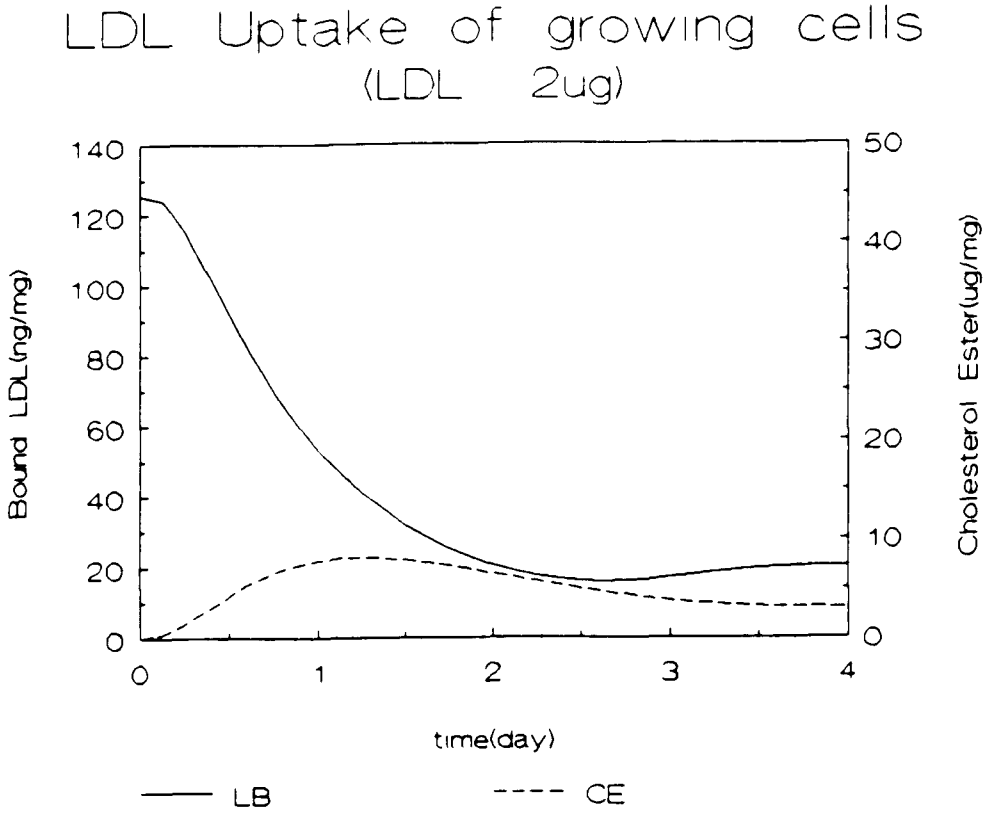
LDL Uptake of growing cells
(LDL 2ug)
Bound LDL(ng/mg)
Cholesterol Ester(ug/mg)
time(day)
LB
CE
0
20
40
60
80
100
120
140
10
30
50
1
2
3
4

# Fig. 23

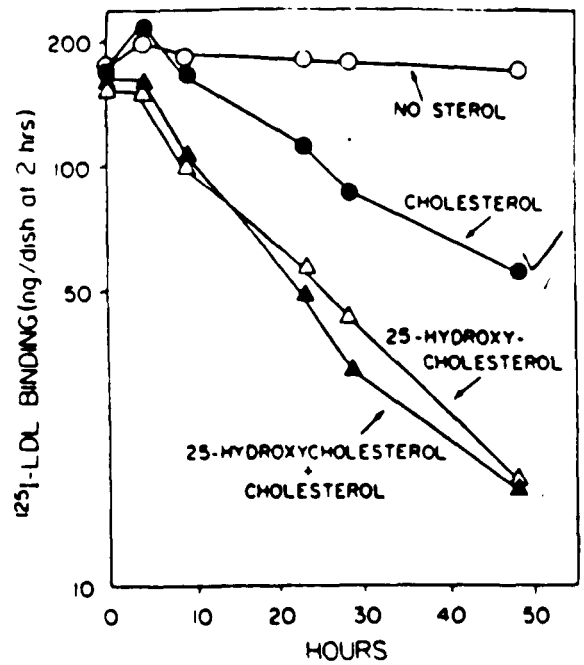


Suppression of $^{125}$I-LDL Binding Activity in Fibroblast Monolayers by 25-Hydroxycholesterol and Cholesterol

# Fig. 24

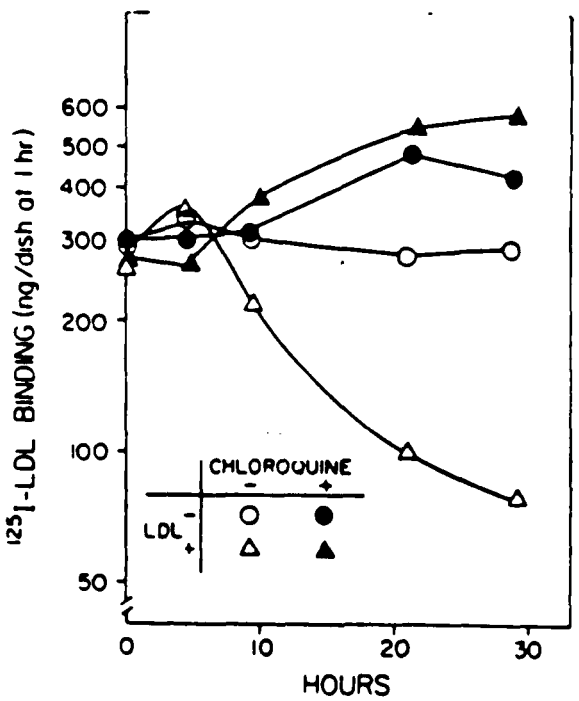


Feedback Suppression of $^{125}$I-LDL Binding Activity in Fibroblast Monolayers by Unlabeled LDL and Its Prevention by Chloroquine

**Fig. 25**

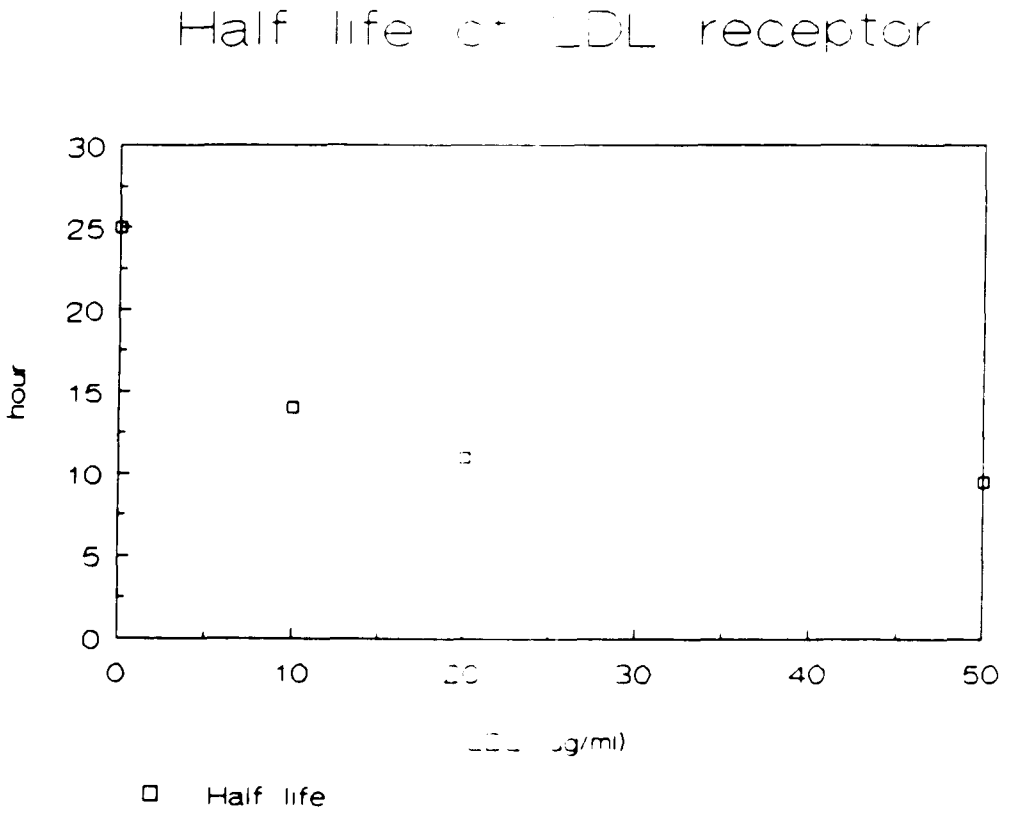
Half life
LDL receptor
30
25
20
15
10
5
0
hour
0
10
30
40
50
Half life

# Fig. 26

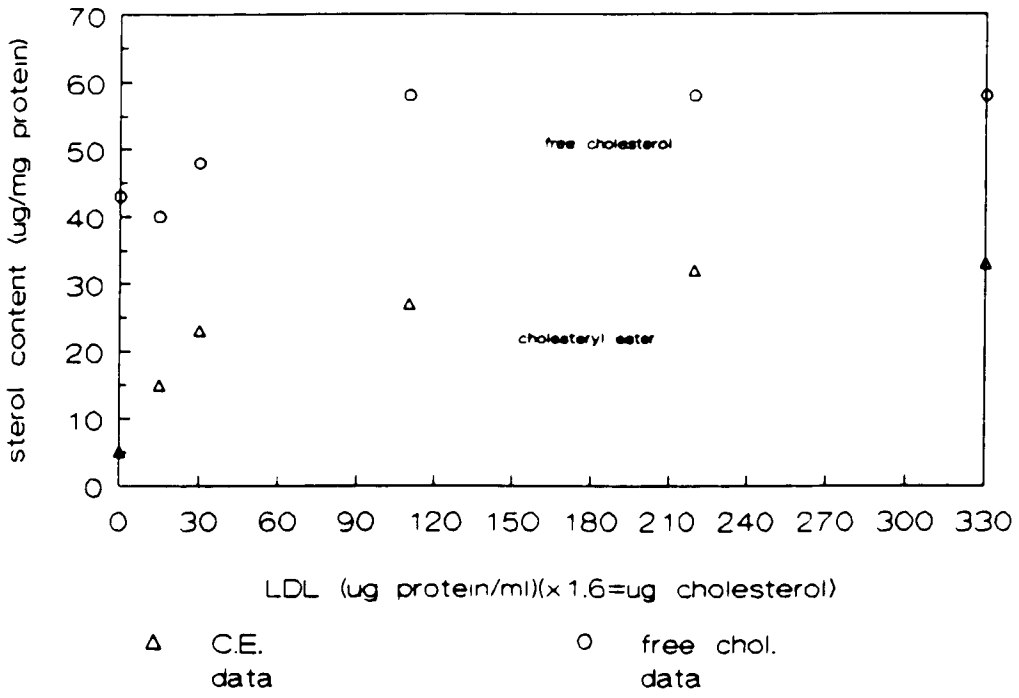
70
60
50
40
30
20
10
0
sterol content (ug/mg protein)
free cholesterol
cholesteryl ester
0 30 60 90 120 150 180 210 240 270 300 330
LDL (ug protein/ml)(x 1.6=ug cholesterol)
Δ C.E. data
O free chol. data

**Fig. 27**

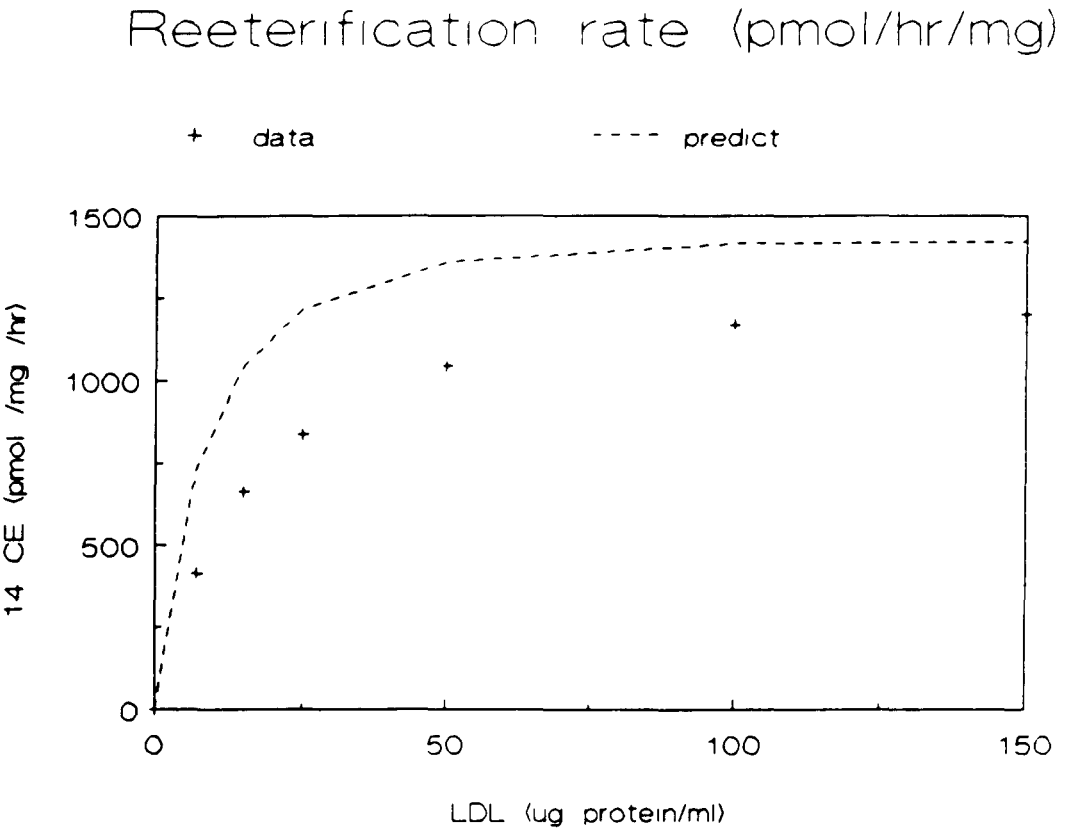
Reeterification rate (pmol/hr/mg)
+ data
---- predict
1500
1000
500
0
14 CE (pmol /mg /hr)
0
50
100
150
LDL (ug protein/ml)

**Fig. 28a**

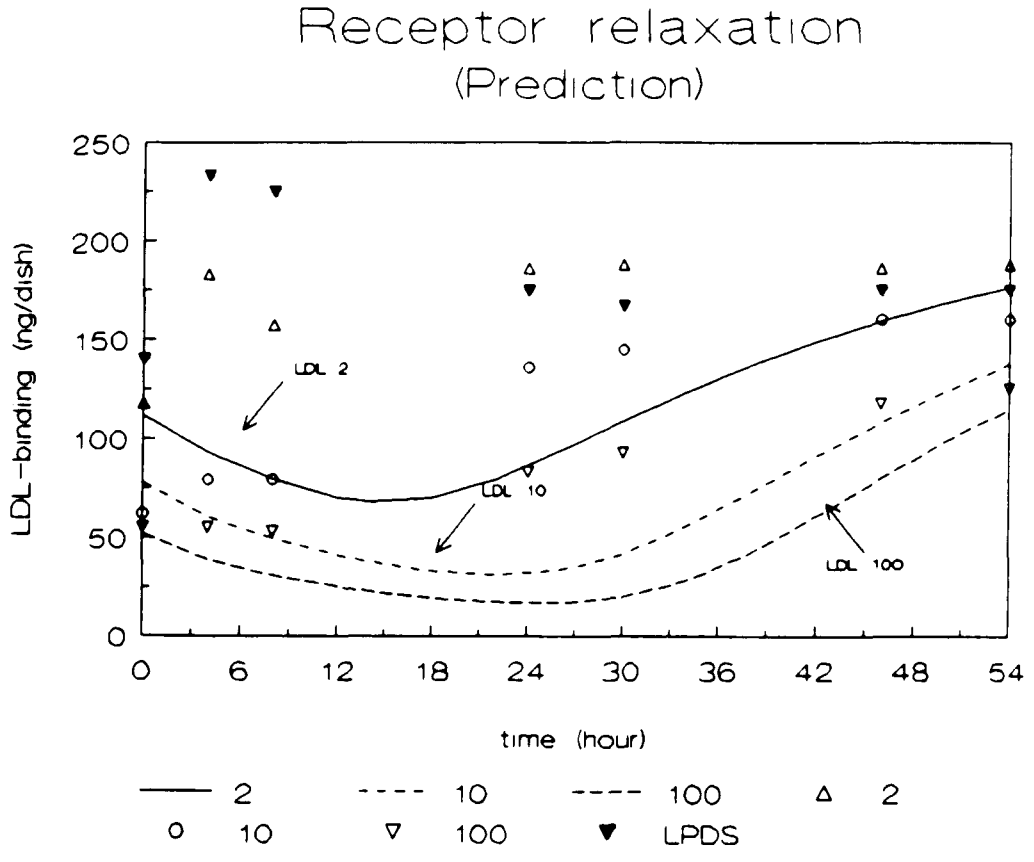
Receptor relaxation
(Prediction)
LDL-binding (ng/dish)
250
200
150
100
50
0
0
6
12
18
24
30
36
42
48
54
time (hour)
LDL 2
LDL 10
LDL 100
2
10
100
2
10
100
LPDS

**Fig. 28b**

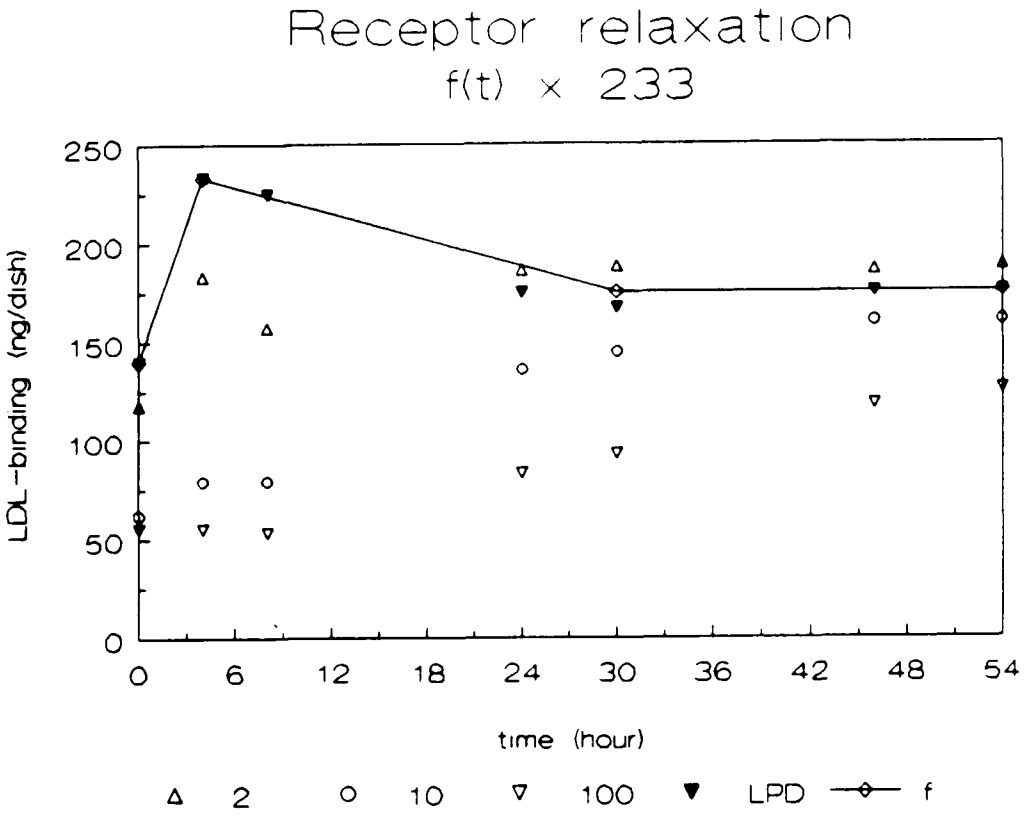
Receptor relaxation
f(t) x 233
LDL-binding (ng/dish)
250
200
150
100
50
0
0
6
12
18
24
30
36
42
48
54
time (hour)
2
10
100
LPD
f

**Fig. 28c**

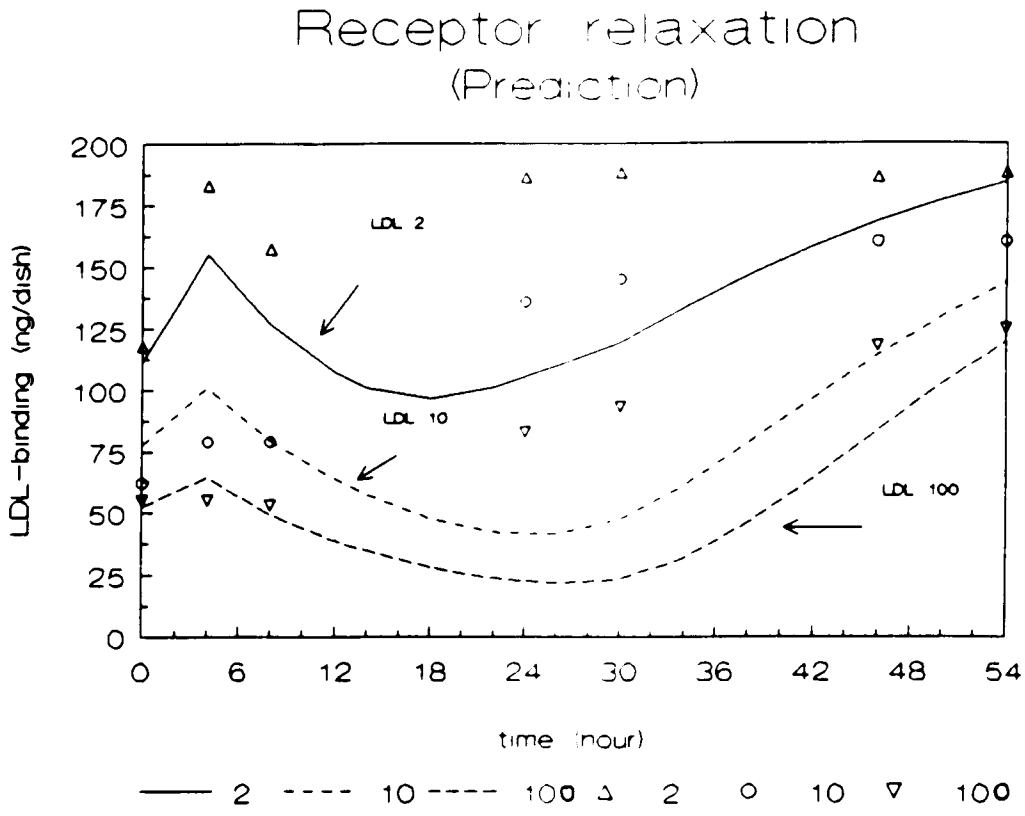
Receptor relaxation
(Prediction)
LDL-binding (ng/dish)
200
175
150
125
100
75
50
25
0
0
6
12
18
24
30
36
42
48
54
time (hour)
LDL 2
LDL 10
LDL 100
2
10
100
2
10
100

**Fig. 28d**

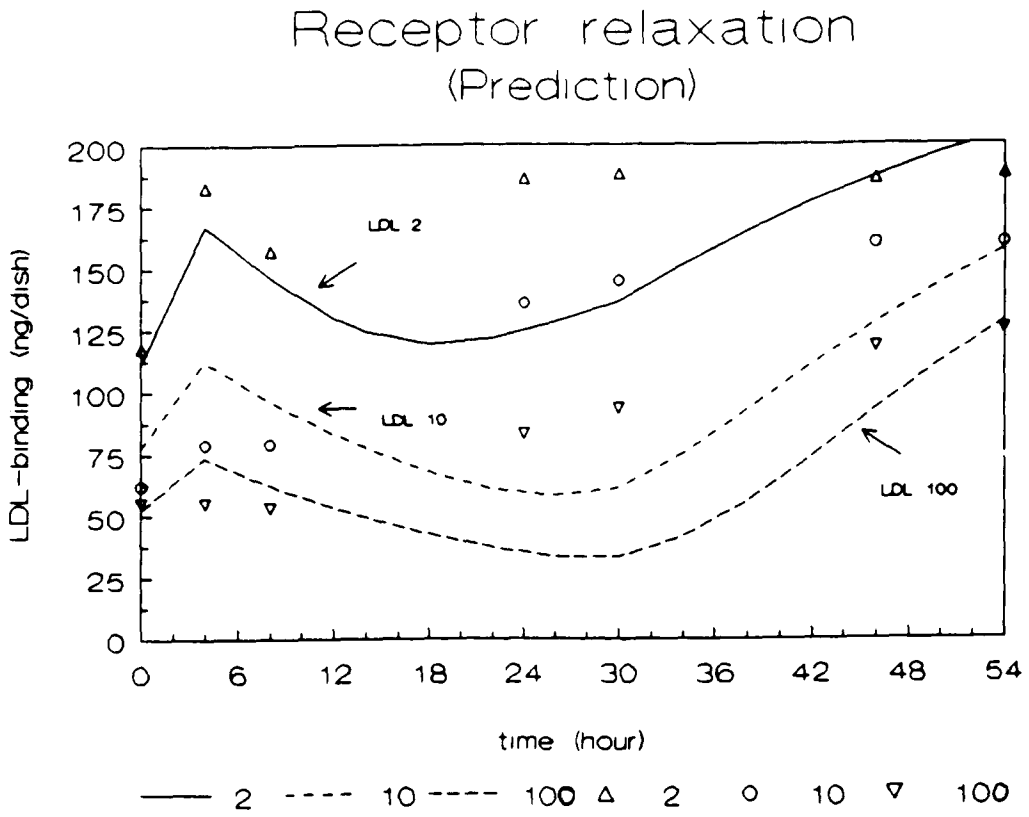
Receptor relaxation
(Prediction)
LDL-binding (ng/dish)
200
175
150
125
100
75
50
25
0
0
6
12
18
24
30
36
42
48
54
time (hour)
LDL 2
LDL 10
LDL 100
2
10
100
2
10
100

**Fig. 28e**

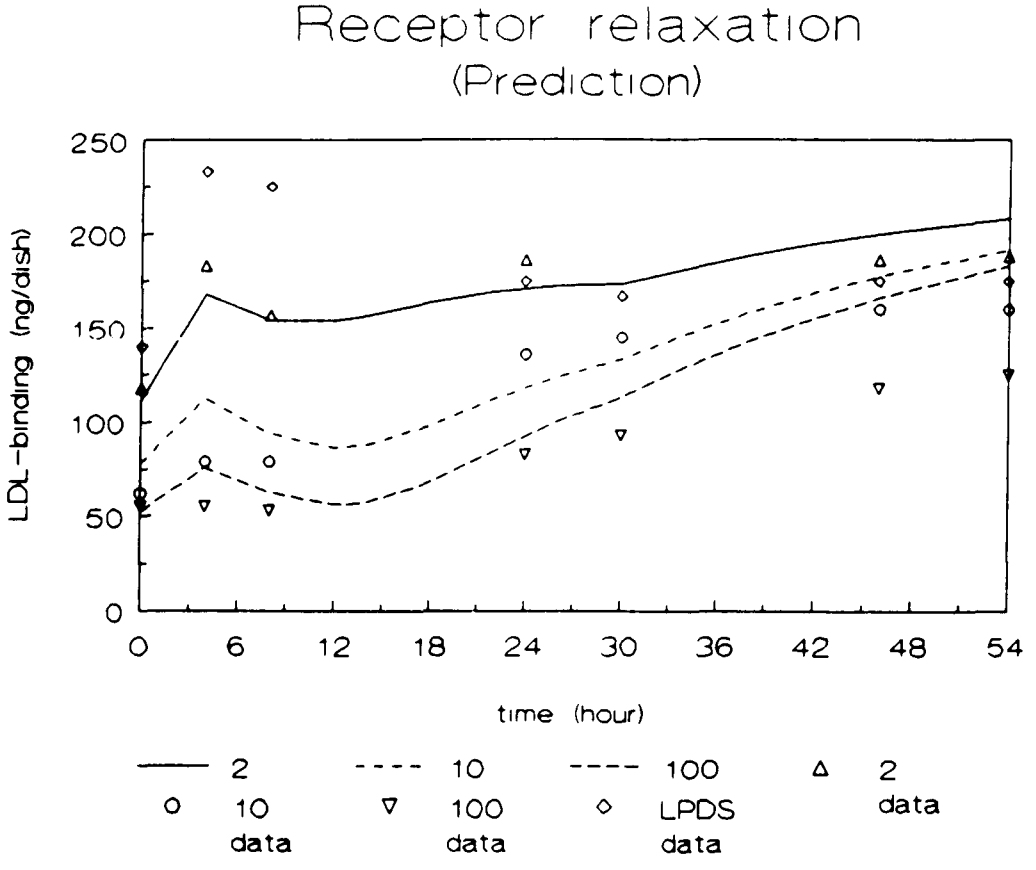
Receptor relaxation
(Prediction)
LDL-binding (ng/dish)
250
200
150
100
50
0
0
6
12
18
24
30
36
42
48
54
time (hour)
2
10
100
2
10 data
100 data
LPDS data
data

# Fig. 29

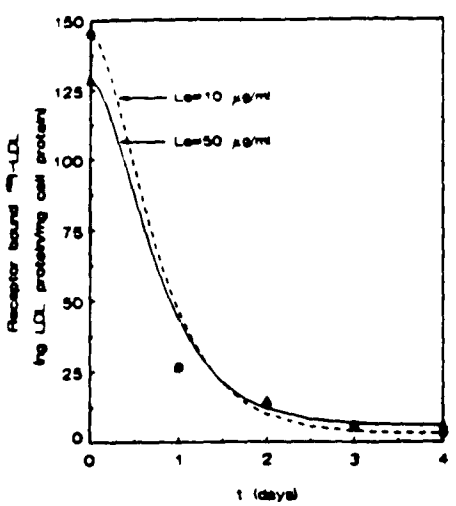


The predicted rate of LDL hydrolysis in the lysosome of the cells at steady state

# Fig. 30

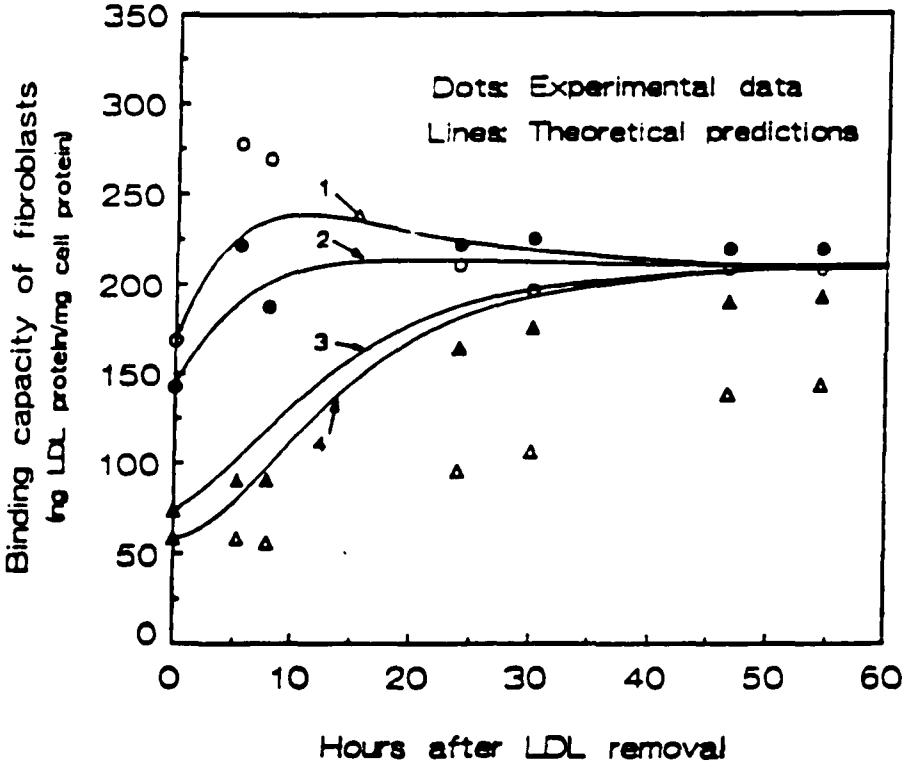
Dots: Experimental data
Lines: Theoretical predictions
Binding capacity of fibroblasts
(ng LDL protein/mg cell protein)
Hours after LDL removal
0
50
100
150
200
250
300
350
0
10
20
30
40
50
60
1
2
3
4

**Fig. 31**

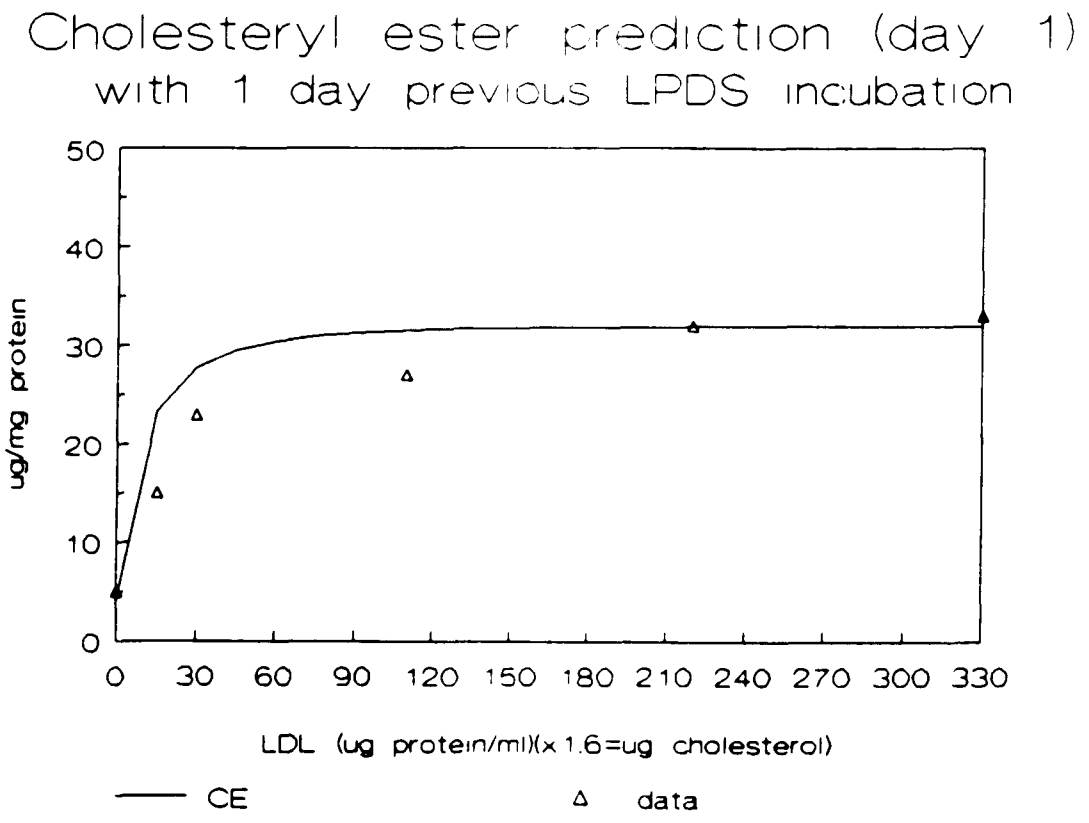
Cholesteryl ester prediction (day 1)
with 1 day previous LPDS incubation
ug/mg protein
50
40
30
20
10
0
0 30 60 90 120 150 180 210 240 270 300 330
LDL (ug protein/ml)(x 1.6=ug cholesterol)
CE
data

# Fig. 32

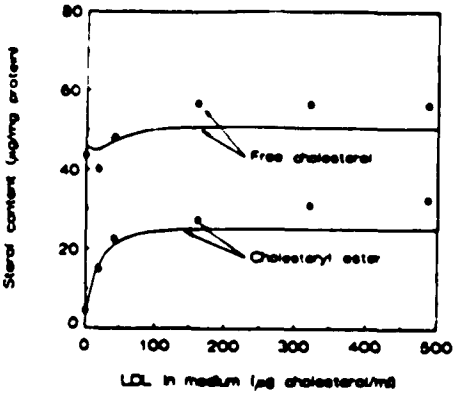


Effect of increasing concentrations of LDL on the content of free (○) and esterified (●) cholesterol in normal fibroblasts

# Fig. 33

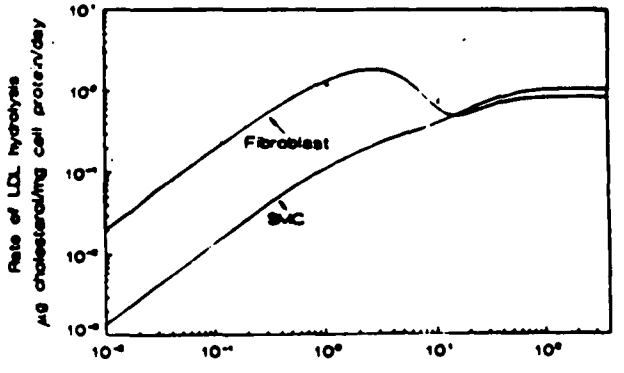


The predicted rate of LDL hydrolysis in the lysosome of the cells at steady state.

**Fig. 34**

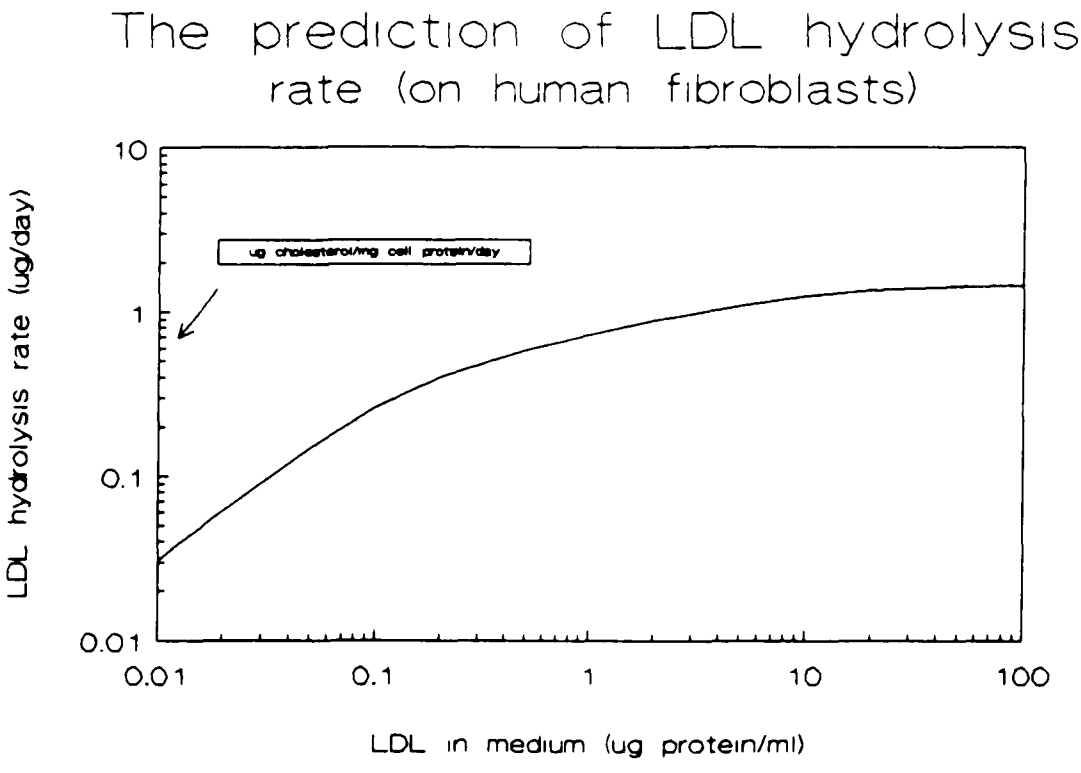
The prediction of LDL hydrolysis rate (on human fibroblasts)
LDL hydrolysis rate (ug/day)
10
1
0.1
0.01
ug cholesterol/mg cell protein/day
0.01
0.1
1
10
100
LDL in medium (ug protein/ml)

**Fig. 35**

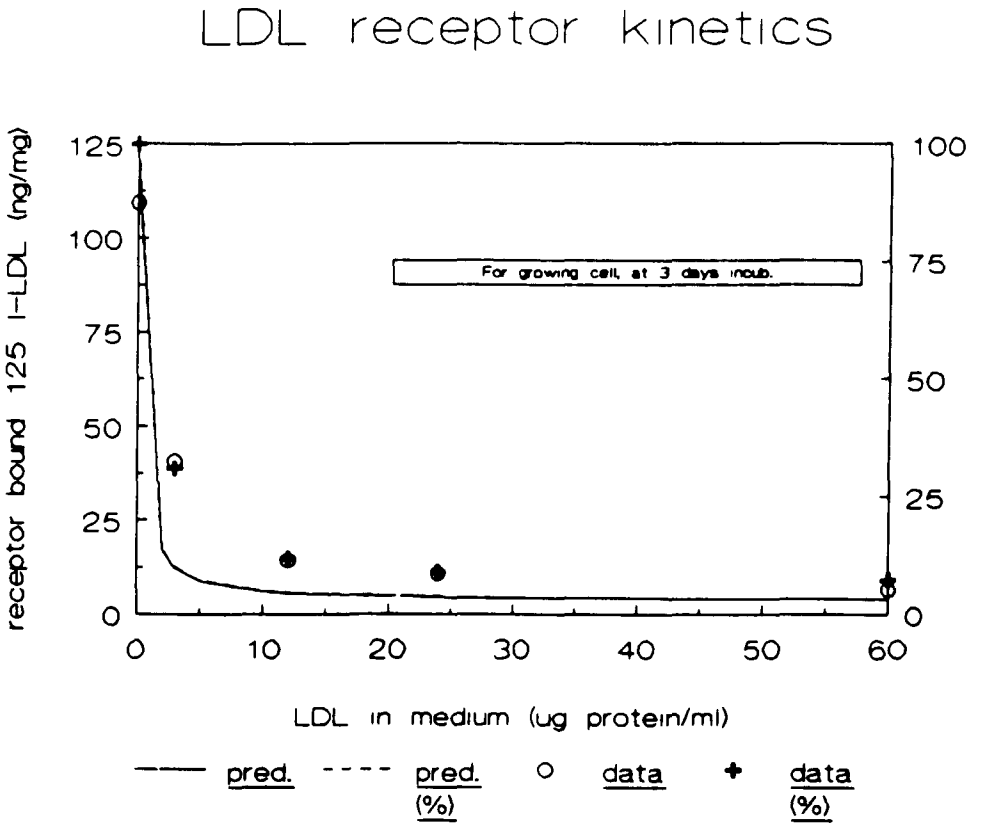


Effect of Prolonged Incubation with Varying Amounts of LDL on $^{125}$I-LDL Binding Activity

## APPENDIX I

In this appendix, we investigate the error in the calculation of $dC^{14}E/dt$ introduced by neglecting $MC^{hy}$ with respect to 1 in the expression for $C^a$. Let $\epsilon = MC^{hy}$, which we estimated to be about 0.1. Assume $\epsilon \ll 1$. Then, in terms of $\epsilon$, $dC^{14}E/dt$ becomes:

$$\frac{dC^{14}E}{dt} = \frac{k_{80}F\epsilon}{\epsilon+(1+\epsilon)Mk_7/(1+MC)} = \frac{k_{80}F\epsilon}{\epsilon+Mk_7/(1+MC)} \left[1- \frac{\epsilon}{1+\epsilon(1+MC)/Mk_7}+O\left(\frac{\epsilon}{1+\epsilon(1+MC)/Mk_7}\right)^2\right]$$

as long as $Mk_7/(1+MC) \leq O(1)$. The approximation in the text corresponds to retaining only the 1 in the square bracket above; it clearly yields an order $\epsilon$ relative error if $Mk_7/(1+MC)$ is order $\epsilon$ or order 1 and an $O(\epsilon^2)$ error if it is $O(\epsilon^2)$.

## Bibliography

1. Barak, L.S. and W.W. Webb. 1981. Fluorescent low density lipoprotein for observation of dynamics of individual receptor complexes on cultured human fibroblasts. *J. Cell Biol.* **90**:595-604.

2. Barak, L.S. and W.W. Webb. 1982. Diffusion of low density lipoprotein-receptor complex on human fibroblasts. *J. Cell Biol.* **95**:846-852.

3. Tank, D.W., W.J. Fredricks, L.S. Barak, and W.W. Webb. 1985. Electric field-induced redistribution and postfield relaxation of low density lipoprotein receptors on cultured human fibroblasts. *J. Cell Biol.* **101**:148-157.

4. Steinberg, D. 1983. Lipoproteins and atherosclerosis: A look back and a look ahead. *Arteriosclerosis*. 3:283-301.

5. Brown, M.S. and J.L. Goldstein. 1986. A receptor-mediated pathway for cholesterol homeostasis. *Science*. **232**:34-47.

6. Brown, M.S. and J.L. Goldstein. 1979. Receptor-mediated endocytosis: Insights from the lipoprotein receptor system. *Proc. Natl. Acad. Sci. USA.* **76**:3330-3337.

7. Anderson, R.G.W., M.S. Brown, U. Beisiegel and J.L. Goldstein. 1982. Surface distribution and recycling of the low density lipoprotein receptor as visualized with antireceptor antibodies. *J. Cell Biol.* **93**:523-531.

8. Brown, M.S. and J.L. Goldstein. 1975. Regulation of the activity of the low density lipoprotein receptor in human fibroblasts. *Cell.* **6**:307-316.

9. Goldstein, J.L. and M.S. Brown. 1977. The low density lipoprotein pathway and its relation to atherosclerosis. *Ann. Rev. Biochem.* **46**:897-929.

10. Fielding, C.J. 1984. The origin and properties of free cholesterol potential gradients in plasma, and their relation to atherogenesis. *J. Lipid Res.* **25**:1624-1628.

11. Brown, M.S. and J.L. Goldstein. 1976. Analysis of a mutant strain of human fibroblasts with a defect in the internalization of receptor-bound low density lipoprotein. *Cell.* **9**:663-674.

12. Linderman, J.J. and D.A. Lauffenburger. 1986. Analysis of intracellular receptor/ligand sorting: Calculation of mean surface and bulk diffusion times within a sphere. *Biophys. J.* **50**:295-305.

13. Gladhaug, I. and T. Christoffersen. 1988. Rapid constitutive internalization of epidermal growth factor receptors in isolated rat hepatocytes. *J. Biolog. Chem.* **263(25)**:12199-12203.

14. Lauffenburger, D.A., J. Linderman, and L. Berkowitz. 1987. Analysis of mammalian cell growth factor receptor dynamics. *Ann. N. Y. Acad. Sci.* **506**:147-162.

15. Waters, C.M., K.C. Oberg, G. Carpenter and K.A. Overholser. 1990. Rate constants for binding, dissociation and internalization of EGF: Effect of receptor occupancy and ligand concentration. *Biochem.* **29**:3563-3569.

16. Gex-Fabry, M., and C. DeLisi. 1984. Receptor-mediated endocytosis: A model and its implications for experimental analysis. *Am. J. Physiol.* **247**:R768-R779.

17. Davies, P.F., G.A. Truskey, H.B. Warren, S.E. O'Connor and B.H. Eisenhaure. 1985. Metabolic cooperation between vascular endothelial cells and smooth muscle cells in co-culture: Changes in low density lipoprotein metabolism. *J. Cell Biol.* **101**:871-878.

18. Truskey, G.A. and P.F. Davies. 1985. Effects of ammonium ion derived from bovine endothelial cells upon low density lipoprotein degradation in cultured vascular smooth muscle cells. *Cell Biol. Int. Reports.* **9(4)**:323-330.

19. Truskey, G.A., C.K. Colton, and K.A. Smith. 1986. 1986 Annual Meeting of the A.I.Ch.E. paper 56f. Miami Beach, Fla.

20. Truskey, G.A., C.K. Colton and P.F. Davies. 1984. Kinetic analysis of receptor-mediated endocytosis and lysosomal degradation in cultured cells. *Annals N.Y. Acad. Sci.* **435**:349-351.

21. Yuan, F., S. Weinbaum, R. Pfeffer and S. Chien. 1991. A mathematical model for the receptor-mediated cellular regulation of the LDL metabolism. *A.S.M.E. J. Biomech. Eng.* **113**:1-10.

22. Saffman, P.G. and M. Delbrück. 1975. Brownian motion in biological membranes. *Proc. Natl. Acad. Sci. U.S.A.* **72**:3111-3113.

23. Berg, H.C. and E.M. Purcell. 1977. Physics of chemoreception. *Biophysical J.* **20**:193-219.

24. Goldstein, B., C. Wofsy and G. Bell. 1981. Interactions of low density lipoprotein receptors with coated pits on human fibroblasts: Estimate of the foward rate constant and comparison with the diffusion limit. *Proc. Natl. Acad. Sci. USA.* **78**:5695-5698.

25. Goldstein, B. and C. Wofsy. 1981. Analysis of coated pit recycling on human fibroblasts. *Cell Biophysics.* **3**:251-277.

26. Wofsy, C. and B. Goldstein. 1984. Coated pits and low density lipoprotein receptor recycling. In *Cell Surface Dynamics.* A. Perelson, C. de Lisi and F. Wiegel, editors. Marcel Deckker Inc., New York. 405-456.

27. Erickson, J., B. Goldstein, D. Holowka and B. Baird. 1987. The effect of receptor density on the forward rate constant for binding of ligands to cell surface receptors. *Biophys. J.* **52**:657-662.

28. Keizer, J., J. Ramirez and E. Peacock-Lopez. 1985. The effect of diffusion on the binding of membrane-bound receptors to coated pits. *Biophys. J.* 47:79-87.

29. Carpenter, G. 1987. Receptors for epidermal growth factor and other polypeptide mitogens. *Ann. Rev. Biochem.* 56:881-914.

30. Das, M. and C.F. Fox. 1978. Molecular mechanism of mitogen action: Processing of receptor induced by epidermal growth factor. *Proc. Natl. Acad. Sci. USA.* 75:2644-2648.

31. Basu, S.K., J.L. Goldstein, R.G.W. Anderson and M.S. Brown. 1981. Monensin interrupts the recycling of low density lipoprotein receptors in human fibroblasts. *Cell.* 24:493-502.

32. Basu, S.K., J.L. Goldstein and M.S. Brown. 1978. Characterization of the low density of lipoprotein receptor in membranes prepared from human fibroblasts. *J. Biol. Chem.* 253:3852-3856.

33. Wiley, H.S. and D.D. Cunningham. 1981. A steady state model for analyzing the cellular binding, internalization and degradation of polypeptide ligands. *Cell.* 25:433-440.

34. Goldstein, J.L., R.G.W. Anderson and M.S. Brown. 1979. Coated pits, coated vesicles and receptor-mediated endocytosis. *Nature* (London). 279:679-685.

35. Brown, M.S. and J.L. Goldstein. 1976. Receptor-mediated control of cholesterol metabolism. *Science.* 191:150-154.

36. Goldstein, J.L. and M.S. Brown. 1974. Binding and degradation of low density lipoproteins by cultured human fibroblasts. *J. Biol. Chem.* 249(16):5153-5162.

37. Goldstein, J.L., S.K. Basu, G.Y. Brunschede and M.S. Brown. 1976. Release of low density lipoprotein from its cell surface receptor by sulfated glycosaminoglycans. *Cell.* 7:85-95.

38. Goldstein, J.L., S.K. Basu and M.S. Brown. 1983. Receptor-mediated endocytosis of low-density lipoproteins in cultured cells. *Methods Enzymol.* 98:241-260.

39. Goldstein, B., R. Greigo and C. Wofsy. 1984. Diffusion-limited forward rate constants in two dimensions. *Biophys. J.* 46:573-586.

40. Webb, W.W. and D. Gross. 1986. Patterns of individual molecuolar motions deduced from fluirescent image analysis. In *Applications of Fluorescence in the Biomedical Sciences.* Alan Liss, Inc. New York. 405-422.

41. Anderson, R.G.W. J.L. Goldstein and M.S. Brown. 1977. A mutation that implies the ability of lipoprotein receptors to localise in coated pits on the cell surface of human fibroblasts. *Nature.* 270:697-699.

42. Box, G.E.P. and N.R. Draper. 1965. The Bayesian estimation of common parameters from several responses. *Biometrica*. 52. 3 *and* 4. 355-365.

43. Kirkpatrick, S., C.D. Gelatt Jr. and M.P. Vecchi. 1983. Optimization by simulated annealing. *Science*. 220:671-680.

44. Vanderbilt, D. and S.G. Louie. 1984. A Monte Carlo simulated annealing approach to optimization over continuous variables. *J. Computational Phys*. 56:259-271.

45. Bremermann, H. 1970. A method of unconstrained global optimization. *Mathematical Biosciences*. 9:1-15.

46. Bremermann, H. 1974. Chemotaxis and optimization. *J. Franklyn Inst*. 297(5):397-404.

47. Goldstein, J.L., M.S. Brown and R.G.W. Anderson. 1977. The low density lipoprotein pathway in human fibroblasts: Biochemical and ultrastructural correlations. In *International Cell Biology 1976-1977*. B.R. Binkley and K.R. Porter, eds., Rockefeller University Press, New York.639-648.

48. Goldstein, J.L., S.E. Dana, J.R. Faust, A.L. Beaudet and M.S. Brown. 1975. Role of lysosomal acid lipase in the metabolism of plasma low density lipoprotein. *J. Biol. Chem*. 250:8487-8495.

49. Steinman, R.M., I.S. Mellman, W.A. Muller and Z.A. Cohn. 1983. Endocytosis and the recycling of plasma membrane. *J. Cell Bio*. 96:1-27.

50. Vlodavsky, I., P.E. Fielding, C.J. Fielding and D. Gospodarowicz. 1978. Role of contact inhibition in the regulation of receptor-mediated uptake of low density lipoprotein in cultured vascular endothelial cells. *PNAS USA*. 75(1): 356-360.

51. Pitas, R.E., T.L. Innerarity, K.S. Arnold and R.W. Mahley. 1979. Rate and equilibrium constants for binding of apo-E $HDL_c$ (a cholesterol-induced lipoprotein) and low density lipoproteins to human fibroblasts: Evidence for multiple receptor binding of apo-E $HDL_c$. *PNAS USA*. 76(5): 2311-2315.

52. Wofsy, C., H. Echavarría-Herras and B. Goldstein. 1985. Effect of preferential insertion of LDL receptors near coated pits. *Cell Biophys*. 7:197-203.

53. Goldstein, J.L., J.R. Faust and M.S. Brown. 1975. Role of the low density lipoprotein receptor in regulating the content of free and esterified cholesterol in human fibroblasts. *J. Clin. Invest*. 55:783-793.

54. Torado, G.J., larzar, G. K. and Green, H. 1966. The Initiation of Cell Division in a Contact-inhibited Mammalian Cell LIne. *J. Cell. and Comp. Physiol*. 66:325-334

55. Brown, M.S. and Goldstein, J.L. 1974. Suppression of 3-Hydroxy-3-methylglutaryl Coenzyme A Reductase Activity and

Inhibition of Growth of Human Fibroblasts by 7-Ketocholesterol. *J. Biol. Chem.* **249**:7306-7314.

56. Levenspiel, O. 1972. Chemical Reaction Engineering. Jhon Wiley and Sons, Inc., New York. 71-73

57. Eisenberg, S. 1980. Plasma lipoprotein conversions: The origin of low density and high density lipoproteins. *Ann. N.Y. Acad. Sci.* **348**:31-47.

58. Shireman, R.B. and J.F. Remsen. 1982. Uptake of [$^{3}$H]cholesterol from low density lipoprotein by cutured human fibroblasts. *Biochimica et Biophysica Acta* **711**:281-289.

59. Goldstein, J.L. and Brunschede, G.Y. and Brown, M.S. 1975. Inhibition of the proteolytic degradation of low density lipoprotein in human fibroblasts by chloroquine, concanavalin A, and triton WR 1339. *J. Biol. Chem.* **250**: 7854-7862.

60. Brown, M.S., Dana, S.E. and Goldstein, J.L. 1975. Receptor-dependent hydrolysis of cholesteryl esters contained in plasma low density lipoprotein. *Proc. Natl. Acad. Sci. USA* *72*:2925-2929.

61. Goldstein, J.L., S.E. Dana and M.S. Brown. 1974. Esterification of low density lipoprotein cholesterol in human fibroblasts and its absence in homozygous familial hypercholesterolemia. *Proc. Natl. Acad. Sci. USA* **71**:4288-4292.

62. Brown, M.S., S.E. Dana and J.L. Goldstein. 1975. Cholesterol ester formation in cultured human fibro blasts. *J. Biol. Chem.* **250**:4025-4027.

63. Kandutch, A.A., H.W. Chen and H.J. Heiniger. 1978. Biological activity of some oxygenated sterols. *Sience* **201**:498-501.

64. Tanaka, R.D., P.A. Edwards, S.F. Lan and A.M. Fogelman. 1983. Regulation of 3-hydroxy-3-methyl glutaryl coenzyme A reductase activity in avian myloblasts. *J. Biol. Chem.* **258**:13331-13339.

65. Chin, D.J., G. Gil, J.R. Faust, J.L. Goldstein, M.S. Brown and K. Luskey. 1985. *Mol. Cell. Biol.* **5**:634-641.

66. Gupta, A., R.C. Sexton and H. Rudney. 1986. Modulation of regulatory oxysterol formation and low density lipoprotein suppression of 3-hydroxy-3-methyl glutaryl coenzyme A reductase activity by ketoconazole. *J. Biol. Chem.* **261**:8348-8356.

67. Wintersteiner, O. and J.R. Ritzman. 1940. *J. Biol. Chem.* **136**:697-708.

68. Assamann, G., D.S. Fredrickson, H.R. Sloan, H.M. Fales and R.J. Heighet, 1975. Accumulation of oxygenerated steryl esters in Wolmaln's desease. *J. Lipid Res.* **16**:28-38.

69. Van Lier, J.E. and L.L. Smith. 1967. Sterol metabolism. I. 26-hydroxycholesterol in the human aota. *Biochemistry* **6**:3269-3278.

70. Björkhem, I. and J.A. Gustafsson. 1974. Mitochondrial w-hydroxylation of cholesterol side chain. *J. Biol. Chem.* **249**:2528-2535.

71. Breslow, J.L., D.A. Lothrop, D.R. Spaulding and A.A. Kandutch. 1975. Cholesterol, 7-ketocholesterol and 25-hydroxycholesterol uptake studies and effect on 3-hydroxy-3-methylglutaryl-coenzyme A reductase activity in human fibroblasts. *Biochim. Biophys. Acta* **298**:10-17.

72. Kandutch, A.A. and H.W. Chen. 1973. Inhibition of sterol synthesis in cultured mouse cells by 7$\alpha$-hydroxycholesterol, 7$\beta$-hydroxycholesterol and 7-ketocholesterol. *J. Biol. Chem.* **248**:8408-8417.

73. Chen, H.W., H.J. Heiniger, and A.A. Kandutch. 1975. Replication of colicin El plasmid DNA added to cell extracts. *Proc. Natl. Acad. Sci. USA* **72**:1950-1954.

74. Goldstein, J.L. and M.S. Brown. 1984. Progress in understanding the LDL receptor and HMG CoA reductase,two membrane proteins that regulate the plasma cholesterol. *J. Lip. Res.* **25**:1450-1461.

75. Luskey, K.L. 1986. Structure and expression of 3-hydroxy-3-methylglutaryl coenzyme A reductase. *Annals N.Y. Acad. Sci.* :249-254.

76. Goldstein, J.L. and M.S. Brown. 1990. Regulation of the mevalonate pathway. *Nature* **343**:425-430.

77. Brown, M.S., S.E. Dana and J.L. Goldstein. 1974. Regulation of 3-hydroxy-3-methylglutaryl coenzyme A reductase activity in cultured human fibroblasts. *J. Biol. Chem.* **249**:780-796.

78. Nakanish, M., J.L. Goldstein and M.S. Brown. 1988. Multivalent control of 3-hydroxy-3-methylglutaryl coenzyme A reductase. *J. Biol. Chem.* **263**:8929-8937.

79. Luskey K.L., J.R. Faust, D.J. Chin, M.S. Brown and J.L. Goldstein. 1983. Amplication of the gene for 3-hydroxy-3-methylglutaryl coenzyme A reductase activity in human fibroblasts. *J. Biol. Chem.* **258**:8462-8469.

80. Brown, M.S., J.R. Faust, J.L. Goldstein, I. Kaneko and A. Endo. 1978. Induction of 3-hydroxy-3-methylglutaryl coenzyme A reductase activity in human fibroblasts incubated with compactin (ML-236B), a competitive inhibitor of the reductase. *J. Biol. Chem.* **253**:1121-1128.

81. Brown, M.S. and J.L. Goldstein. 1980. Multivalent feed back regulation of HMG CoA reductase, a control mechanism coordinating isoprenoid synthesis and cell growth. *J. Lipid Res.* **21**:505-517.

82. Goldstein, J.L., S.E. Dana, J.R. Faust, A.L. Beaudet and M.S. Brown. 1975. Role of lysosomal acid lipase in the metabolism of plasma low density lipoprotein. *J. Biol. Chem.* **250**:8487-8495.

83. Stryer, L. 1988. *Biochemistry*. W.H. Freeman and Company, New York. 555-559.

84. Fielding, C.J. and P.E. Fielding. Metabolism of cholesterol and lipoproteins. In *Biochemistry of Lipids and Membranes* 1985. Vance, D.E. and J.E. Vance, eds., The Benjamin/Cummings Publishing Company, Inc., Menlo Park, California. 404-474.

85. Goldstein, J.L., S.E. Dana, G.Y. Brunschede and M.S. Brown. 1975. Genetic heterogeniety in familial hypercholesterolemia: Evidence for two different mutations affecting functions of low density lipoprotein receptor. *Proc. Natl. Acad. Sci. USA* **72**:1092-1096.

86. Suckling, K.E. and E.F. Stange. 1985. Role of acyl-CoA:cholesterol acyltransferase in cellular cholesterol metabolism. *J. Lipid Res.* **26**:647-671.

87. Slotte, J.P., G. Hedström, S. Rannström and S. Ekman. 1989. Effects of sphingomyelin degradation on cell cholesterol oxidizability and steady-state distribution between the cell surface and the cell interior. *Biochimica et Biophysica Acta* **985**:90-96.

88. Slotte, J.P., E.L. Bierman. 1988. Depletion of plasma-membrane sphingomyelin rapidly alters the distribution of cholesterol between plasma membranes and intracellular cholesterol pools in cultured fibroblasts. *Biochem. J.* **250**:653-658.

89. Billheimer, J.T., D.A. Cromley and E.S. Kempner. 1990. The functional size of acyl-coenzyme A:cholesterol acyltransferase and acyl-CoA hydrolase as determined by radiation inactivation. *J. Biol. Chem.* **265**:8632-8635.

90. Doolittle, G.M. and T.Y. Chang. 1982. *Solubilization, partial purification and reconstitution in phosphatidylcholine-cholesterol liposomes of acyl-CoA:cholesterol transferase.*

91. Phillips, M.C., W.J. Johnson and G.H. Rothblat. 1987. Mechanisms and consequences of cellular cholesterol exchange and transfer. *Biochimica et Biophysica Acta* **906**:223-276.

92. Karlin, J.B., W.J. Johnson, C.R. Benedict, G.K. Chacko, M.C. Phillips and G.H. Rothblat. 1987. Cholesterol flux between cells and high density lipoprotein. *J. Biol. Chem.* **262**:12557-12564.

93. Clair, R.W. St. and M.A. Leight. 1983. Cholesterol efflux from cells enriched with cholesterol esters by incubation with hypercholesterolemic monkey low density lipoprotein. *J. Lip. Res.* **24**:183-191.

94. Rothblat, G.H. and M.C. Phillips. 1982. Mechanism of cholesterol efflux from cells. *J. Biol. Chem.* **257**:4775-4782.

95. Grandison, A.S. and C. Green. 1979. Transfer of cholesterol between different regions of the rat hepatocyte surface membrane. *Int. J. Biochem.* **10**:623-627.

96. Lange, Y., J. Dolde and T.L. Steck. 1981. The rate of transmembrame movement of cholesterol in the human erythrocyte. *J. Biol. Chem.* **256**:5321-5323.

97. Wu, J. and J.M. Bailey. 1980. Lipid metabolism in cultured cells: studies on lipoprotein-catalyzed reverse cholesterol transport in normal and homozygous familial hypercholesterolemic skin fibroblasts. *Archives of biochemistry and biophysics* **202**:467-473.

98. Brown, M.S. and J.L. Goldstein. 1974. Familial hypercholesterolemia: Defecting binding of lipoprotein to cultured fibroblasts associated imported regulation of 3-hydroxy-methyl coenzyme A reductase activity. *Proc. Natl. Acad. Sci. USA* **71**:788-792.

99. Brown, M.S. and J.L. Goldstein. 1974. Expression of the familial hypercholesterolemia gene in heterogegotes: Mechanism for a dominant disorder in man. *Science* **185**:61-63.

100. Goldstein, J.L. and M.S. Brown. 1973. Familial hypercholesterolemia: Identification of a defect in the regulation of 3-hydroxy-3-methylglutaryl coenzyme A reductase activity associated with overproduction of cholesterol. *Proc. Natl. Acad. Sci. USA* **70**:2804-2808.

101. Brown, M.S. and J.L. Goldstein. 1975. Regulation of the activity of the low density lipoprotein receptor in human fibroblasts. *Cell* **6**:307-316.

102. Gevers, W., G.A. Coetzee and D.R. Westhuyzen. Biological clinical implications of LDL receptors. In *Biochemistry and biology of plasma lipoproteins*. Scanu, A.M. and A.A. Spector, eds., Marcel Deckker Inc., New York. 331-358.

103. Reed, B.C. and M.D. Lane. 1980. Insulin receptor synthesis and turnover in differentiating 3T3-L1 preadipocytes. *Proc. Natl. Acad. Sci. USA.* **77**:285-289.

104. Yamamoto, T., C.G. Davis, M.S. Brown, W.J. Schneider, M.L. Casey, J.L. Goldstein and D.W. Russel. 1984. The human LDL receptor: A cysteine-rich protein with multiple alu sequences in its mRNA. *Cell* **39**:27-38.

105. Goldstein, J.L., M.K. Sobani, J.R. Faust and M.S. Brown. 1976. Heterozygous familial hypercholesterolemia failure of normal allele to compensata for mutant allele at a regulated genetic locus. *Cell* **9**:195-203.

106. Bailey, J.E. and F.O. David. 1986. *Biochemical engineering fundamentals*. McGraw-Hill, Inc., New York., 429.

107. Brown, M.S. and J.L. Goldstein. 1990. Scavenging for receptors. *Nature*. **343**:508-509.

108. Darnell, J.E., H.F. Lodish and D. Baltimore. 1986. *Molecular Cell Biology*. Scientific American Book Inc., 363.

109. Brown, M.S., S.E. Dana and J.L. Goldstein. 1973. Regulation of 3-hydroxy-3-methylglutaryl coenzyme A reductase activity in human fibroblasts by lipoproteins. *Proc. Natl. Acad. Sci. USA* 70:2162-2166.

110. Brown, M.S. and J.L. Goldstein. 1984. How LDL Receptors Influence Cholesterol and Atherosclerosis. *Scientific Am.* 251:58-66.

111. Yuan, F., S. Chien and S. Weinbaum. 1991. A New View of Convective-Diffusive Transport Process in the Arterial Intima. *J. Biomech. Engineering*. 113:314-329.